

**Endothelial eNOS and red blood cell eNOS
independently regulate blood pressure and nitric oxide
metabolites**

Inaugural dissertation

for the attainment of the title of doctor
in the Faculty of Mathematics and Natural Sciences
at the Heinrich Heine University Düsseldorf

presented by

Francesca Leo
from Massa, Italy

Düsseldorf, January 2022

From the Myocardial Infarction Research Laboratory, Clinic for Cardiology,
Pulmonology and Angiology, Medical Faculty, Heinrich-Heine-University of
Düsseldorf.

Published by permission of the
Faculty of Mathematics and Natural Sciences at
Heinrich Heine University Düsseldorf

Supervisor: Univ.-Prof. Dr. Dr. rer. nat. Miriam M. Cortese-Krott
Co-supervisor: Univ.-Prof. Dr. rer. nat. Jens Fischer

Date of the oral examination: 19.01.2022

I declare under oath that I have produced my thesis independently and without any undue assistance by third parties under consideration of the ‘Principles for the Safeguarding of Good Scientific Practice at Heinrich Heine University Düsseldorf’.

This dissertation was neither in the same nor in a similar form in another examination procedure submitted. I also declare that I have not yet received or attempted to acquire any further degree.

Francesca Leo

To my family

Parts of this dissertation were already published in peer-reviewed scientific journals and presented on scientific conferences.

Original publications:

Francesca Leo*, Tatsiana Suvorava* ; Sophia K. Heuser, Junjie Li, Anthea LoBue, Frederik Barbarino, Eugenia Piragine, Rebekka Schneckmann, Beate Hutzler, Miranda E. Good, Bernadette O. Fernandez, Lukas Vornholz, Stephen Rogers, Allan Doctor, Maria Grandoch, Johannes Stegbauer, Eddie Weitzberg, MD, Martin Feelisch, Jon O. Lundberg, Brant E. Isakson, Malte Kelm, Miriam M. Cortese-Krott (2021). “Red Blood Cell and Endothelial eNOS Independently Regulate Circulating Nitric Oxide Metabolites and Blood Pressure.” *Circulation*. Online ahead of print.

The contribution to the paper “Red blood cell and endothelial eNOS independently regulate circulating nitric oxide metabolites and blood pressure” consisted in producing all the data regarding blood pressure and echocardiography of the animal models presented, including the tables reporting the data. Moreover, planification of the experiments and treatment of the mice was carried out. I contributed to the correction of the manuscript and to answer to the reviewers during revision phase.

Francesca Leo, Thomas Krenz, Georg Wolff, Mathias Weidenbach, Christian Heiss, Malte Kelm, Brant Isakson, Miriam M. Cortese-Krott (2020). "Assessment of tissue perfusion and vascular function in mice by scanning laser Doppler perfusion imaging." *Biochemical Pharmacology* 176: 113893.

The contribution to the paper "Assessment of tissue perfusion and vascular function in mice by scanning laser Doppler perfusion imaging" consisted in the correction and revision of the manuscript. I took care of the preparation of the answers to the reviewers during the revision phase.

Reviews:

Junie Li, Anthea LoBue, Sophia K. Heuser, **Francesca Leo**, Miriam M. Cortese-Krott (2021). (Using diaminofluoresceins (DAFs) in nitric oxide research.” *Nitric Oxide*. In Press, Journal Pre-proof.

The contribution to the review “Using diaminofluoresceins (DAFs) in nitric oxide research” consisted in the correction and revision of the text before submission and during the revision phase.

Francesca Leo, Beate Hutzler, Claire A. Ruddiman, Brant E. Isakson, Miriam M. Cortese-Krott (2020). "Cellular microdomains for nitric oxide signaling in endothelium and red blood cells." *Nitric Oxide* 96: 44-53.

The contribution to the review "Cellular microdomains for nitric oxide signaling in endothelium and red blood cells" consisted in the writing of a paragraph of the manuscript. Moreover, I took care of the correction of the paper before submission, and I prepared an answer to the reviewers during the revision phase.

Posters and oral presentations:

1. 01-02.06.2021, Düsseldorf, Germany: **Cardiovascular Disease (CaVaD) Symposium 2021**
(Poster presentation: "Red blood cell and endothelial eNOS independently regulate circulating nitric oxide metabolites and blood pressure"; Francesca Leo, Tatsiana Suvorava, Sophia K. Heuser, Junjie Li, Anthea LoBue, Frederik Barbarino, Eugenia Piragine, Rebekka Schneckmann, Beate Hutzler, Miranda E. Good, Bernadette O. Fernandez, Lukas Vornholz, Stephen Rogers, Allan Doctor, Maria Grandoch, Johannes Stegbauer, Eddie Weitzberg, Martin Feelisch, Jon O. Lundberg, Brant E. Isakson, Malte Kelm, Miriam M. Cortese-Krott)
2. 07-08.12.2020, Düsseldorf, Germany (online): **Methods in Cardiovascular Research**
Oral presentation: "Invasive blood pressure measurement: Millar catheter"
3. 27.11.2019 in Pisa, Italy: **IRPES 2019 – Innovative Research in Pharmaceutical & Environmental Sciences**
(Poster presentation: "Reactivation of eNOS in the endothelium rescues eNOS KO mice from endothelial dysfunction and hypertension"; Francesca Leo, Eugenia Piragine, Lukas Vornholz, Nadine Thomas, Tatsiana Suvorava, Miriam M. Cortese-Krott)
4. 07-08.10.2019 in Düsseldorf, Germany: **Besuch und Betreuung der „Autumn School“ des Kooperationspartner University of Virginia mit dem Internationalen Graduiertenkolleg IRTG 1902 von Prof. Gödecke**

(Poster presentation: “Specific reactivation of eNOS in the endothelium of adult mice rescues from endothelial dysfunction and hypertension”; Francesca Leo, Eugenia Piragine, Lukas Vornholz, Nadine Thomas, Tatsiana Suvorava, Brant E. Isakson, Miriam M. Cortese-Krott)

5. 02-08.02.2019 in Ventura, (CA) USA: **Gordon Research Seminar and Gordon Research Conference Nitric Oxide 2019**

(Poster presentation: “Role of the NO-cGMP pathway in RBCs in systemic hemodynamics”; Francesca Leo, Evanthia Mergia, Julia Hocks, Doris Koesling, Tatsiana Suvorava, Malte Kelm, Miriam M. Cortese-Krott)

6. 29.11.2018-01.12.2018 in Charlottesville, (VA) USA: **Besuch und Betreuung der „Autumn School“ des Kooperationspartner University of Virginia mit dem Internationalen Graduiertenkolleg IRTG 1902 von Prof. Gödecke**

(Poster presentation: „Specific reactivation of eNOS in the endothelium rescues from endothelial dysfunction and hypertension”; Francesca Leo, Nadine Thomas, Lukas Diederich, Julia Hocks, Brant E. Isakson, Tatsiana Suvorava, Malte Kelm, Miriam M. Cortese-Krott)

7. 08-10.10.2018 in Tübingen, Germany: **Hot topics in Signal Transduction & cGMP Research**

(Poster presentation: “Role of the NO-cGMP pathway in RBCs in systemic hemodynamics”; Francesca Leo, Evanthia Mergia, Nadine Thomas, Doris Koesling, Tatsiana Suvorava, Malte Kelm, Miriam M. Cortese-Krott)

8. 15-16.03.2018 in Düsseldorf, Germany: **Cardiovascular Disease (CaVaD) Symposium 2018**

(Poster presentation: “Role of the Arg1/NOS3 pathway in RBCs in systemic hemodynamics”; Francesca Leo, Tatsiana Suvorava, Malte Kelm, Miriam M. Cortese-Krott)

(Oral presentation: “Red blood cells can regulate vascular tone”)

Abstract

Background and hypothesis. It is well known that nitric oxide (NO) produced in the vessel wall by an endothelial nitric oxide synthase (eNOS) regulates vascular tone and blood pressure (BP). Besides their role as oxygen transporters, red blood cells (RBCs) are known as scavengers of NO bioactivity. However, it has been shown that RBCs, similar to endothelial cells (ECs), carry an active and functional eNOS. The physiological role and involvement of red cell eNOS in NO metabolism and regulation of vascular tone and BP are not known. The hypothesis of this study was that red cell eNOS contributes to the regulation of NO metabolites, vascular tone, and BP.

Aim and Goals. This study aimed to elucidate the functional significance and specific role of red cell eNOS as compared to endothelial eNOS in controlling vascular hemodynamics and systemic NO metabolism.

The goals of this study were the following: (1) The creation and characterization of tissue-specific eNOS knock-out (KO) and knock-in (KI) mice by using tissue-specific Cre-induced gene inactivation or reactivation; (2) the analysis of systemic hemodynamics of the generated mice; (3) the evaluation of NO metabolites distribution at baseline and after administration of nitrate.

Methods. Tissue-specific “loss” and “gain-of-function” models for eNOS were generated using tissue-specific Cre-induced gene inactivation or reactivation. These mice were characterized for Cre-induced DNA recombination by polymerase chain reaction (PCR), for eNOS expression by real-time quantitative PCR and immunoblotting, for *ex vivo* and *in vivo* vascular endothelial function by determining ACh-induced responses in an organ bath and flow-mediated dilation (FMD) by ultrasound. BP and peripheral resistance were assessed by Millar catheter and echocardiography. Blood count was determined by a coulter counter.

Results. KO and KI models for eNOS in the ECs and RBCs were successfully generated and showed tissue-specific DNA recombination and lack or presence of eNOS expression in the targeted tissues. EC eNOS KO mice showed a loss in endothelial function, decreased NO metabolites, and increased BP, with no effects in cardiac parameters. *Vice versa*, reactivation of eNOS in the endothelium fully rescued the global eNOS KO from hypertension. Interestingly, RBC eNOS KO mice were hypertensive with decreased circulating NO metabolites but a fully preserved endothelial function. Notably, reactivation of eNOS specifically in the RBCs rescued the mice from hypertension and increased NO-heme levels in RBCs. Nitrate administration determines an increase in circulating nitrite levels and a BP decrease in EC eNOS KO and control mice but no changes in the BP of RBC eNOS KO mice.

Summary and conclusion. These data demonstrate that red cell eNOS plays an important role in the modulation of BP and systemic hemodynamics, which is independent of the role played by vascular eNOS.

Zusammenfassung

Hintergrund und Hypothese: Es ist bekannt, dass Stickstoffmonoxid (NO), welches in der Gefäßwand durch die endotheliale Stickstoffmonoxid-Synthase (eNOS) produziert wird, den Gefäßtonus und den Blutdruck reguliert. Neben ihrer Rolle als Sauerstofftransporter, sind Erythrozyten (RBCs) als Scavenger der NO-Bioaktivität bekannt. Es wurde jedoch gezeigt, dass Erythrozyten, ähnlich wie Endothelzellen (EC), eine aktive und funktionelle eNOS tragen. Die physiologische Rolle und der Einfluss der erythrozytären eNOS auf den NO Metabolismus, die Regulation des Gefäßtonus, sowie den Blutdruck ist unbekannt. Die Hypothese dieser Arbeit war, dass die erythrozytäre eNOS zur Regulation des NO Metabolismus, dem Gefäßtonus und dem Blutdruck beiträgt.

Ziele: Hauptziel dieser Studie war es, die funktionelle Bedeutung und spezifische Rolle der Erythrozyten-eNOS, im Vergleich zur endothelialen eNOS, bei der Kontrolle der vaskulären Hämodynamik und des systemischen NO-Stoffwechsels zu klären. Die Zielsetzungen dieser Studie waren die folgenden: (1) Die Entwicklung und Charakterisierung von gewebespezifischen knock-out (KO) und knock-in (KI) Mausmodellen durch die Verwendung von gewebespezifischer Cre-induzierter Gen-Inaktivierung bzw. – Reaktivierung; (2) die Analyse der systemischen Hämodynamik der Mauslinien des Interesses; (3) Die Untersuchung der Verteilung der NO-Metaboliten zu Beginn und nach der Gabe von Nitrat.

Methoden: Durch gewebespezifische Cre-induzierte Gen-Inaktivierung oder – Reaktivierung wurden gewebespezifische “loss” und “gain-of-function”-Modelle für eNOS generiert. Im Rahmen der Charakterisierung dieser Mäuse erfolgte die Untersuchung auf Cre-induzierte DNS-Rekombination durch Polymerase-Kettenreaktion (PCR), auf eNOS-Expression durch quantitative Echtzeit-PCR und Immunoblotting und der vaskulären Endothelfunktion *ex vivo* und *in vivo* durch Bestimmung der ACh-induzierten Reaktion in einem Organbad, sowie der Fluss-vermittelten Dilatation (FMD) durch Ultraschall. Blutdruck und peripherer Widerstand wurden mittels Millar-Katheter und Echokardiographie analysiert. Die Erstellung des Blutbilds erfolgte mit einem Coulter-Zähler.

Ergebnisse. KO und KI Modelle für eNOS in Endothelzellen und Erythrozyten wurde erfolgreich generiert und zeigte gewebespezifische DNS-Rekombination bzw. das Fehlen oder Vorhanden sein von eNOS-Expression in den Zielgeweben. EC eNOS KO Mäuse zeigten einen Verlust der Endothelfunktion, verminderte NO-Metaboliten und erhöhten Blutdruck, ohne Auswirkungen auf kardiale Parameter. Umgekehrt bewahrte die Reaktivierung von eNOS im Endothelium die globalen KO Mäuse vor Bluthochdruck. Interessanterweise waren RBC eNOS-KO Mäuse hypertensiv mit verminderten zirkulierenden NO-Metaboliten, jedoch einer vollständig erhaltenen Endothelfunktion. Bemerkenswert ist, dass eine Reaktivität von eNOS ausschließlich in den Erythrozyten die Mäuse vor Hypertonie schützt und

es zu einer Erhöhung von NO-Häm in den Erythrozyten kommt. Die Gabe von Nitrat bewirkt einen Anstieg der zirkulierenden Nitritspiegel und eine Senkung des Blutdrucks in EC eNOS KO- und Kontrollmäusen, aber keine Veränderung im Blutdruck der RBC eNOS-KO Mäuse

Zusammenfassung und Schlussfolgerung: Diese Daten zeigen, dass die erythrozytäre eNOS eine wichtige Rolle bei der Regulation des Blutdruckes und der systemischen Hämodynamik spielt, welche unabhängig von der Rolle der vaskulären eNOS ist.

Index of contents

Abstract	VIII
Zusammenfassung	IX
Index of figures	XV
Index of tables	XVII
Abbreviations	XVIII
1. Introduction	1
1.1 Hypertension and cardiovascular disease	1
1.2 Regulation of vascular tone and blood pressure	5
1.3 Systemic NO metabolism and the nitrate/nitrite/NO pathway	8
1.4 Role of RBCs in the regulation of vascular tone	10
1.5 Red blood cells as regulators of the systemic NO metabolism	12
1.6 The use of a loxP-Cre method for tissue-specific gene targeting	14
2. Aim of the study	15
3. Materials and methods	17
3.1 Chemicals	17
3.1.1 Solutions	18
3.1.2 Antibodies	19
3.1.3 Commercial kits	19
3.1.4 Equipment	20
3.1.1 Softwares	20
3.2 Animals	21
3.3 Creation of tissue-specific mice lines	22
3.3.1 Generation of eNOS ^{flox/flox} mice	22
3.3.2 Generation of eNOS ^{inv/inv} mice	22
3.3.3 Generation of EC/RBC eNOS KO mice	22

3.3.4	Generation of EC/RBC eNOS KI mice	23
3.3.5	Generation of global eNOS KO mice.....	23
3.4	<i>Dietary nitrate supplementation of the mice in the drinking water</i>	23
3.5	<i>Collection of blood and mouse tissues</i>	24
3.5.1	Blood collection and separation of plasma and RBCs	24
3.5.2	Tissues collection	24
3.6	<i>Hematological phenotyping of tissue-specific mice models</i>	25
3.7	<i>Blood collection and separation of RBCs for immunofluorescence</i>	25
3.7.1	Immuno transmission electron microscopy (TEM).....	26
3.8	<i>Isolation of endothelial cells from lungs</i>	26
3.9	<i>Isolation of erythroid cells from bone marrow</i>	27
3.10	<i>Molecular characterization of mice models of eNOS KO and eNOS KI</i>	28
3.10.1	Analysis of tissue-specific DNA recombination by qPCR	28
3.10.2	Analysis of eNOS expression in isolated cells and tissues by RT-qPCR	29
3.10.1	Western blotting	32
3.10.2	Immunoprecipitation of mouse anti-eNOS using EPOXY270 Beads	33
3.11	<i>Characterization of systemic hemodynamics</i>	34
3.11.1	Measurement of vascular function <i>in vivo</i>	34
3.11.2	Analysis of cardiac function by high-resolution ultrasound	35
3.11.3	Blood pressure measurements by Millar catheterization	35
3.11.4	Measurement of endothelial function/vascular reactivity <i>ex vivo</i>	36
3.11.5	Determination of nitrite levels in plasma	37
3.12	<i>Statistical Analyses</i>	38
4.	Results	39
4.1	<i>Analysis of eNOS and AE-1 localization on RBC membrane</i>	39
4.2	<i>Generation of tissue-specific conditional eNOS KO mice</i>	41
4.3	<i>Determination of eNOS protein expression levels to characterize global eNOS KO and EC eNOS KO and RBC eNOS KO</i>	43
4.3.1	Characterization of EC eNOS KO mice	43

4.3.2	Characterization of RBC eNOS KO mice	44
4.4	<i>Blood count</i>	46
4.5	<i>Evaluation of the impact of the absence of EC eNOS and RBC eNOS on cardiovascular homeostasis and systemic hemodynamics</i>	47
4.5.1	Vascular endothelial function is lost in EC eNOS KO and preserved in RBC eNOS KO mice 47	
4.5.2	FMD is lost in EC eNOS KO and preserved in RBC eNOS KO mice	48
4.5.3	EC eNOS KO mice and RBC eNOS KO mice are hypertensive	50
4.5.4	No differences are detected in cardiac parameters in EC eNOS KO and RBC eNOS KO mice but significant increase in systemic vascular resistance	51
4.6	<i>Generation of tissue-specific conditional eNOS KI mice</i>	54
4.6.1	Test of the efficiency of the gene reactivation construct.....	54
4.6.2	eNOS gene dosage effect in global eNOS KI mice.....	56
4.6.3	Tissue-specific eNOS KI mice	57
4.7	<i>Determination of eNOS protein expression levels in EC eNOS KI and RBC eNOS KI mice</i>	58
4.7.1	Characterization of tissue-specific eNOS KI mice.....	58
4.8	<i>Blood count</i>	61
4.9	<i>Evaluation of the impact of eNOS on cardiovascular homeostasis and systemic hemodynamics after tissue-specific eNOS reactivation</i>	62
4.9.1	Vascular endothelial dilation to acetylcholine is reestablished in EC eNOS KI mice	62
4.9.2	FMD is restored in EC eNOS KI mice	64
4.9.3	EC eNOS KI mice and RBC eNOS KI show decreased BP	64
4.9.4	No differences are detected in cardiac parameters and systemic vascular resistance in EC eNOS KO and RBC eNOS KO mice	66
4.10	<i>Summary</i>	68
4.11	<i>Evaluation of NO metabolites concentration in blood and tissues</i>	69
4.11.1	Circulating nitrite decreases in EC eNOS KO and RBC eNOS KO, and NO-heme levels change in RBC eNOS KO/KI mice	69
4.12	<i>Effects of nitrate supplementation on systemic hemodynamics</i>	74
4.12.1	Blood pressure and NO metabolites in EC- and RBC eNOS KO after nitrate supplementation.....	74

4.12.2 Plasma nitrite levels are increased in EC eNOS KO and WT controls but not in RBC eNOS KO mice after nitrate supplementation 78

5. Discussion 80

5.1 *New functional models of tissue-specific eNOS KO and eNOS KI mice were generated* 82

5.2 *Reintroduction of eNOS in the endothelium rescues from hypertension and restores vascular endothelial function and FMD. Circulating nitrite levels are decreased in EC eNOS KO mice* 83

5.3 *Red cell eNOS modulates blood pressure independently from vascular eNOS. Circulating nitrite is decreased in RBC eNOS KO mice, and the levels of NO-heme are changed in RBC eNOS KO/KI mice* 87

5.4 *Administration of nitrate in the drinking water affects BP of WT and EC eNOS KO mice and has no effects on BP and plasma nitrite levels of RBC eNOS KO mice* 88

5.5 *How does red cell eNOS regulate BP?* 89

5.6 *Summary and perspective* 93

6. References 94

7. Acknowledgements 109

8. Curriculum vitae 111

Index of figures

Figure 1 – Circulatory system	2
Figure 2 – Structural characterization of blood vessels	4
Figure 3 – NO pathway to vasodilation in smooth muscle cells	7
Figure 4 – Oral administration of nitrate and NO formation	9
Figure 5 – Arg1-eNOS-sGC pathway in RBCs.....	13
Figure 6 – Graphical abstract	15
Figure 7 – Representative scheme for TAM treatment.....	23
Figure 8 – Representative scheme for nitrate supplementation in the drinking water	24
Figure 9 – Immunohistochemistry staining of RBCs from WT mice for eNOS and AE-1 identification ..	39
Figure 10 – Transmission electron microscopy on isolated RBCs of WT mice.....	40
Figure 11 – Genomic construct for gene deletion of eNOS.....	41
Figure 12 – Crossing strategies for the generation of eNOS KO mice	42
Figure 13 – Characterization of EC eNOS KO mice	44
Figure 14 – Characterization of RBC eNOS KO mice	45
Figure 15 – Vascular endothelial dilator function is lost in EC eNOS KO and preserved in RBC eNOS KO	48
Figure 16 – Flow-mediated dilation evaluation in EC eNOS KO and RBC eNOS KO mice.....	49
Figure 17 – Red cell eNOS and endothelial eNOS both contribute to blood pressure homeostasis.....	50
Figure 18 – RBC eNOS has an impact on SVR	52
Figure 19 – Genomic construct for gene reactivation of eNOS	54
Figure 20 – Test efficiency of the gene reactivation construct.....	54
Figure 21 – Representation of the three alleles used to test the generation of the KI model.....	55
Figure 22 – Characterization of global eNOS KI mice.....	56
Figure 23 – Generation of tissue-specific eNOS KI mice	57
Figure 24 – Characterization of EC eNOS KI mice.....	58
Figure 25 – Characterization of EC eNOS KI and RBC eNOS KI mice	59
Figure 26 – Vascular endothelial function is restored in EC eNOS KI mice after TAM treatment.....	63
Figure 27 – FMD is restored in EC eNOS KI after tamoxifen treatment	64
Figure 28 – Red cell eNOS and endothelial eNOS both contribute to blood pressure homeostasis.....	65
Figure 29 – No differences in SVR are detected after tissue-specific eNOS reintroduction	66

Figure 30 – Red cell eNOS and endothelial eNOS both contribute to plasma nitrite, but red cell eNOS is the major determinant of circulating NO-heme..... **70**

Figure 31 – Measurement of nitrate concentration in Tap water and Vittel water..... **74**

Figure 32 – The nitrate concentration in the tap water affects BP in WT and EC eNOS KO but not in RBC eNOS KO mice **76**

Figure 33 – Plasma nitrite is increased in EC eNOS KO and WT mice. No differences are detected in RBC eNOS KO mice **78**

Index of tables

Table 1 – List of chemicals with manufacturer and headquarter of the manufacturer	17
Table 2 – List of solutions	18
Table 3 – List of antibodies used for immunofluorescence and WB	19
Table 4 – List of commercial kits with manufacturer and headquarter of the manufacturer	19
Table 5 – List of equipment with manufacturer and headquarter of the manufacturer	20
Table 6 – Softwares, developer and headquarters of the manufacturer	20
Table 7 – Probes used to genotype knock-out mice, designed and used by Transnetyx.....	28
Table 8 – Probes used to genotype knock-in mice, designed and used by Transnetyx.....	29
Table 9 – Final amount of cDNA extracted from different tissues used for reverse transcription	30
Table 10 – TaqMan Genes used for expression assays.....	31
Table 11 – Antibodies concentrations used for WB and IP.....	32
Table 12 – Blood count parameters evaluated in EC eNOS KO and RBC eNOS KO mice.....	46
Table 13 – Blood pressure and heart rate in all the eNOS KO strains investigated	51
Table 14 – Systemic hemodynamics assessed in a sub-cohort of mice by measurements of echocardiography and Millar in the same individual.....	53
Table 15 – Generation of heterozygous and homozygous global eNOS KI.....	55
Table 16 – Blood count parameters evaluated in EC eNOS KI and RBC eNOS KI mice.....	61
Table 17 – Blood pressure and heart rate in all the eNOS KI strains investigated.....	65
Table 18 – Systemic hemodynamics as assessed in a sub-cohort of mice by measurements of echocardiography and Millar in the same individual	67
Table 19 – NO metabolites in blood and organs of EC eNOS KO, RBC eNOS KO, and corresponding WT littermate controls	71
Table 20 – NO metabolites in blood and organs of EC eNOS KI, RBC eNOS KI, and corresponding CondKO littermate controls	72
Table 21 – Blood pressure parameters and heart rate measured by Millar catheterization after supplementation of different NITRATE concentrations to tissue-specific eNOS KO mice.....	77
Table 22 – Plasma circulating nitrite levels and MAP of EC eNOS KO, RBC eNOS KO, and corresponding WT littermate controls before and after nitrate supplementation.....	79

Abbreviations

5'GTP	guanosine-5-triphosphate
ACh	acetylcholine
AE-1	anion exchanger 1
AMI	acute myocardial infarction
Arg1	Arginase 1
BC eNOS	Blood cell eNOS (eNOS expressed in the blood cells)
BM	bone marrow
BP	blood pressure
BSA	bovines serum albumin
CAD	coronary heart disease
cGMP	cyclic guanosine monophosphate
CLD	chemiluminescence detector
cNOS	constitutive nitric oxide synthase
CO	cardiac output
CondKO	conditional global knockout
CVDs	cardiovascular disease
DBP	diastolic blood pressure
DC	detergent compatible
deoxyHb	deoxygenated hemoglobin
EC eNOS KI	endothelial cell eNOS knock-in mice
EC eNOS KO	endothelial cell eNOS knock-out mice
ECs	endothelial cells
EDRF	endothelium-derived relaxing factor
EDTA	ethylenediaminetetraacetic acid
EDV	end diastolic volume
EF	ejection fraction
ELB	erythrocyte lysis buffer
eNOS	endothelial nitric oxide synthase
EPR	electron paramagnetic resonance
ESV	end systolic volume
FACS	fluorescence activated cell sorting
FMD	flow-mediated dilation

FS	fractional shortening
GBD	Global Burden of Disease
GC	guanylyl cyclase
gKO	global eNOS knockout
Gra	granulocytes
GSNO	S-nitrosoglutathione
GSNOR	S-nitrosoglutathione reductase
Hb	hemoglobin
HCT	hematocrit
HEPES	4-(2-hydroxyethyl)-1-piperazineethanesulfonic
HGB	hemoglobin
HR	heart rate
I/R	ischemia-reperfusion
iNOS	inducible nitric oxide synthase
KI	knock-in
KO	knock-out
L-Arg	L-arginine
L-Orn	L-ornithine
LDS	lithium dodecyl sulfate
LV	left ventricle
Lymph	lymphocytes
MAP	mean arterial pressure
MCH	mean hemoglobin concentration
MCHC	mean corpuscular hemoglobin concentration
MCV	mean corpuscular volume
MEJ	myoendothelial junction
MLCK	myosin light-chain kinase
MLCP	myosin light-chain phosphatase
Mo	monocytes
MPV	mean platelet volume
NADPH	nicotinamide adenine dinucleotide phosphate
NEM	N-Ethylmaleimide
Neo	neomycin cassette
nNOS	neuronal nitric oxide synthase

NO	nitric oxide
NO ₂	nitrogen dioxide
NO-heme	nitrosyl hemoglobin
NOS	nitric oxide synthase
PBS	phosphate buffer saline
PCR	polymerase chain reaction
PDE	phosphodiesterase
PE	phenylephrine
PKG	protein kinase G
PSLA	parasternal long axis
PLTs	platelets
qPCR	real-time polymerase chain reaction
RBC eNOS KI	red blood cell eNOS knock-in mice
RBC eNOS KO	red blood cell eNOS knock-out mice
RBCs	red blood cells
RDW	red blood cell distribution width
RT	reverse transcription
Rt	room temperature
SAX	short axis
SDS	sodium dodecyl sulfate
SBP	systolic blood pressure
SD	standard deviation
sGC	soluble guanylate cyclase
SMCs	smooth muscle cells
SNP	sodium nitroprusside
SRA	sample reducing agent
SV	stroke volume
SVR	systemic vascular resistance
TAM	tamoxifen
TBS	tris-buffered saline
T-TBS	tris-buffered saline plus tween 20
TBS	tris-buffered saline
TEM	transmission electron microscopy
WB	western blot

WBC	white blood cells
WT	wildtype

1. Introduction

1.1 Hypertension and cardiovascular disease

Hypertension is a frequent, chronic, age-related disorder characterized by increased arterial blood pressure (BP). It often is a determinant of debilitating cardiovascular and renal complications, and it is considered a significant risk factor for coronary artery disease (CAD), acute myocardial infarction (AMI), and stroke. Cardiovascular disease (CVDs) still represent one of the leading causes of death globally [1] and include pathological conditions that have severe repercussions on heart function, like stroke, heart failure, and heart rhythm abnormalities. Other CVDs affect the vasculature; few examples are peripheral artery disease, thromboembolic disease, and venous thrombosis. High BP is usually noted in combination with other cardiovascular risk factors [2].

A recent study carried by the Global Burden of Disease (GBD) examined the burden of CVDs among the US States and found that a large proportion of CVDs is attributable to (in decreasing order of contribution) diet, high systolic BP, high body mass index, high total cholesterol levels, high fasting plasma glucose level, and tobacco smoking [1]. For this reason, the symptoms developed because of a pathological condition vary according to the patient's daily habits (poor diet, alcohol consumption, smoke, lack of physical exercise) [3] or due to other previous pathologies (hypertension, diabetes mellitus, obesity).

Hypertension is estimated to account for about 13% of CVD deaths [4]. It is possible to intervene in a preventive manner by treating risk factors, such as hypertension, blood lipids, and diabetes. Primary hypertension, also defined as "essential hypertension," accounts for about 4.5% of all causes of diseases in most countries worldwide, causing about 7 million deaths every year [5]. Most patients with hypertension die from the cardiovascular consequences of this disease.

Physicians rely on Riva-Rocci's technique and the auscultation of the Korotkoff sounds in a non-invasive way using the sphygmomanometer to diagnose hypertension. However, in some cases, it is necessary to proceed with invasive measurements by arterial catheterization; in many animal experiments, this procedure involves the carotid artery catheterization; for human patients, the brachial artery is commonly used [6].

BP modulation is strictly dependent on vascular function. Blood circulates through the body in blood vessels. Blood vessels can be classified according to the amount of oxygen that is carried by the blood. Arteries transport oxygen-rich blood from the heart to smaller arterioles and capillaries or sinusoids, promoting oxygen exchange to the different organs and tissues. Poor-oxygenated blood is then taken up by

the venules that transport it to the veins and return it back to the heart. This cycle represents the “macrocirculation” (Figure 1).

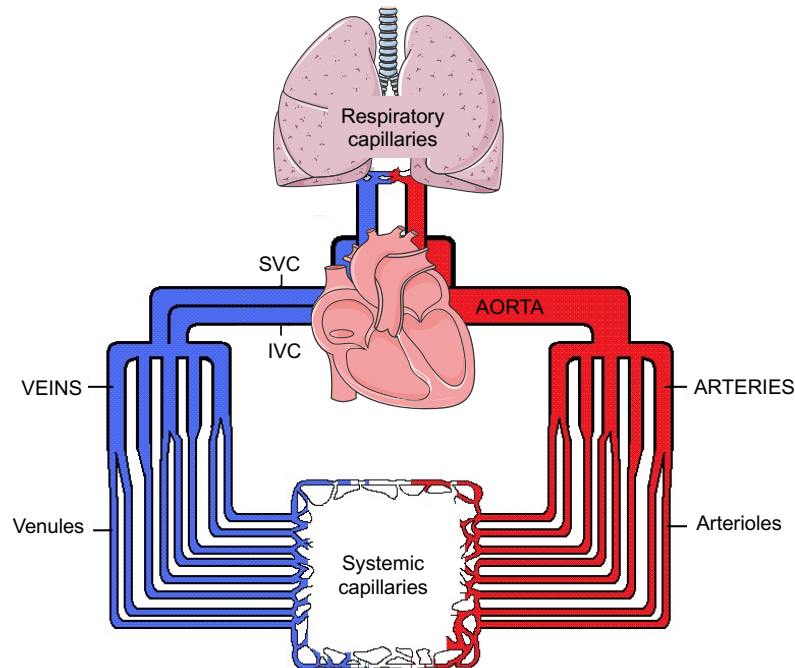


Figure 1 – Circulatory system

Abbreviations: SVC, superior vena cava; IVC, inferior vena cava.

Essential components of the human cardiovascular system are the heart, blood, and blood vessels. The systemic circulation can be seen to function in two parts: *macrocirculation*, which provides oxygenated blood to the peripheries (organs and tissues), and *microcirculation*, or pulmonary circulation, where blood is oxygenated. The cardiovascular systems of humans are closed, meaning that the blood never leaves the network of blood vessels. In contrast, oxygen and nutrients diffuse across the blood vessel layers and enter interstitial fluid, which carries oxygen and nutrients to the target cells, and carbon dioxide and wastes in the opposite direction.

A further classification of the blood vessels can be done based on their diameter and structural composition [7]. Blood vessels are organized into three different layers, known as *tunica intima*, *media*, and *externa*. Blood vessels are classified according to the composition and abundance of these three layers (Figure 2).

Arteries can be divided into elastic arteries and muscular arteries. Elastic arteries are the largest arteries near the heart (the aorta and its major branches), with diameters ranging from 2.5 - 1 cm. Their large lumen allows them to serve as low-resistance conduits and promotes blood flow between the heart and the medium-sized muscular arteries. For this reason, elastic arteries are also called conductive vessels. The major component of the wall of the conductive vessels is elastin.

Muscular arteries lie distal to the elastic arteries and supply the different organs or parts of them. They range in diameter from 1 - 0.3 cm. By actively changing the artery's lumen, the *tunica media* regulates the amount of blood flowing to an organ according to the specific needs of that organ. The smooth muscle of

the *tunica media* of muscular arteries is packed between two thick sheets of elastin. These elastic membranes help to dampen the pulsatile pressure produced by the heartbeat.

Arterioles are the smallest arteries (3 mm - 10 μ m). Arterioles show the most remarkable difference in pressure; for this reason, they are also known as resistive vessels, and their *tunica media* contains only one or two layers of smooth muscle cells (SMCs). The diameter of each arteriole is rather regulated by local factors (pH, oxygen tension) or by the sympathetic nervous system (hormones). Arteriolar resistance depends on the contraction of vascular SMCs. Structural changes in the wall-to-lumen ratio are termed vascular remodeling [8].

Capillaries are the smallest blood vessels, with a diameter of 8 - 10 μ m. In capillaries, erythrocytes pass through in a single line. Capillaries are composed of only a single layer of endothelial cells (ECs) surrounded by a basement membrane and allow the exchange of oxygen, carbon dioxide, and nutrients between blood and the fluid between cells.

Venules are the smallest veins and are 8 - 100 μ m in diameter. The smallest venules are called postcapillary venules, and they function very much like capillaries. Larger venules have a *tunica media* that consists of one or two layers of SMCs and a thin *tunica externa*.

Veins are also elastic vessels that transport blood from the peripheral tissues to the heart. Veins differ from arteries structurally because of their larger lumen with a diameter varying from 2 - 9 mm (small to medium-size veins) until more than 2.5 cm (large veins). Their *tunica externa* is thicker than the *tunica media*, and inside the lumen, there are special valves necessary for the proper return of the blood to the heart. The largest vein of the body is the *vena cava*, which returns systemic blood to the heart. Veins have less elastin in their walls than arteries because veins do not need to dampen any pulsations that are smoothed out by arteries before the blood reaches the veins. As a result, the wall of a vein is thinner than that of a comparable artery (Figure 2).

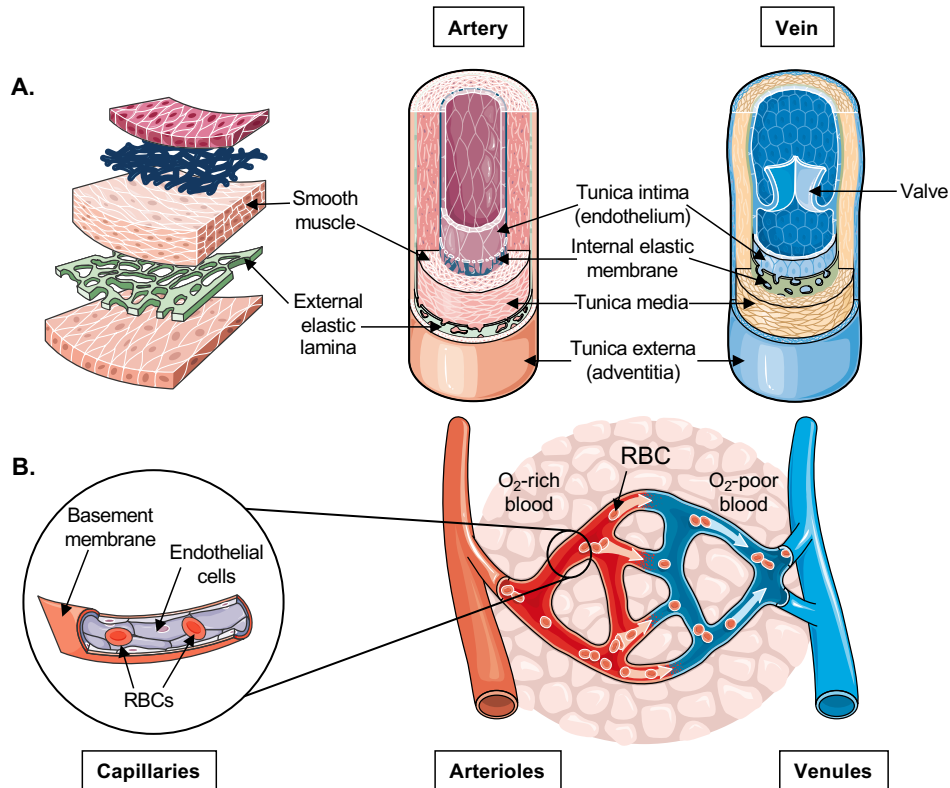


Figure 2 – Structural characterization of blood vessels

(A) This diagram indicates the composition of *tunica intima*, *media*, and *externa* of arteries and veins. Arteries are richer in elastin, the major component of the elastic lamina. Veins have a larger diameter and contain valves inside the lumen to guarantee a proper venous return to the heart. (B) Arterioles and venules are the medium size vessels directly connected to arteries and veins. From arterioles, the blood moves to capillaries, venules, veins, and back to the heart. Capillaries are composed only of a single layer of endothelial cells, with a basement membrane keeping them together. Capillaries are the smallest vessels and are responsible for gas exchanges within the different organs and tissues.

The functional differences of the pathway in red blood cells (RBCs) or the vasculature may become prominent under specific pathophysiological conditions such as endothelial dysfunction or blood disorders. Endothelial dysfunction is observed in the early stage of CVDs [9]; for example, endothelial dysfunction has been identified in normotensive young adults with a family history of hypertension [9].

In addition, essential hypertension is often accompanied by an increase in systemic vascular resistance (SVR); in this context, the diameter of the resistive vessels is one of the main determinants of systemic BP. Therefore, it is crucial to understand the pivotal role of the endothelium as it has a high prognostic value in the early detection of diseases and classification of cardiovascular risk factors.

1.2 Regulation of vascular tone and blood pressure

BP homeostasis is primarily regulated at distal conduit arteries, proximal and distal resistance arteries, and pre-capillary sphincter arteries. BP declines substantially while blood passes through the high-resistance arterioles and capillary beds; thus, BP in the veins is much lower than in the arteries.

The inner wall of the vasculature is composed of a layer of endothelial cells that regulate multiple vascular functions, such as vascular tone, circulation of blood cells, inflammation, and platelet activity [10], by releasing numerous dilatory and constrictor substances [11].

One of the main substances with vasodilatory function released by the endothelium is nitric oxide (NO), a short-live signaling molecule identified initially as “endothelium-derived relaxing factor” (EDRF) for its ability to induce relaxation of pre-constricted aortic vascular preparations [12-14]. NO is relatively stable compared to other endogenously produced free radicals like superoxide anion radical ($O_2^{\bullet-}$) and hydroxyl radical (OH^{\bullet}). Its half-life and reactivity in cells and tissues depend on the localization of NO enzymatic/non-enzymatic source, the local availability of substrates, the flux/rate of production, and the presence of molecules efficiently reacting with NO [15]. NO plays a crucial role in regulating vascular tone and blood flow [16] and is a central signaling entity in the cardiovascular system [12]. Moreover, it is a critical player in neurotransmission [17], cellular proliferation, host defense, leukocyte adhesion, platelet aggregation, and inflammatory processes [18].

NO is highly reactive, and it is able to diffuse from ECs into the adjacent SMCs, where it mediates vasodilator effects in a complex intracellular signaling pathway [19].

NO is biosynthesized endogenously by the nitric oxide synthase (NOS) that catalyzes the conversion of L-arginine (L-Arg) to equimolar amounts of NO and L-citrulline in the presence of oxygen and the cofactors calcium, calmodulin, tetrahydrobiopterin (BH_4), and nicotinamide adenine dinucleotide phosphate (NADPH), in its reduced form [20].

In mammals, there are three different isoforms for the gene encoding NOS: NOS1 is coding for the neuronal nitric oxide synthase (nNOS), which is expressed in specific neurons of the brain; NOS2 for the inducible nitric oxide synthase (iNOS), which is expressed in macrophages and under pro-inflammatory conditions in a wide range of cells and tissues; and NOS3 for endothelial nitric oxide synthase (eNOS).

eNOS and nNOS are also known as constitutive NOS (cNOS) and are activated after stimulation of specific receptors by various agonists and mechanical forces, like shear stress [21].

The NOS isoform that is constitutively expressed in the vascular endothelial cells of the blood vessels is eNOS and is responsible for NO production and modulation of the vascular tone [12]. NO produced by eNOS in ECs is considered the central regulator of vascular tone and systemic hemodynamics [22].

As already mentioned, the *tunica intima* of the blood vessels is formed by a single layer of vascular endothelial cells that communicate on one side (luminal or apical side) with the vessel lumen and on the other side with the *tunica media* via the internal elastic lamina (abluminal or basal side). In the vessel wall, eNOS is found both at the apical and basal side of the ECs. The NO produced by eNOS is mainly released abluminally from ECs to the SMCs, and only a minor amount is released into the bloodstream.

In addition, in resistance arteries (arterioles, pre-, and postcapillaries), NO goes through myoendothelial junctions (MEJs), and it is transferred from ECs to SMCs depending on the redox state of hemoglobin alpha [23, 24] (Figure 3).

The importance of vascular eNOS for the cardiovascular system and the regulation of vascular tone and systemic hemodynamics became clear when global eNOS KO (eNOS^{-/-}) mice were analyzed. Different eNOS^{-/-} lines were generated and used, evidencing a strong impact of eNOS in modulating coronary hemodynamics and systemic BP; all strains of eNOS^{-/-} mice showed a hypertensive phenotype [25-27].

In the SMCs, the target of NO is the guanylyl cyclase (GC). NO binds reversibly to the Fe²⁺ of the heme group of the GC (heme-nitrosylation), inducing a conformational change and activating the enzyme [28].

This leads to an increase of intracellular cyclic guanosine-3-5-monophosphate (cGMP), produced from guanosine-5-triphosphate (5'GTP) [29, 30]. In the vessel wall, GC mediates smooth muscle relaxation.

cGMP binds to protein kinase G (PKG) in the SMCs and inhibits intracellular calcium (Ca²⁺) entry, causing inactivation of myosin light-chain kinase (MLCK), accompanied by dephosphorylation of myosin light chain by the myosin light-chain phosphatase (MLCP) [31, 32]. This process leads to smooth muscle relaxation and vasodilatation (Figure 3). The signal is shut down by phosphodiesterase (PDE) intervention that promotes the reconversion of cGMP into its precursor 5'GTP.

GC exists as a heterodimer, and there are two isoforms known, α 1-GC and α 2-GC. The distribution and biological function of the two isoforms of GC was investigated by Mergia and colleagues, using mice deficient in either α 1- or α 2-GC [33]. In platelets, α 1-GC is the only isoform present, responsible for NO-induced inhibition of aggregation. Comparable levels of α 1-GC and α 2-GC were identified in the brain. In aortic tissue, α 1-GC was recognized as the major isoform (94%), mediating vasodilation.

An essential regulator of NO production is arginase 1 (Arg1), an enzyme that competes with eNOS for the same substrate L-Arg, catalyzing the hydrolysis of L-Arg to ornithine (L-Orn) and urea [34, 35]. It exists in two different isoforms (types I and II), which differ in tissue distribution, subcellular localization, and physiological function. Intervention on Arg1 activity may modulate the pool of L-Arg available for NO production by limiting it, for example, during hypoxia or in the presence of reactive oxygen species [34]. On the other hand, inhibition of Arg1 activity may increase endothelium-derived NO formation and improve endothelium-dependent vasodilatation, for example, in CAD conditions [35-37].

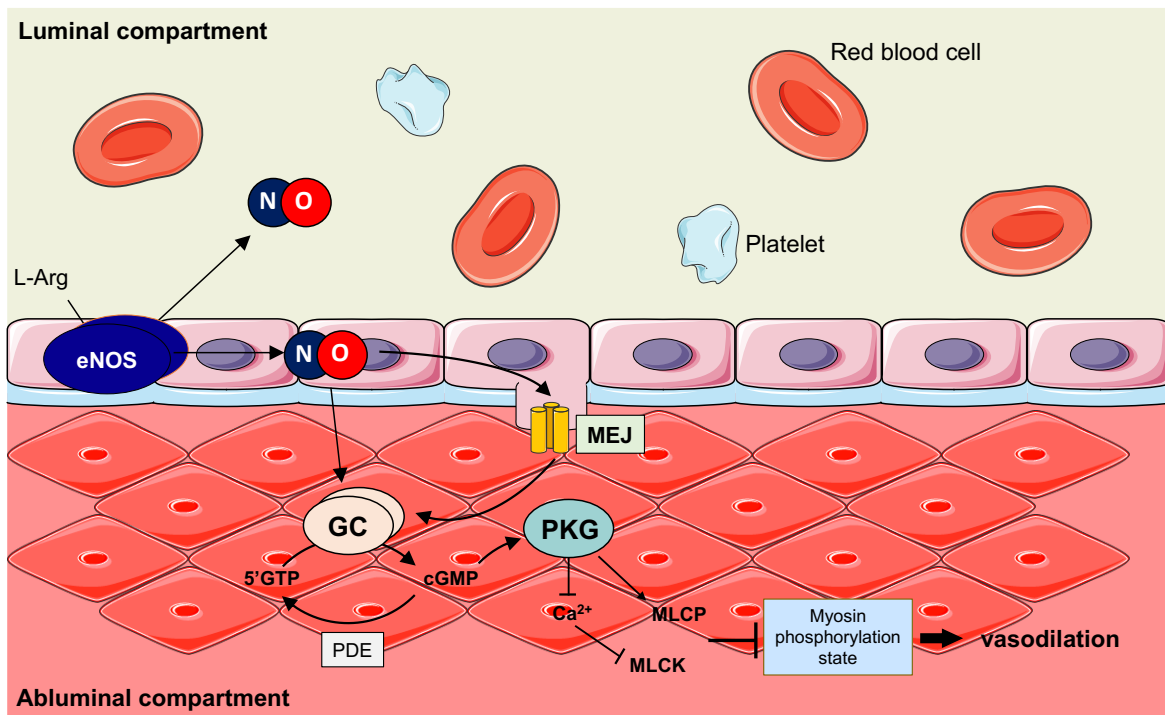


Figure 3 – NO pathway to vasodilation in smooth muscle cells

After its formation from L-Arg, the NO produced by eNOS is primarily released abluminally from ECs to the extracellular space and to the adjacent SMCs, where it binds to the GC and activates the production of cGMP from 5'GTP. cGMP binds to PKG and activates MLCP, inhibiting intracellular Ca²⁺ entry and leading to a decreased activity of a MCLK. Myosin phosphorylation state gets reduced, leading to smooth muscle relaxation and vasodilatation and thus regulating blood pressure. A minor amount of NO is released into the bloodstream. In resistance arteries (arterioles, pre- and postcapillaries), NO goes through myoendothelial junctions (MEJs) and is transferred from ECs to SMCs.

1.3 Systemic NO metabolism and the nitrate/nitrite/NO pathway

Other regulatory components of BP are the nature, distribution, and kinetics of the several NO-metabolites found in plasma, RBCs, and vascular tissues [38-40]. Under normal physiological conditions, the primary enzymatic source of NO in the body is thought to be eNOS [41, 42], with lesser contributions of the nNOS and the iNOS (in monocytes/macrophages). It was suggested that eNOS-derived NO might exert endocrine effects, which are thought to be mediated mainly by nitrite and other semi-stable circulating metabolites. These include nitrate, nitroso compounds, and possibly nitro fatty acids [38-40] formed in blood and tissues by several reactions.

There are two primary sources of nitrite and nitrate: endogenous, which involves the direct synthesis of NO by eNOS from L-Arg and its further oxidation into nitrite and nitrate; and an exogenous source, through the diet.

Inorganic nitrite and nitrate introduced with the diet were considered toxic substances for the body, leading to the development of gastric cancer [43, 44]. However, in the last decades, numerous studies have focused on the beneficial possibilities that the intake of these substances can promote.

Administration of inorganic nitrite or nitrate increases NO-like bioactivity, promoting vasodilation, blood flow increase, and arterial pressure lowering through the generation of cGMP. Nitrite shows significant bioactivity under low oxygen tension conditions and acidic conditions, leading to the conversion of nitrite into NO and promoting a series of cGMP-dependent down signaling events [39, 45].

Under low oxygen tension conditions, nitrite was recognized as a possible source of NO through a nitrite reductase activity operated by deoxyhemoglobin (deoxyHb). The challenges to the nitrite reductase hypothesis are many; the first is how NO could escape from red blood cells after its formation, considering the rich hemoglobin content in the cytoplasm. Moreover, the dissociation of NO from deoxyHb is regulated by a slow dissociation rate constant [46, 47].

Under normal physiological conditions, nitrite is an effective nitrosating and nitrosylating entity regardless of its route of administration [48]. Once the exogenous nitrate is introduced into the organism, it enters the entero-salivary circulation directly, where a fundamental role is played by commensal bacteria [49, 50]. Both nitrite and nitrate from the diet can be a source of NO [51], especially in pathological conditions where a NO deficiency is recognized [52]. The introduction of nitrate generally induces an increase in its circulating plasma levels. Subsequently, up to 25% of the nitrate present in the circulation (representing the nitrate derived from the diet and the NOS-derived form) is recovered by the salivary glands and concentrated in the saliva [53-55]. Commensal bacteria catalyze the conversion to nitrite in the oral cavity [56]. Once reached the acidic gastrointestinal tract (pH 1-1.5), nitrite is protonated to HNO_2 and further

decomposed into NO and other species [57, 58] (Figure 4). In addition to the gastrointestinal path described, nitrate can follow other metabolic pathways, such as on the skin [59] or in the urine [60].

Vasodilatory functions and the essential physiological role of nitrate in modulating BP have been controversial [61]. However, its active role as a bioactive molecule has been recognized in promoting a lowering of BP [48, 56].

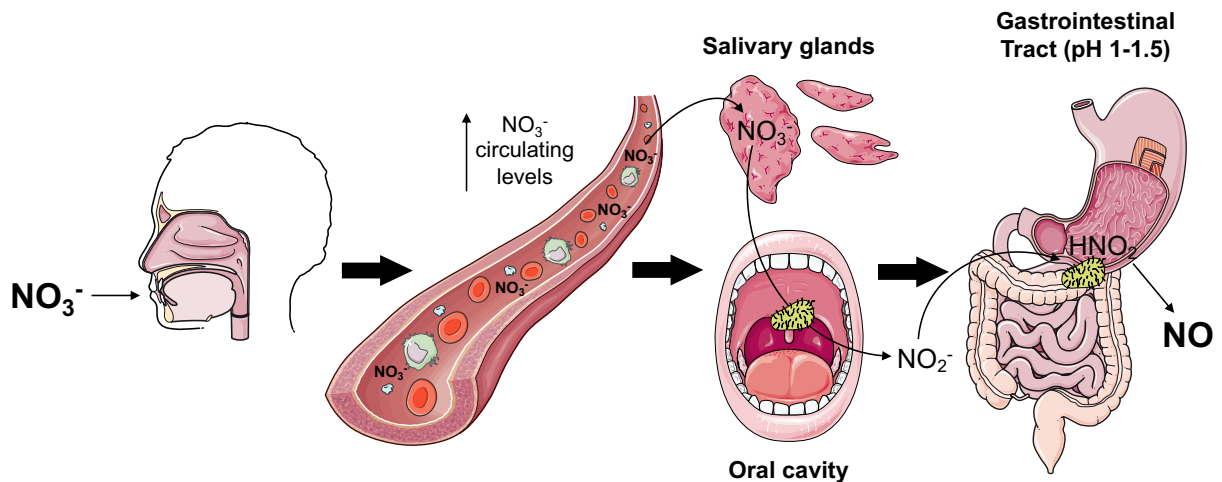


Figure 4 – Oral administration of nitrate and NO formation

After external nitrate administration, circulating nitrite/nitrate levels increase. Nitrate is uptaken by the salivary glands in the oral cavity. Commensal bacteria catalyze the conversion to nitrite. The acidic pH (1-1.5) of the stomach leads to the protonation of nitrite to form HNO_2 and in the gut NO , through a direct action of commensal bacteria.

1.4 Role of RBCs in the regulation of vascular tone

RBCs are highly specialized cells that descend from hematopoietic stem cells in the bone marrow (BM). Their precursor cells are called erythroblasts, and before being released into the bloodstream, they lose their nuclei, mitochondria, and endoplasmic reticulum, losing the ability to synthesize proteins. Maturation of RBC progenitor cells lasts approximately one week before becoming fully functional RBCs. RBC half-life is of approximately 120 days in humans [62].

RBCs represent the most abundant cell type of the whole blood and are responsible for the exchange and transport of gas and nutrients to the various tissues of the organism. RBCs' biochemical, biophysical, and mechanical properties and their structural characteristics are optimized for their function.

RBC ability to transport oxygen is due to the presence in their cytosol of 10 mM concentration of a metalloprotein called "hemoglobin" (Hb), a tetramer composed of two α and two β subunits containing respectively a prosthetic heme group with a central iron ion in its reduced form (Fe^{2+}) [63]. This complex can reversibly bind oxygen in the lungs and allows it to be transported in circulation and released in tissues. RBCs are characterized by a biconcave "donut" shape that provides them with an extensive surface for gas exchange and contributes to the deformability of RBCs. The term deformability refers to the ability of RBCs to modify their structure to squeeze through blood vessels smaller than their diameter (8 μm) [64]. Cellular deformability is of high importance and affects oxygen delivery to the tissues [65].

An essential regulator for RBC deformability is blood viscosity. Blood viscosity is strictly connected with systemic hemostasis and depends on the concentration of RBCs and the intracellular Hb content; higher Hb levels increase intracellular viscosity and modify RBC deformability [66].

Changes in the RBC rheological properties within the microcirculation may profoundly affect tissue perfusion.

In addition to their role as gas transporters and exchangers, RBCs have been recognized to possess more non-canonical functions, and an active role of RBCs was proposed in the modulation of vascular tone [67]. Because of the high Hb levels contained within RBCs, they were considered for a long time simply NO scavengers, inactivating endothelium-derived NO via rapid reaction with Hb to form methemoglobin and nitrate, thereby limiting NO available for vasodilatation [28, 52, 54, 68, 69]. In particular, the reaction of NO with Hb leads to the formation of a nitrosylated Hb (NO-heme) with a high-speed reaction rate of $10^7 \text{ M}^{-1}\text{s}^{-1}$ [70], whereas the dissociation to Hb and NO is extremely slow [46].

However, in the last decades, RBCs have been proposed to actively control the vascular tone by transporting and releasing vasoactive molecules in response to hypoxia and shear forces. Mechanisms of release and potential sources of NO in RBCs are still a matter of debate, but candidates include iron-nitrosyl-hemoglobin [71], S-nitrosohemoglobin [72-74], and nitrite [75, 76].

Similar to ECs, RBCs express a functional eNOS producing NO [77-80], but as mentioned, the high amount of Hb makes it controversial whether a significant amount of NO is formed and exported as a result of eNOS activity [81, 82]. One possibility is that although one single RBC produces 9.8 fmol/min of NO, the abundance of erythrocytes in the bloodstream might be significant for a physiologically relevant role of RBCs on blood pressure regulation [77].

Moreover, a hypothesis particularly investigated to explain a possible escape of NO from RBCs suggests the formation of intermediate species that can later promote the release of NO; among these, N₂O₃ or possible isomers can be found [83-85].

Particular interest as a possible transmembrane channel for NO species, and in particular nitrite has aroused in the anion exchanger-1 (AE-1), a membrane protein that accounts for 25% of the RBC membrane and has attracted much attention in the last decade. The first evidence on the ability of AE-1 to transport nitrite was observed in 1997 [86]. Furthermore, a study dating back to 2009 has shown that AE-1 appears to be involved in the export of nitrite from RBCs [75], and this hypothesis has been more recently strengthened by other working groups [87, 88].

In addition, RBCs are thought to contribute to the regulation of systemic NO bioavailability by releasing ATP when subjected to hypoxia or shear stress, which seems to be dependent on the activation of erythrocytic pannexin-1 channels [89-91], inducing eNOS-dependent vasorelaxation and an increase in blood flow [91-95].

To investigate the functional significance and specific role of red cell eNOS in a direct comparison of endothelial eNOS, tissue-specific eNOS lines are necessary.

The hypertensive phenotype previously observed in the eNOS^{-/-} lines was attributed to the absence of eNOS in the ECs [25-27]. However, the discovery of the existence of a functional eNOS in the blood cells (BCs) made necessary a reevaluation of these findings and further investigations to evaluate a possible role of red cells eNOS in the modulation of blood pressure and thus investigate the possibility that the hypertensive phenotype was due to eNOS expressed in the blood rather than the one expressed in the endothelium [77, 78, 96-101].

In 2013 chimera mice were generated supporting a role for an eNOS expressed in the blood cells (BC eNOS) in the regulation of BP and nitrite homeostasis [67]. Chimera animals resulted from a BM cross-transplantation strategy between WT and eNOS^{-/-} mice to elucidate the contribution of circulating BC eNOS to intravascular nitrite formation and physiological BP regulation *in vivo*. Chimera mice showed a significant increase in BP after localized eNOS removal from the blood compartment. Platelets or leukocyte depletion from the whole blood did not impact the high BP of the mice, suggesting RBCs as responsible cell type for the hypertensive phenotype. High BP was correlated with decreased circulating nitrite levels, supporting the previous findings on eNOS^{-/-} mice [25-27].

Although these studies provided strong evidence for BC eNOS in control of BP and nitrite production, the use of BM from chimera mice presented severe methodological limitations, such as lack of specificity for erythroid cells and the irradiation-dependent activation of inflammatory pathways, that might cause up-regulation of iNOS [102], contributing to the general pool of NO metabolites.

However, conditional transgenic models allowing examination of the specific role of endothelial eNOS, compared to eNOS expressed in RBCs in systemic hemodynamics control, are still lacking.

An approach avoiding the disadvantages encountered by previous studies [67] will enable the identification of the mechanisms responsible for blood pressure changes and will allow indicating EC eNOS or RBC eNOS as primarily responsible for BP modulation.

1.5 Red blood cells as regulators of the systemic NO metabolism

As already mentioned, RBCs for a long period were considered scavengers of NO due to the reaction of the central Fe²⁺ in the heme group of Hb with NO, leading to the formation of nitrate and methemoglobin. Therefore, it was controversial whether significant amounts of NO were formed and exported from the RBCs due to eNOS activity.

Different mechanisms have been proposed to mediate NO signaling across the RBC membrane despite the high Hb levels. One proposed mechanism occurring under normoxic conditions is based on the compartmentalization of NO synthesis in RBCs. One theory focuses on the synthesis of NO directly in the proximity of the RBC membrane and the immediate diffusion of the hydrophobic NO through the membrane to escape the fast scavenging reaction with Hb [103].

Another possible mechanism to avoid Hb inhibition of NO signaling could be the mediation by NO metabolites.

Under hypoxic conditions, RBCs have been shown to induce vasodilation, and these findings were attributed to different NO metabolites [71, 73, 104-106] and bioactivation mechanisms [105, 107, 108]. One of the proposed mechanisms involved the nitrosylation of the heme group of Hb followed by NO transfer to cysteine-93 of the Hb β -chain [73]. According to this proposed mechanism, NO release was regulated by conformational changes of Hb tetramer structure. However, multiple further findings have questioned the proposed mechanism [82, 109-111].

The more accepted mechanism is the NO-dependent vasorelaxation, derived by a nitrite reductase activity of deoxyHb that produces NO from nitrite [48, 77, 78, 104, 105]. In support of this finding, RBCs store high concentrations of nitrite [76]. Moreover, a gradient of nitrite from arterial to venous plasma supports

the theory according to which nitrite is used for hypoxic vasodilation [112]. DeoxyHb was shown to be essential for the reduction of nitrite to NO under hypoxic conditions [113].

Despite the discovery of an active eNOS inside the RBCs, its physiological role and involvement in RBC physiology, NO metabolism, BP modulation, and vascular tone remains controversial [28, 69, 114-117].

Human RBCs also express the enzyme Arg1 [118]. Endothelial cell Arg1 has emerged as an important regulator of NO production by competing with eNOS for their common substrate L-Arg [34, 35]. The role of Arg1 in RBCs is unknown; it has been hypothesized a role of Arg1 in the regulation of eNOS and export of NO bioactivity [119]. However, further investigations are still needed.

Recently an active GC was also identified in RBCs, indicated as “soluble” guanylyl cyclase (sGC) [120]. The localization of sGC in direct vicinity to eNOS could mediate NO downstream signaling, supporting the theory of compartmentalization of NO synthesis in RBCs [120].

To summarize, a complete pathway involving Arg1-eNOS-sGC has been identified within RBCs [118-120]. However, the role of eNOS in RBCs and how the NO produced is released into the circulation, avoiding Hb scavenging, is still unknown (Figure 5).

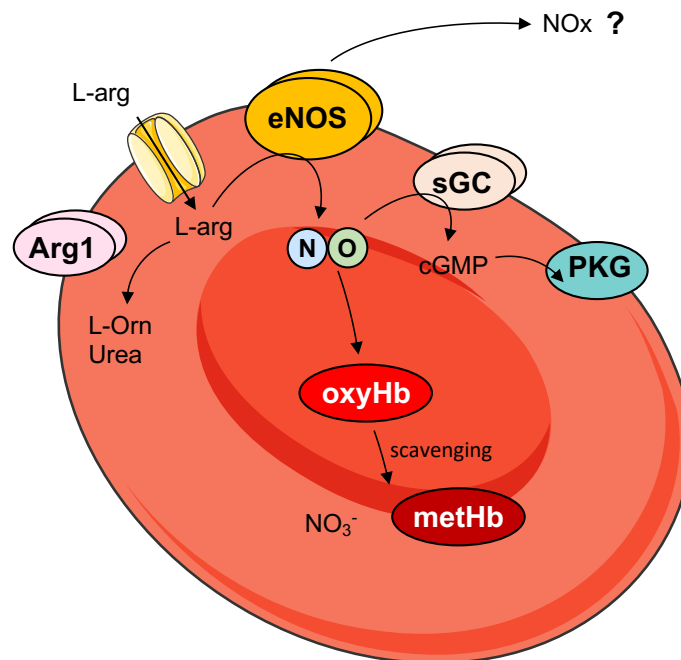


Figure 5 – Arg1-eNOS-sGC pathway in RBCs

A complete pathway involving Arg1, eNOS, and sGC has been identified in RBCs. It remains unclear how the NO produced is released into the circulation, avoiding the scavenging of the hemoglobin.

1.6 The use of a loxP-Cre method for tissue-specific gene targeting

The first steps for the generation of tissue-specific gene alterations emerged with introducing the transgenic Cre expression model [121, 122].

The advent of the bacteriophage P1 Cre-LoxP site-specific recombination system allowed the gene-targeting approach to study gene function in mice. Using this technology, tissue-specific gene knock-out (KO) or knock-in (KI) models can be produced [123, 124].

Cre recombinase catalyzes site-specific DNA recombination between 34 bp recognition (loxP) sites. If two loxP sites are introduced in the same orientation into a genomic locus, the presence of Cre results in the deletion of the DNA sequence flanked by the loxP sites. Cre-mediated gene manipulation requires transient transfection of the mutant loxP-containing endothelial stem (ES) cells with a vector encoding Cre recombinase. An additional round of selection is necessary to verify if ES cell clones carry the desired deletion. This additional manipulation of the cells in culture might affect the ability of ES cells to generate germ cells in chimeric mice, which is a severe problem in gene targeting technology.

The Cre-loxP recombination system has also been used to manipulate genes in a cell type-specific [125, 126] or inducible [127] manner.

When two loxP sites are introduced into the genome, flanking an essential part of a target gene without affecting its function, Cre-mediated deletion of the loxP-flanked fragment will lead to the inactivation of the gene. It is also possible to restrict gene inactivation *in vivo* to a particular cell type by crossing mice with a loxP-flanked target gene with transgenic mouse strains expressing Cre recombinase under the control of a cell type-specific or inducible promoter.

In 2004, a first gene inactivation model restricted to erythroid tissues was generated [121]. Transgenic mouse lines expressing Cre recombinase only in erythroid cell lineages were generated by placing Cre transcription under the control of the human β -globin gene promoter and β -globin locus control region to restrict Cre expression to erythroid cell lineages.

Generation of tissue-specific mouse models will be essential to investigate the specific role of eNOS in the endothelium or the RBCs.

2. Aim of the study

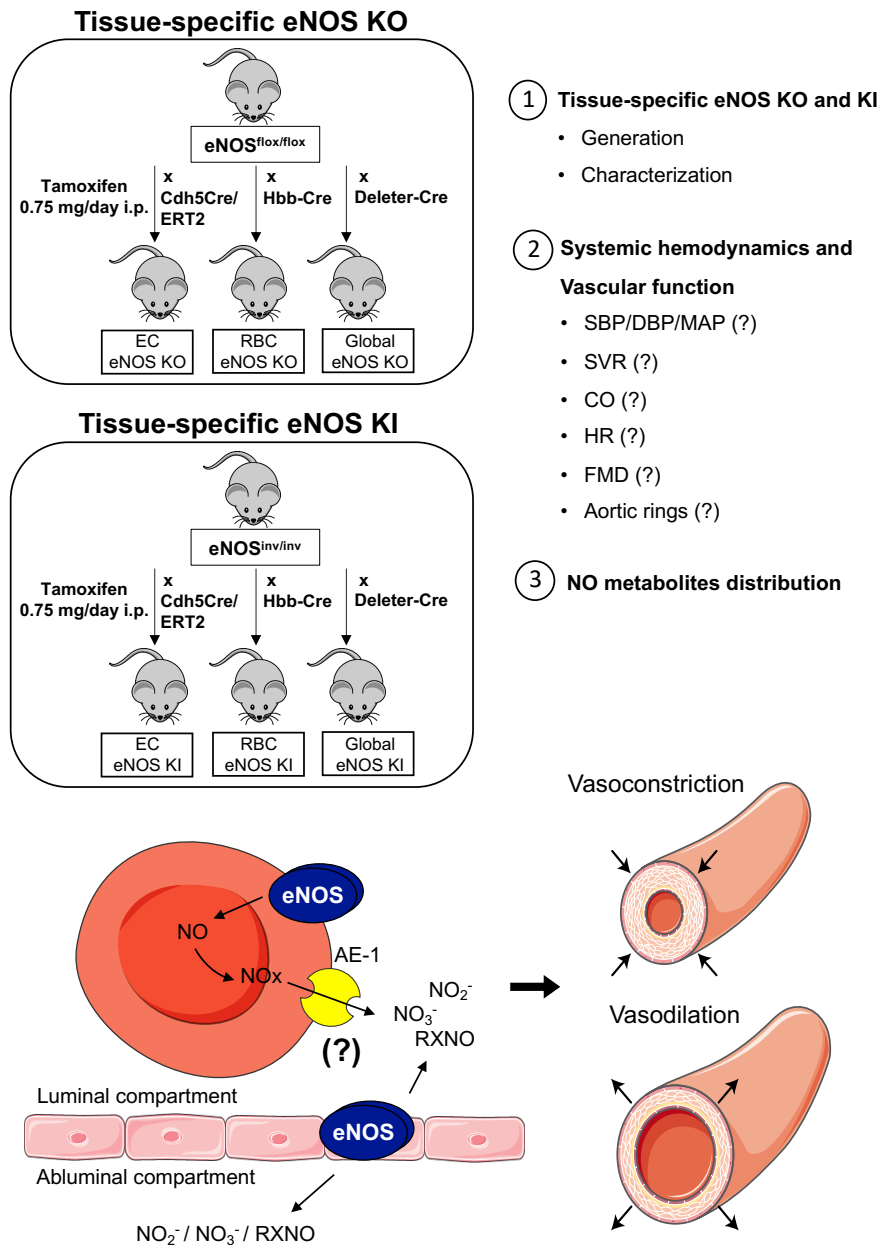


Figure 6 – Graphical abstract

The hypothesis of this study was that red cell eNOS contributes to the regulation of NO metabolites, vascular tone, and BP. This study aimed to elucidate the functional significance and specific role of red cell eNOS directly compared to endothelial eNOS in controlling vascular hemodynamics and systemic NO metabolism. To accomplish this, we generated tissue-specific “loss” and “gain-of-function” models for eNOS by using tissue-specific Cre-induced gene inactivation or reactivation. The goals of this study are the following: (1) The creation and characterization of tissue-specific eNOS KO and KI mice by using tissue-specific Cre-induced gene inactivation or reactivation; (2) the analysis of systemic hemodynamics of the strains of interest; (3) the evaluation of NO metabolites distribution before and after administration of nitrate.

Endothelial cells (ECs) express an active eNOS that regulates NO metabolites and vascular tone.

Next to their classical role of gas transporters, numerous studies suggested that red blood cells (RBCs) possess more non-canonical functions in the cardiovascular system. RBCs express an active eNOS, but the role of eNOS expressed in RBCs in the regulation of vascular tone is unknown.

This study hypothesized that red cell eNOS contributes to the regulation of NO metabolites, vascular tone, and BP.

Therefore, the aim was to elucidate the functional significance and specific role of red cell eNOS directly compared to endothelial eNOS in controlling vascular hemodynamics and systemic NO metabolism. To accomplish this, we generated tissue-specific “loss” and “gain-of-function” models for eNOS by using tissue-specific Cre-induced gene inactivation or reactivation.

This work is focused on three main goals:

- 1- The creation and characterization of tissue-specific eNOS KO and KI mice.

To verify the successful generation of tissue-specific eNOS KO and tissue-specific eNOS KI mice, the proper removal/reintroduction of eNOS in RBCs (BM) or ECs (aorta) will be evaluated, both via quantitative polymerase chain reaction (qPCR) and western blot (WB) analysis. Moreover, PCR on isolated cells and tissues will be carried out.

- 2- The analysis of systemic hemodynamics of the strains of interest.

Next to *in vivo* hemodynamic measurements, the vascular endothelial function will also be assessed *ex vivo* to exclude the effects of the loxP-Cre system on vessel functionality. Cardiovascular parameters will also be investigated by high-resolution ultrasound.

- 3- The evaluation of NO metabolites distribution before and after administration of nitrate.

Analytical chemiluminescent detection (CLD) technique will be applied for the determination of plasma nitrite levels.

3. Materials and methods

3.1 Chemicals

Table 1 – List of chemicals with manufacturer and headquarter of the manufacturer

Chemical	Manufacturer	Headquarter
Methanol	VWR	Radnor, USA
β ME-Ethanol	Merck	Darmstadt, Germany
PBS (without Ca/Mg)	Sigma-Aldrich	St. Louis, USA
Nonidet p40 Substrate	Fluka	Buchs, Switzerland
S-Deoxycholate	Fluka	Buchs, Switzerland
10% SDS ultra-pure	Thermo Fisher Scientific	Waltham, USA
Isoflurane	Piramal Critical Care	USA
IBMX	Sigma-Aldrich	St. Louis, USA
NaCl	Thermo Fisher Scientific	Waltham, USA
KCl	Thermo Fisher Scientific	Waltham, USA
KH_2PO_4	Sigma-Aldrich	St. Louis, USA
Na_2HPO_4	Thermo Fisher Scientific	Waltham, USA
Triton X-100	Sigma-Aldrich	St. Louis, USA
MgSO_4	Sigma-Aldrich	St. Louis, USA
CaCl_2	Sigma-Aldrich	St. Louis, USA
NaHCO_3	Sigma-Aldrich	St. Louis, USA
BSA	Sigma-Aldrich	St. Louis, USA
Fish skin gelatin	Sigma-Aldrich	St. Louis, USA
D-Glucose	Sigma-Aldrich	St. Louis, USA
Tamoxifen	Sigma-Aldrich	St. Louis, USA
Peanut oil	Sigma-Aldrich	St. Louis, USA
NEM	Sigma-Aldrich	St. Louis, USA
EDTA	Sigma-Aldrich	St. Louis, USA
DNase I	Sigma-Aldrich	St. Louis, USA
Collagenase I	Worthington Biochemical Corporation	Troisdorf, Germany
SDS	Sigma-Aldrich	St. Louis, USA
LDS	Thermo Fisher Scientific	Waltham, USA
10X Bolt™ Sample Reducing Agent	Thermo Fisher Scientific	Waltham, USA
Tween20	Sigma-Aldrich	St. Louis, USA
Glycine	Sigma-Aldrich	St. Louis, USA
Skim milk powder	Sigma-Aldrich	St. Louis, USA
2,2-dichloro-1,1-difluoroethyl methyl ether 97%	Alfa Aesar	Haverhill, USA
Sulfanilamide	Sigma-Aldrich	St. Louis, USA
Potassium ferricyanide	Sigma-Aldrich	St. Louis, USA

Iodine	Sigma-Aldrich	St. Louis, USA
Sodium nitrite	Sigma-Aldrich	St. Louis, USA
Potassium hexacyanoferrate (III)	Sigma-Aldrich	St. Louis, USA
CD31 Microbeads, mouse	Milteny Biotec	Milteny Biotec, Bergisch Gladbach, Germany
CD45 Microbeads, mouse	Milteny Biotec	Milteny Biotec, Bergisch Gladbach, Germany
FcR Blocking Reagent, mouse	Milteny Biotec	Milteny Biotec, Bergisch Gladbach, Germany

3.1.1 Solutions

Table 2 – List of solutions

Solution	Preparation
Phosphate Buffer Saline (PBS)	CaCl ₂ ·2H ₂ O 0.9 mM, MgCl ₂ ·6H ₂ O 0.5 mM, KCl 2.7 mM, KH ₂ PO ₄ 1.5 mM, NaCl 136.9 mM, Na ₂ HPO ₄ 8.1 mM
Hanks' Balanced Salt Solution (HBSS)	NaCl 0.14 M, KCl 5 mM, CaCl ₂ 1 mM, MgSO ₄ ·7H ₂ O 0.4 mM, MgCl ₂ ·6H ₂ O 0.5 mM, Na ₂ HPO ₄ ·2H ₂ O 0.3 mM, KH ₂ PO ₄ 0.4 mM, D-Glucose 6 mM, NaHCO ₃ 4 mM
RBC permeabilization buffer	PBS with NP40 0.2%
Blocking buffer for immunofluorescence	PBS with fish skin gelatin 10%, Triton X-100 0.25%), BSA 0.5% and goat serum 10%
Krebs-Henseleit buffer	CaCl ₂ 1.6 mM, MgSO ₄ 1.2 mM, KCl 5 mM, KH ₂ PO ₄ 1.2 mM, NaCl 118 mM, NaHCO ₃ 24.2 mM, glucose 10 mM
Tamoxifen solution	Dilute in EtOH to a final concentration of 60 mg/ml. dissolve at 60°C and dilute in peanut oil 1:6.
HEPES buffer	NaCl 98.9 mM, KCl 4.7 mM, CaCl ₂ ·2H ₂ O 1.9 mM, MgSO ₄ ·7H ₂ O 1.2 mM, NaHCO ₃ 25 mM, KH ₂ PO ₄ 1 mM, Na-Hepes 20 mM, D-Glucose 11.1 mM
TBS 20x	Tris Base 200 mM, NaCl 2M, ddH ₂ O
Transfer buffer Bio-Rad system 10x	Tris Base 250 mM, Glycine 1.92M, MilliQ Water
Stripping buffer	10% SDS, Tris 1.5M, β ME-Ethanol, MilliQ Water
Tris-glycine-buffer Bio-Rad system	Tris Base 250 mM, glycine 1.92M, SDS 35 mM, MilliQ Water
T-TBS 1x	TBS 20x, MilliQ Water, tween20 0.1%
Blocking buffer for WB	Skim milk powder 5%, T-TBS 1x
LDS buffer (1X)	400 µl LDS 4X; 1200 µl H ₂ O
Digesting solution for ECs isolation	25 mL HBSS, Collagenase (450 U/mL)/ DNase I (60 U/mL)
Phosphate Buffer Saline/NEM/EDTA	0.5 mL EDTA 500 mM, 10mL NEM 100 mM, PBS to 100 mL
Potassium Ferricyanide	1.646 g in 100 mL PBS
KI/I ₂	0.404744 g of KI, 0.142979 g of I ₂ , 3.75 mL of water MilliQ and 50 mL of AcOH;
Sulfanilamide	0.5 g in 10 mL, 1 M HCl
Oxidative solution for NO-heme detection	K ₃ Fe[(CN) ₆] 1.6465 g dissolved in 10 mL of PBS
Separation buffer for cells isolation	0.5% (v/w) BSA, 2mM EDTA in PBS
Erythrocyte lysis buffer	Ammoniochloride 0.8% + 10 mM EDTA + DNase 10 U/mL
Separation buffer (PEB)	BSA 0.5%, 2mM EDTA in PBS 1x (pH 7.4)

3.1.2 Antibodies

Table 3 – List of antibodies used for immunofluorescence and WB

Antibody	Code	Manufacturer
Mouse anti-eNOS	MA5-15559	Thermo Fisher Scientific, St. Louis, USA
Rabbit anti-AE1	D3X1R-#20112S	Cell Signaling, Denvers, USA
Alexa Fluor® 568 Fab goat anti-mouse IgG for eNOS	A11019	Life Technologies Corporation, Eugene, USA
Alexa Fluor® 647 Fab goat anti-rabbit IgG for AE-1	A21246	Life Technologies Corporation, Eugene, USA
Mouse anti-eNOS for WB and IP	624086	Erembodegem, Belgium (custom made)
Monoclonal anti- α tubulin	T6199	Sigma Aldrich, St. Louis, USA
Monoclonal anti- β actin	A1978	Sigma Aldrich, St. Louis, USA
Goat anti-mouse Ig	554002	BD Pharmingen, San Diego, USA
Ter119 anti-mouse PE	130-117-363	Milteny Biotec, Bergisch Gladbach, Germany

3.1.3 Commercial kits

Table 4 – List of commercial kits with manufacturer and headquarter of the manufacturer

Kit	Manufacturer	Headquarter
RNase-Free DNase Set	Qiagen	Hilden, Germany
QuantiTect Rev. Transcription Kit	Qiagen	Hilden, Germany
ECL Prime detection reagent kit	GE Healthcare	Little Chalfont, UK
Ambion DNA-free Kit	Thermo Fisher Scientific	Waltham, USA
RNeasy Mini Kit	Qiagen	Hilden, Germany
Dynabeads antibody coupling kit	Invitrogen	Carlsbad, (CA) USA
SuperSignal™ West Pico Plus chemiluminescent substrate	Thermo Fisher Scientific	Waltham, USA
SuperSignal™ West Femto Maximum Sensitivity Substrate	Thermo Fisher Scientific	Waltham, USA
Bio-Rad Protein Assay Kit	BioRad	Hercules, USA

3.1.4 Equipment

Table 5 – List of equipment with manufacturer and headquarter of the manufacturer

Equipment	Name	Manufacturer	Headquarter
Microplate reader	FLUOstar Optima	BMG LABTECH	Ortenberg, Germany
Biomolecular imager	Image Quant LAS4000	GE Healthcare	Little Chalfont, UK
	ChemiDOC™ Imaging System	Bio-Rad Laboratories GmbH	München, Germany
Full spectrum microvolume UV-Vis analyzer	Nanodrop 2000	Thermo Fisher Scientific	Waltham, USA
Real-Time PCR Instrument	StepOnePlus Real-Time PCR Systems	AB Applied Biosystems	Waltham, USA
Peristaltic pump		Cole-Parmer GmbH	Wertheim, Germany
Blood Counter	Vet ABC™ Hematology Analyzer	Scil animal care company – division of Henry Schein Animal Health	Gurnee, USA
Aortic rings analyzer	Graz Tissue Bath System	Hugo Sachs	Baden-Württemberg, Germany
Confocal microscope	OLYMPUS IX81/FV1000	Biocompare	San Francisco, USA
Blood pressure analyzer	MPVS Ultra	ADInstruments	Sidney, Australia
Tissue homogenator for cells isolation	GentleMACS Dissociator	Milteny Biotec	Bergisch Gladbach, Germany
FACS	MACSQuant Analyzer 10	Milteny Biotec	Bergisch Gladbach, Germany

3.1.1 Softwares

Table 6 – Softwares, developer and headquarters of the manufacturer

Software	Developer	Headquarter
Prism 9.1.1	GraphPad	San Diego, CA, USA
Image Studio Lite	LI-COR Biosciences	Lincoln, USA
IOX – blood pressure measurements	EMKA	Paris, Frances
LabChart	ADInstruments	Sidney, Australia
Brachial Analyzer 5	Medical Imaging Applications	Coralville, IA
Vevo2100	Visual Sonics Inc.	Toronto, Canada
Olympus Fluoview FV1000 version 4.1a	Olympus	Center Valley, USA
PoewerChrom	eDAQ	Colorado Springs, USA
FACS Flowing Software	Turku Bioscience	Turku, Finland

3.2 Animals

All experiments were approved by the LANUV according to the European Convention for the Protection of Vertebrate Animals used for Experimental and other Scientific Purposes (Council of Europe Treaty Series No. 123). Animals used at the University of Virginia were handled according to protocols approved by the University of Virginia IACUC. Animal care was provided following the institutional guidelines of the Heinrich Heine University or the University of Virginia and Emory Animal Care and Use Committees and followed the National Institutes of Health (NIH) guidelines for the care and use of laboratory animals. Experimental planning and execution followed the ARRIVE recommendations [128]. For experiments, 2-6 months old male mice up to 30 g were used. Mice of the same genotype and age were randomly assigned to experimental groups.

Immunofluorescence experiments were conducted by me at the University of Virginia (VA), USA. For these particular experiments wildtype mice were provided by Prof. Dr. B. E. Isakson (E. Berne Cardiovascular Research Center; Department of Molecular Physiology and Biophysics; VA, USA). WT male mice (B6NTac) were bought from Taconic Biosciences (NY, USA).

Mice expressing Cre recombinase in erythroid cells under the control of the promoter of the hemoglobin beta chain (C57BL/6-Tg(Hbb-Cre)12Kpe/J) [121] were obtained by Jackson Laboratory (JAX stock #008314) and crossed for more than ten generations with C57BL/6J.

Tamoxifen (TAM)-inducible endothelial-specific Cre mice (Tg(Cdh5Cre/ERT2)1Rha) [129] were kindly provided by Prof. Dr. E. Lammert (Heinrich-Heine-University of Düsseldorf, Düsseldorf, Germany). The inducible models of endothelial-specific Cre mice were generated after a necessary treatment with TAM (Sigma-Aldrich, St. Louis, USA). Around 200 ml of TAM (approximately 25-30 g body weight) were given for five consecutive days every 24 hours via intraperitoneal (i.p.) injections in a concentration of 75 mg/kg. On day 21 after the injections, the explantation of the organs took place.

DeleterCre (C57Bl/6.C-Tg(CMVCre)1Cgn/J) [122] mice expressing Cre in all tissues were kindly provided by Prof. C. Pfeffer (Heinrich Heine University of Düsseldorf).

3.3 Creation of tissue-specific mice lines

3.3.1 Generation of eNOS^{flox/flox} mice

The eNOS^{flox/flox} mice were created in the Myocardial Infarction Research Laboratory of the Heinrich Heine University of Düsseldorf.

For the generation of eNOS^{flox/flox} mice, an orphan loxP site and an FRT-neo-FRT-loxP resistance cassette were simultaneously inserted into the eNOS genomic locus to target exon 2 for Cre-mediated excision. Sequencing confirmed base pair-precise modification of the eNOS genomic locus and integrity of all functional elements. The plasmid was linearized and electroporated in A9 ES cells (hybrid C57/129), 300 clones were picked, and 12 positive clones on 100 were screened by Southern Blot at 5' arm. Further screening was done by long-range PCR because of the lack of specificity of the 3'-probe designed for southern analysis. Two males derived from ES cells were obtained and bred with C57BL/6J mice for at least ten generations.

3.3.2 Generation of eNOS^{inv/inv} mice

To generate eNOS^{inv/inv} mice, an inverted exon 2 and two additional Lox511 sites were introduced in the eNOS^{flox/flox} construct, which allowed the Cre-induced reactivation of eNOS in a tissue of interest. The plasmids were sequenced, linearized, and electroporated in A9 ES cells (hybrid C57/129), 300 clones picked, and positive clones were screened by Southern Blot at 5' arm and by long-range PCR.

3.3.3 Generation of EC/RBC eNOS KO mice

Homozygous eNOS^{flox/flox} mice were crossed with Cdh5Cre/ERT2^{pos} mice to obtain eNOS^{flox/flox} Cdh5Cre/ERT2^{pos} and eNOS^{flox/flox} Cdh5Cre/ERT2^{neg} mice; to induce endothelial-specific activation of the Cre recombinase, Cre positive and negative mice of each line were treated with TAM (75 mg/kg/day) for five consecutive days. Experiments were conducted 21 days after the last injection (Figure 7).

Homozygous eNOS^{flox/flox} mice were crossed with erythroid-specific HbbCre^{pos} mice to obtain erythroid-specific eNOS KO mice (eNOS^{flox/flox} HbbCre^{pos}, RBC eNOS KO) and their respective WT littermate controls (eNOS^{flox/flox} HbbCre^{neg}).



Figure 7 – Representative scheme for TAM treatment

To induce a specific removal/reintroduction of eNOS from the endothelial cells it was necessary a 5-day TAM treatment on 8 weeks old mice. Experiments were conducted 21 days after the last day of injection.

3.3.4 Generation of EC/RBC eNOS KI mice

Homozygous $eNOS^{inv/inv}$ mice were crossed with $Cdh5Cre/ERT2^{pos}$ mice to obtain $eNOS^{inv/inv} Cdh5Cre/ERT2^{pos}$ and $eNOS^{inv/inv} Cdh5Cre/ERT2^{neg}$ mice. TAM treatment was necessary to induce endothelial-specific activation of the Cre recombinase (Figure 7).

The founder line $eNOS^{inv/inv}$ was crossed with erythroid-specific $HbbCre^{pos}$ mice to obtain erythroid-specific eNOS KI mice ($eNOS^{inv/inv} HbbCre^{pos}$, RBC eNOS KI) and their WT littermate controls ($eNOS^{inv/inv} HbbCre^{neg}$).

Global eNOS KI mice were used as proof of concept to verify the functionality of the gain of function model and the global eNOS reintroduction.

3.3.5 Generation of global eNOS KO mice

To generate global eNOS KO mice, the founder $eNOS^{flox/flox}$ mice were crossed with DeleterCre ($C57Bl/6.C-Tg(CMVCre)1Cgn/J$) mice expressing Cre in all tissues.

3.4 Dietary nitrate supplementation of the mice in the drinking water

Mice were given tap water ad libitum directly from the sink of the laboratory (nitrate around 230 μ M) except when indicated. In specific experiments mice were given different nitrate concentrations dissolved in drinking water:

- 1- Water containing low nitrate amount (Vittel water, source: Vittel, Vogesen, France);
- 2- A prepared solution containing 200 μ M of nitrate, comparable to the amount present in the tap water. Considering that an average mouse weighs 30 mg and drinks around 6 ml of water/day, the

dose of nitrate assumed with the prepared solution is 0.074 mg, corresponding to a concentration of 2.48 mg/kg.

Mice received the water for 24 hours and then BP was measured via Millar catheterization (Figure 8).

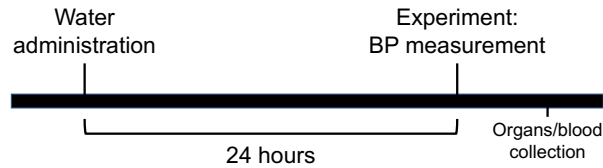


Figure 8 – Representative scheme for nitrate supplementation in the drinking water

Drinking water containing different nitrate concentrations was administered for 24h to the mice before blood pressure measurement with Millar catheterization of the right carotid artery.

3.5 Collection of blood and mouse tissues

3.5.1 Blood collection and separation of plasma and RBCs

Mice were anesthetized with isoflurane by an oral intubation (3% induction and 2% maintenance) and fixed on a heated platform (set to 39°C, body temperature approx. 36°C) in a supine position. Whole blood was withdrawn by cardiac puncture with a syringe coated with EDTA 0.5 M, and collected in a 2 ml tube, containing 0.1 ml of EDTA 0.5 M, to prevent coagulation. Plasma was collected after centrifugation (800 g, 10 minutes, 4 °C) and frozen in liquid nitrogen. The buffy coat was discarded. RBCs were collected from the bottom of the tube and placed in a separate tube for further analysis.

3.5.2 Tissues collection

Organs were explanted after systemic perfusion with cold phosphate-buffered solution (PBS) pH 7.4 and immediately frozen in liquid nitrogen. Bone marrow was isolated from femurs and tibias of both legs and used for DNA and RNA isolation for further analysis.

3.6 Hematological phenotyping of tissue-specific mice models

Mice were anesthetized with isoflurane and blood was taken via retro-orbital collection, using a disposable glass Pasteur pipette. Vet ABC™ Hematology Analyzer was used for blood count analysis. Different parameters were analyzed: red blood cell count (RBC), hematocrit (HCT), hemoglobin (HGB), red blood cell distribution width (RDW), mean corpuscular hemoglobin concentration (MCHC), mean hemoglobin concentration (MCH), mean corpuscular volume (MCV), white blood cell count (WBC), number and percentage of lymphocytes, granulocytes and monocytes (Lymph# and Lymph%, Gra# and Gra%, Mo# and Mo%), platelet count (PLT) and mean platelet volume (MPV).

3.7 Blood collection and separation of RBCs for immunofluorescence

To collect blood for immunofluorescence assay, mice were anesthetized with 2,2-dichloro-1,1-difluoroethyl methyl ether 97% (Alfa Aesar, Haverhill, Massachusetts, USA) and exsanguinated via cardiac puncture with syringes coated with EDTA 0.5 M (Sigma-Aldrich) to prevent coagulation. Whole blood was centrifuged (2300 rpm; Fisher, accuSpin Micro 17), plasma and buffy coat were removed by aspiration. The remaining RBC pellet was washed three times in a modified Krebs-Heinseleit (K-H) buffer and centrifuged. Washed RBCs were then diluted at 1:200 for immunostaining.

To detect eNOS and AE-1 by immunofluorescence, diluted RBCs were mounted onto slides via cytopspin for 3 minutes at 800 g and fixed afterward with PBS/PFA 4%. After fixation, PFA was washed away, and a permeabilization step was carried out using a 0.2% NP40 in PBS buffer. After washing RBCs were blocked for 1 hour (PBS + fish skin gelatin 10%, Triton X-100 0.25%, BSA 0.5%, 10% goat serum).

Primary antibodies were stained with a 1:200 dilution, and incubation took place overnight at 4°C (eNOS anti-mouse MA5-15559, Thermo Scientific; AE-1 anti-rabbit D3X1R, Cell Signaling). Next, RBCs were washed with PBS, and the secondary antibodies were stained for 2 hours at dark at room temperature (Rt) (goat anti-mouse Fab Alexa Fluor 568; goat anti-rabbit Fab Alexa Fluor 647; Invitrogen). After three more washes, a mounting medium was added, and a coverslip was applied. Slides were imaged using an Olympus IX81/FV1000 confocal microscope at 100X objective.

3.7.1 Immuno transmission electron microscopy (TEM)

Isolated RBCs were fixed with PBS/PFA 4%, embedded, and labeled with primary antibodies (eNOS anti-mouse MA5-15559, Thermo Scientific; AE-1 anti-rabbit D3X1R, Cell Signaling) and secondary antibodies (goat anti-mouse #25133, 15nm size; goat anti-rabbit #25116, 25nm size, Electron Microscopy Sciences). Images were taken on a Joel 1220.

3.8 Isolation of endothelial cells from lungs

Endothelial cells were extracted with the MACS-Method by two independent magnetic separation steps consisting of a negative selection using anti-CD45 microbeads and a positive selection using anti-CD31 microbeads.

After the opening of the thorax and systemic perfusion with cold PBS, lungs were explanted entirely and put in a C-tube filled with 10 mL of digesting solution (HBSS, Collagenase 450 U/ml, DNase I 60 U/ml). C-tubes were positioned in the gentle MACS for homogenization (Program: m spleen 01.01; Milteny, Bergisch Gladbach, Germany). After 45 minutes of incubation at 37°C, homogenates were filtered through a 70 µm EASY strainer. A first centrifugation step at 300 g, 4°C for 10 minutes was carried out. The supernatant was discarded, and RBCs contained in the cell pellet were lysed in 5 ml of lysis buffer for 5 minutes at Rt. 15 ml of PBS were added, and centrifugation was carried out (300 g, 4°C for 10 minutes). The supernatant was removed, and the cell pellet resuspended in 180 µl of separation buffer (PEB). CD45 microbeads were added to remove leukocytes (20 µl) and let incubate for 15 minutes at 4°C. After adding 10 ml of PEB, centrifugation was carried out at 300 g, 4°C for 10 minutes, the supernatant was discarded, and the pellet resuspended in 500 µl PEB. The cell suspension was then added to the separation columns, and the flow was collected in a 15 ml falcon prefilled with 10 ml PEB. CD45 negative (CD45⁻) fraction was collected and centrifuged at 300 g, 4°C for 10 minutes. After removal of the supernatant, the pellet was resuspended in 180 µl PEB.

20 µl CD31 microbeads were added to the tube and let incubate in the fridge for 15 minutes. 10 ml of PEB were added, and the tube was centrifuged at 300 g, 4°C for 10 minutes. After aspiration of the supernatant and resuspension of the pellet in 500 µl PEB, a second separation step was conducted, collecting the flow-through in a 15 ml falcon prefilled with 10 ml PEB. The CD31 positive (CD31⁺) endothelial cells were retained in the column. The flow-through contained the CD31 negative (CD31⁻) fraction. To obtain endothelial cells, columns were removed from the magnetic support and put in a 15 ml falcon prefilled with 5 ml PEB. By further adding 5 ml of PEB to the columns and flushing them with a plunger, CD31⁺

endothelial cells were collected in the prefilled tube. After centrifugation (300 g, 4°C for 10 minutes) of CD31⁺ and CD31⁻ fraction supernatant was discarded, and the pellet resuspended in 1 ml PEB. Next, the cell suspension was centrifuged at 800 g at 4°C for 10 minutes. After removing the supernatant, the final cell pellet was resuspended in 20 µl PBS and 200 µl of RNA later snap-frozen in liquid nitrogen and stored at -80°C.

The purity and yield of cells were determined by flow cytometric analysis using specific antibodies according to standard procedures. The percentage of CD31⁺ cells was obtained by this method was a minimum of 95%.

3.9 Isolation of erythroid cells from bone marrow

Bone marrow was isolated from both legs' femur and tibias, and each bone was cut at the sides to be opened. The bones were put in a 0.5 ml tube with a hole at the bottom, placed in a 2 ml tube prefilled with 200 µl of PEB. Centrifugation at maximal speed was carried out for 20 seconds. The small tube was discarded, and 800 µl PEB added to the 2 ml tube. The cell pellet was resuspended and centrifuged at 400 g for 10 minutes. The supernatant was removed, and 1 ml of erythrocyte lysis buffer (ELB) was added. The solution was then transferred to a 15 ml falcon containing 2 further ml of ELB (to reach a final volume of 3 ml), followed by incubation on ice for 10 minutes. The cell suspension was filtered with a 40 µm filter, and the resulted solution was centrifuged at 350 g for 10 minutes at 4°C. Supernatant was discarded.

To remove CD45⁺ cells, the cell pellet was resuspended in 210 µl PEB and 30 µl of FcR-Blocker. The suspension was incubated in the fridge (4-8°C) for 10 minutes. Next, 60 µl of CD45 microbeads were added and incubated in the fridge for 15 minutes. 5 ml of PEB buffer were added to wash the solution, and a centrifugation step was carried out (350 g; 10 minutes; 4°C). The supernatant was removed and 500 µl PEB were added to resuspend the cells.

The cell suspension was then added to the separation columns, and the flow-through was collected in a 15 ml falcon. 3 ml of PEB buffer were applied three times to wash the columns, and the flow-through was collected in the 15 ml falcon. CD45⁻ fraction was collected in the tube, and 5 further ml of PEB were added to a final volume of 14 ml. The cell suspension was centrifuged at 350 g, 4°C for 10 minutes, the supernatant was removed, and cells were resuspended in 500 µl PEB.

The separation step was repeated a second time by collecting the flow-through in a 15 ml falcon and washing the column three times with 3 ml PEB to collect the CD45⁻ fraction in the falcon. The CD45⁻ fraction was used for sorting Ter119⁺. The column were removed from the magnet, and 5 ml of PEB were

added. The flow-through represented the CD45⁺ fraction.

The cells were resuspended in 210 µl PEB and 30 µl FcR-Blocker and incubated in the fridge (4-8°C) for 10 minutes. Next, 60 µl of Ter119 microbeads were added (microbeads were vortexed before using) and incubated for 15 minutes on ice. 5 ml of PEB were added to wash, and centrifugation was carried out (350 g, 10 minutes, 4°C). The supernatant was removed, and the solution was resuspended in 150 ml of PEB buffer.

Separation columns were prepared by washing with 3 ml, and the cell suspension was added to the columns. The membranes of the columns were washed by adding three times 3 ml of PEB buffer, and the flow-through containing Ter119⁻ fraction was collected. The positive fraction was collected by removing the columns from the magnet and adding 5 ml of PEB. The Ter119⁺ fraction was centrifuged at 350 g for 10 minutes at 4°C, the supernatant was removed, and cells were transferred into a 2 ml tube. Centrifugation was carried out (10000 g; 10 minutes; 4 °C). The supernatant was discarded, and 20 µl PBS buffer and 200 µl of RNA were added later. Samples were stored at -80°C.

3.10 Molecular characterization of mice models of eNOS KO and eNOS KI

3.10.1 Analysis of tissue-specific DNA recombination by qPCR

The Cre recombinase-dependent genetic locus recombination was determined by extracting genomic DNA from targeted and non-targeted tissues and analyzed by real-time polymerase chain reaction (qPCR) with specific primers and probes designed to recognize the floxed allele and the allele with targeted deletion (Transnetyx, Cordova, TN). A threshold was defined by using tissues from global eNOS KO mice obtained by the same floxed construct for data analysis.

The tissues analyzed were the aorta and BM. The analysis was carried out by Transnetyx, Cordova, TN.

Table 7 – Probes used to genotype knock-out mice, designed and used by Transnetyx

	Probe	Binds to	Forward sequence	Reverse sequence
P1	Cre	Cre-Recombinase sequence	TTAATCCATATTGGCAGAACGAAAACG	CAGGCTAAGTGCCTTCTCTACA
P2	WT	eNOS wildtype allele	CCACCTCCTAAGGCTGTTGT	GCCCACCCTCCTCTTCCT
P3	FLOX	flox/flox allele	GGCGGCCGCATAACTTC	CAGACTGCCTTGGGAAAAGC
P6	EX	binds if eNOS Exon2 is cut	ACCTCCTAAGGCTGTTGTGAGA	GCCAAAGGCTTGCTGCAATT

Table 8 – Probes used to genotype knock-in mice, designed and used by Transnetyx

	Probe	Binds to	Forward sequence	Reverse sequence
P1	Cre	Cre-Recombinase sequence	TTAATCCATATTGGCAGAACGAAAACG	CAGGCTAAGTGCCTTCTCTACA
P4	WT	eNOS wildtype allele	AGGAAGGACCAGAGGGATCAAG	ATGGGATGAGATTGGTTGCTTAGG
P5	INV	inverted eNOS allele	CTCCTCTTCCTGACACTTTCTGT	GCTTGCTGCAATTGATAACTTCGTA
P7	FLIP	flipped eNOS allele (reinverted)	GGAACCTCAGATCTCCATAACTTCGT	ACCCCTCCTCTTCCTGACACTTT

3.10.2 Analysis of eNOS expression in isolated cells and tissues by RT-qPCR

Extraction of total RNA, reverse transcription (RT), pre-amplification, and qPCR from ECs or mouse tissues was carried out using commercial kits according to the manufacturer's instructions.

3.10.2.1 RNA extraction

RNA from animal tissues was isolated and purified with RNAeasy Mini Kit (Qiagen, Hilden, Germany). The tissues were homogenized on ice (4°C) in RLT buffer and β -Mercaptoethanol (10 ml/ml) with a tissue ruptor at full speed (Qiagen, Hilden, Germany) until the lysate was homogeneous (30-60 seconds). The eluate was transferred to a new tube and incubated at 55°C for 10 minutes with 590 μ l of RNase-free water and 10 ml of proteinase K solution, and then cleared by centrifugation at Rt for 3 minutes at 10000 g. The supernatant was transferred to a new tube, and ethanol was added and gently mixed by pipetting.

The sample was transferred on an RNAeasy mini spin column and centrifuged at maximal speed (10000 g) at 15-25 °C for 15 seconds. The eluate was discarded. RW1 buffer was added twice (700 μ l followed by 350 μ l) to the column to wash the membrane, centrifugation was carried out (15-25 °C, 15 minutes, 10000 g), and the flow-through was discarded.

DNA was digested by using the RNase-Free DNase Set. 80 μ l of DNase incubation mix (10 μ l of DNase I stock solution in 70 μ l buffer RDD) were added directly to the RNAeasy mini spin column membrane and placed at Rt for 15 minutes. RW1 buffer was used to wash the column and cleared by centrifugation (15-25°C, 15 minutes, 10000 g); the flow-through was discarded.

Next, 500 μ l of buffer RPE/ethanol solution were added to the column and centrifuged (15-25°C, 15 minutes, 10000 g), and the flow through was discarded. The column was placed in a new collection tube

and centrifuged at full speed for 1 minute to eliminate any possible buffer RPE/ethanol carryover. 30-50 μ l of RNase-free water were added to the column to elute RNA.

The RNA concentration was determined by absorption measurement at the wavelength of 260 nm using a NanoDrop 2000 (Thermo Fisher Scientific, Waltham, USA).

3.10.2.2 Reverse transcription

The reverse transcription of the isolated RNA samples was done with the QuantiTect Reverse Transcription Kit (Qiagen, Hilden, Germany). Isolated RNA samples were vortexed and centrifuged. Then, the RNA samples were diluted in 12 ml of nuclease-free water (table 9).

Table 9 – Final amount of cDNA extracted from different tissues used for reverse transcription

Tissue type	Final cDNA amount
Heart	1 μ g in 20 μ l
Aorta	500 ng in 20 μ l
BM	2 μ g in 20 μ l
CD31 ⁺ from heart	38 ng in 20 μ l
CD31 ⁺ from lung	42 ng in 20 μ l
Ter119 ⁺	208 ng in 20 μ l

2 μ l of gDNA Wipe Out Buffer were added to the diluted samples. Afterward, samples were vortexed, centrifuged, incubated for 2 minutes at 42°C, and immediately put on ice (4°C). 6 μ l of reverse transcription Master Mix were added to each sample. The Master Mix includes 1 μ l Quantscript RT, 4 μ l Quantristrip RT-Buffer and 1 μ l RT Primer Mix per RNA sample. One additional sample (pre-RT) representing the sample control that did not undergo reverse transcription was prepared, consisting of the sample with the highest amount of RNA. To this sample, RNase-free water was added instead of Master Mix. The samples, including Master Mix, were vortexed and centrifuged, incubated for 15 minutes at 42°C, and afterward for 3 minutes at 95°C. The reverse transcription was completed, and the samples could be stored at -20°C for some days or at -80°C for a longer time or used directly for qPCR.

3.10.2.3 Pre-amplification of cDNA

When necessary, the primer mix was prepared by adding 5 ml of each primer (eNOS, Cre, Rplp0), and RNase-free water was added to a total volume of 500 μ l.

12.5 µl of the RT-product were added to 12.5 µl of the primer-mix and 25 µl PreAmp Supermix (1725160, BioRad).

The program used for carrying out qPCR consisted of 3 minutes at 95°C, 15 seconds at 95°C, and 4 final minutes at 58°C. The second and third steps were repeated for 10 cycles.

3.10.2.4 qPCR with TaqMan-Assay

The qPCR was performed with 2x TaqMan Gene Expression Fast Advanced Master Mix (Thermo Fisher Scientific, Waltham) and different 20x TaqMan Gene Expression assays (Thermo Fisher Scientific, Waltham, USA) (Table 10).

Table 10 – TaqMan Genes used for expression assays

Gene	Assay ID	Dye
Rplp0	Mm00725448_s1	VIC-MGB
eNOS	Mm00435197_g1	FAM
Cre	Mr00635245_cn	FAM

The ribosomal protein large P0 (rplp0) is a constitutively expressed housekeeping gene, and it was used as an endogenous control for the qPCR analysis.

The Master Mix was prepared by adding 10 µl of Fast Advanced Master Mix per sample, 1 µl of the 20x TaqMan probe for the Housekeeper, and 1 µl for the gene of interest. These volumes were multiplied for the total number of the wells + 5/6. Each sample was measured in triplicates. Before performing the qPCR, the cDNA samples were diluted in nuclease-free water, spun down, and pipetted to the wells to a final volume of 8 µl.

The qPCR was performed using StepOnePlus Real-Time PCR Systems (AB Applied Biosystems, Waltham, USA). The running method comprised a first *holding stage* of 50°C for 2 minutes, followed by 2 further minutes at 95°C. The *cycling stage* (40 cycles) was carried out with 95°C for 3 seconds and 60°C for 30 seconds.

Expression data were normalized to the geometric mean of housekeeping gene rplp0 to control the variability in expression levels and were analyzed using $2^{-\Delta\Delta CT}$ or $2^{-\Delta CT}$. Ct values higher than 38 were not included in the calculations and were considered "no signal".

3.10.1 Western blotting

3.10.1.1 Tissue lysates/protein detection

Heart and aorta were homogenized on ice in RIPA buffer (1% NP40, 0.5% sodium deoxycholate, 0.1% SDS in PBS pH 7.4) containing a cocktail of protease/phosphatase inhibitor mini tablet (Thermo Fisher Scientific, Waltham, USA). Subsequently, the homogenate was vortexed for 30 seconds, followed by 30 seconds of sonification in the ultrasonic bath for three consecutive times. After 15 minutes of incubation at 4°C, while rotating, lysates were centrifuged at 400 g for 15 minutes at 4°C, and the supernatant was separated from the pellet. Protein detection was performed with a detergent compatible (DC) protein assay (BioRad, Hercules, USA) that uses a colorimetric method to determine protein concentration following detergent solubilization. The principle of the assay is according to the Lowry method for protein determination with some modifications [130]. The protein assay was measured at 650-750 nm with a FLUOstar Optima microplate reader (BMG LABTECH, Rotenberg, Germany).

3.10.1.2 SDS-Page/Membrane transfer and antibody incubation

Tissue lysates were separated by SDS-polyacrylamide gel (4-12% Bis-Tris and 7% Tris Acetate) (Thermo Fisher Scientific, Waltham, USA) under denaturing conditions and transferred to 0.2 µm nitrocellulose membrane (GE Healthcare, Little Chalfont, UK). A molecular weight MagicMarker XP was applied to the gel (Thermo Fisher Scientific, Waltham, USA). The membranes were blocked with 5% milk in T-TBS for 1 hour at Rt. Samples were incubated overnight at 4°C with primary antibodies for eNOS and the housekeeper (α -tubulin or β -actin as indicated). Membranes were washed in T-TBS six times for 5 minutes each. Incubation with secondary antibodies was carried out for 1 hour at Rt and the membranes were finally washed in T-TBS (table 11).

Table 11 – Antibodies concentrations used for WB and IP

Antibody	Code	Dilution	Application
Monoclonal anti- α tubulin	T6199	1:5000 in 5% BSA in T-TBS	WB
Monoclonal anti- β actin	A1978	1:1000 in 5% BSA in T-TBS	WB
Mouse anti-eNOS for WB and IP	624086	1:100 in 5% BSA in T-TBS	WB
Goat anti-mouse Ig	554002	1:7500 in in 5% BSA in T-TBS	WB
Goat anti-mouse Ig	554002	1:5000 in 5% milk in T-TBS	IP

3.10.1.3 Detection of protein bands

For chemiluminescence detection, bands were detected using SuperSignal™ ECL substrates and Image Quant (GE Healthcare Little Chalfont, UK). 1 ml of ECL Prime detection reagent mix was applied on the membrane and incubated for 5 minutes. The ECL Prime detection reagent kit (Thermo Fisher Scientific, Waltham, USA) includes solution A: luminol solution and solution B: peroxide solution. Solution A and B were mixed 1:1 (v/v) immediately before use.

3.10.2 Immunoprecipitation of mouse anti-eNOS using EPOXY270 Beads

To perform immunoprecipitation (IP), the Ab was coupled to Dynabeads using a commercial Antibody Coupling Kit (Invitrogen, Carlsbad, USA). The kit supplies all buffers needed for the coupling and washing steps.

Ab is covalently coupled to Dynabeads® M-270 Epoxy beads, minimizing the risk of bound antibody contaminating the final eluate. Dynabeads® M-270 Epoxy beads exhibit ultra-low background binding and do not require blocking before use.

10 mg of Dynabeads® M-270 Epoxy were weighted in a 1.5 ml Eppendorf tube, and beads were washed with 1 ml of C1 solution and vortexed or resuspended by pipetting (the C1 + Ab volume is equal to C2 volume. The total reaction volume (C1 + μ l Ab + C2) should be 100 μ l per mg beads.

The Eppendorf tube was placed on the magnet for 1 minute to allow the beads to collect at the tube wall. The supernatant was removed. The Ab and C1 solution were added to the washed beads and mixed by gentle vortexing or pipetting. C2 solution was added and mixed by gentle vortexing or pipetting. The tubes were incubated on a roller at 37°C overnight (16-24 hours) to allow the proper antibody coupling. The tubes were placed on the magnetic holder for 1 minute to allow the beads to collect at the tube wall, and the supernatant was discarded.

800 μ l of HB solution, 800 μ l of LB, and 800 μ l of SB solution were added to the tube in three different steps and mixed by vortexing or pipetting. After adding every solution and before proceeding with the next one, the tube was placed on the magnet for 1 minute, and the supernatant was removed.

The tube was incubated on a rotator at Rt for 15 minutes, placed on the magnet for 1 more minute, and the supernatant was discarded.

Ab-coupled beads were resuspended in 100 μ l of SB per mg beads to a final concentration of 10 mg/ml and stored at 2-8°C until use.

At the end of the protocol, the beads were covalently coupled with the Ab and ready for IP. The sample was used at a concentration of 80 mg/ml, depending on the protein concentration defined by

BioRad protein assay. To the defined volume of the lysate, 70 μ l of Ab-coupled beads and 100 μ l of PBS 10X were added, and MilliQ water was further added to the tube to a final volume of 1 ml. The sample was incubated overnight under rotation at 4°C.

The tube was placed on the magnetic holder for 1 minute to remove the supernatant. Beads were washed with 200 μ l of PBS, and the sample was resuspended in a new tube. The sample was placed for 1 more minute on the magnet, the supernatant was discarded, and the magnet removed. After adding 100 μ l of PBS and gentle resuspension, the tube was placed on the magnet for 1 additional minute. The supernatant was removed, and the pellet was resuspended in 20 μ l of LDS buffer 4X diluted 1:4 and stored at -20°C or used immediately.

For gel loading, 2.5 μ l of LDS 1X were added with 2.5 μ l of sample reducing agent 10X (SRA) and loaded to the gel for SDS-Page.

3.11 Characterization of systemic hemodynamics

3.11.1 Measurement of vascular function *in vivo*

Vascular function was measured as flow-mediated dilation (FMD) with a Vevo 2100 with a 30-70 MHz linear array microscan transducer (Visual Sonics Inc., Toronto, Canada) as described [131]. The method analyses the changes in vessel diameter of the iliac artery in response to shear stress after vascular occlusion by using a cuff. Isoflurane anesthetized mice were placed on a heated examining plate to maintain the core body temperature at $37 \pm 1^\circ\text{C}$; heart rate was monitored to range between 400-600 bpm, and breathing rate was maintained at 100 breaths/min. During the experiment, a nose cone was placed over the animal's nose and mouth to deliver 2-3% isoflurane to maintain the anesthesia. Three paws of the mouse were secured to the electrode pads with conducting gel, and the last paw was left free to perform the FMD measurements. The hindlimb area of the mouse was first shaved, and the excess of hair was removed by using an epilation cream (Veet) and further cleaned and disinfected with a diluted alcoholic solution (70% ethanol in MilliQ water). To measure the FMD of the mouse, a vascular occluder was placed around the lower limb to induce occlusion of the iliac artery for 5 minutes, followed by 5 further minutes of reperfusion.

A baseline representing picture was taken before the occlusion of the cuff, and pictures were acquired every 30 seconds for 5 minutes. Other pictures were acquired when the reperfusion started every 20-30 seconds for the following 5 minutes. Thus, a total of 23-25 pictures were acquired in 10 minutes.

Pictures were analyzed using Brachial Analyzer 5 software (Medical Imaging Applications, Coralville, IA) to evaluate the diameter of the iliac artery at different time points before (baseline), during, and after occlusion of the vessel.

Measurements were expressed as a percentage of the baseline value acquired before vascular occlusion.

3.11.2 Analysis of cardiac function by high-resolution ultrasound

Transthoracic echocardiography was performed using a high-resolution ultrasound system (18-38 MHz; Vevo 2100, Visual Sonics Inc., Toronto, Canada) and the manufacturer's analysis software [131]. The procedure was started by securing the isoflurane-anesthetized mouse to an animal-handling platform in a supine position. A nose cone was placed over the animal's nose and mouth to deliver 2-3% isoflurane to maintain the anaesthesia. The paws of the mouse were secured to the electrode pads with conducting gel. An appropriate ECG was secured, body temperature at 37°C and respiratory rate for physiological assessment during imaging was checked. After shaving the chest and upper abdomen of the mouse, the procedure was started.

B-mode of the parasternal long-axis (PSLA) view, short-axis (SAX) view, and 2-D guided M-mode images were recorded by placing the transducer along the long axis of the left ventricle (LV) and directing it to the right side of the neck of the mouse. The transducer was rotated clockwise by 90°, and the LV short-axis view was visualized. Trans mitral inflow Doppler spectra were recorded in an apical four-chamber view by placing the microscan transducer at the tip of the mitral valves. Angle correction was used for accurate flow velocity measurements. Aortic valve flow was also evaluated.

Quantification of LV volume, stroke volume (SV), cardiac output (CO), and ejection fraction (EF) were calculated in M-mode by identification of maximal and minimal cross-sectional area. Additionally, LV systolic function was determined as fractional shortening (FS) in the longitudinal axis. Finally, LV end-systolic (ESV) and end-diastolic volumes (EDV) were measured by analyzing the characteristic flow profile of the mitral valve Doppler flow, which was visualized in apical four-chamber view [131].

3.11.3 Blood pressure measurements by Millar catheterization

Mice were anesthetized with isoflurane that was kept at 2-3% during the entire procedure. Invasive assessment of hemodynamic parameters was carried out in the *aorta ascendens* using a 1.4 F Millar pressure-conductance catheter (SPR-839, Millar Instruments, Houston, TX, USA). After removing the fur from the neck of the mouse, a 1-2 cm midline neck incision was made from just below the mandible to the

thoracic inlet. Under a dissecting microscope, the right carotid artery was exposed and carefully separated from other neighboring structures, including the *vagus* nerve. Once the carotid artery was isolated, a silk suture was applied distally (closer to the head) for the complete ligation of the vessel. A second silk suture was placed loosely proximally (closer to the heart) to allow secure positioning of the catheter laterally. Finally, a small clamp occluder was placed between the first two silk sutures to allow obstruction of blood flow. A small incision (arteriotomy) was made distal to the clamp. The tip of the catheter was placed in the small incision in the direction of the heart, the clamp was open, and after placing the catheter deeper along the artery, it was secured in place by tying the second loose suture once that catheter was advanced past the ligature.

Pressure data were analyzed with dedicated software (LabChart, ADInstruments, Sidney, Australia) to determine systolic blood pressure (SBP), diastolic pressure (DBP), and heart rate (HR). In addition, mean arterial pressure (MAP) was measured considering these two parameters:

$$MAP = \frac{(SBP+2*DBP)}{3}$$

3.11.4 Measurement of endothelial function/vascular reactivity *ex vivo*

Mice were anesthetized using a combination of ketamine (100 mg/kg, Pfizer Inc., New York City, USA) and xylazine (10 mg/kg, Bayer AG, Leverkusen, Germany). After lack of pain reflexes in the hind paws, organs were dissected, and the thoracic aorta was carefully freed from fat, isolated, and transferred into HEPES buffer. The artery was carefully flushed to remove residual blood and cut into 2 mm aortic rings. For each mouse, two to three aortic rings were transferred to the organ baths (Harvard Apparatus, Cambridge, USA), which were heated to 37°C, containing Krebs-Henseleit buffer, and were constantly gassed with carbogen (5% v/v carbon dioxide and 95% v/v oxygen). To equilibrate aortic rings, organ bath buffer was exchanged by fresh buffer every 15 minutes for 1 hour until the vessel tension was stable at 1 g. For receptor-independent constriction, 80 nM KCl was added. The treatment was removed by changing buffer in the organ bath for 15 minutes until tension reached baseline values. To test for endothelium-dependent relaxation, vessels were pre-constricted by the initial dose of phenylephrine (PE). This dose was followed by cumulative doses of acetylcholine (ACh) starting from 0.1 nM to 10 µM. After the last dose, treatment was again removed by changing the organ bath buffer for 5 minutes. By administering cumulative doses of PE, resulting in a concentration of 0.1-10 µM in the organ bath, the functionality of SMCs was

tested. This treatment was followed by sodium nitroprusside (SNP) in concentrations from 0.01 nM to 10 μ M.

3.11.5 Determination of nitrite levels in plasma

Biological specimens were harvested 24 hours after administration of drinking water containing different nitrate concentrations. Moreover, the day before the experiment, Eppendorf tubes were washed in MilliQ water to remove possible nitrate contaminations. Blood was collected by heart puncture (1 ml) and placed in 2 ml Eppendorf tubes prefilled with 0.1 ml of NEM/EDTA solution 100 mM. After the addition of blood in the tube, the final concentration of NEM/EDTA was 10 mM. Whole blood was centrifuged at 3000 g for 3 minutes at 4°C, plasma was collected in a nitrate-free Eppendorf tube, buffy coat was discarded, and RBCs were collected in a separate clean tube. Every organ was immediately weighted, and wet weight was noted. Tissues were stored at -80°C.

On the day of the experiment, tissues were diluted and homogenized in a solution of NEM/PBS/EDTA (dilution with lysis buffer in v:v): heart, lung, liver, kidney, spleen, and skeletal muscle were diluted 1:12.5, the aorta was diluted 1:40 in NEM/PBS/EDTA solution. Homogenization was continuously operated on ice (4°C) for 30 seconds up to 1 minute.

To analyze RBCs, it was essential to induce hemolysis of the cells, promoting the release of NO species. For this reason, RBC preparation was done using a dilution of 1:3 of RBCs in a lysis solution of NEM/EDTA/MilliQ water instead of PBS.

Plasma was injected into the instrument without performing any dilution.

Nitrosyl hemoglobin (NO-heme) levels were quantified by group-specific denitrosation in an oxidative solution of potassium hexacyanoferrate(III) in PBS.

The concentration of nitrite and various nitroso species was determined after reductive cleavage by an iodide/triiodide-containing reaction mixture (45 mmol/l potassium iodide (KI) and 10 mmol/l iodine (I₂) in glacial acetic acid). Determination of the NO released into the gas phase was achieved by its chemiluminescent reaction with ozone (O₃) to form nitrogen dioxide (NO₂). A proportion of nitrite arose in an electronically excited state (NO₂*), which, on decay to its ground state, emitted light in the near-infrared region and could be quantified by a photomultiplier; the intensity of light emitted (luminescence) was directly proportional to NO concentration.

The samples were injected first in a warm chamber at 60°C (nitrite) or 37°C (NO-heme), and the NO released from the reductive/oxidative reaction solution passed through a cold chamber at the temperature of 4°C.

The outlet of the gas stream from the cold chamber traveled through a scrubbing bottle containing sodium hydroxide (1 mol/l; 0°C) in order to trap traces of acid and iodine before the transfer into the detector (CLD 77AM sp, Eco Physics) [38, 132].

To keep baseline noise at a minimum and achieve consistent results, nitrogen flow was kept constant throughout the entire measurement cycle, indicated by a pressure gauge placed between the outlet of the scrubbing bottle and the detector inlet (approximately 0.05 bar).

Standards and sample aliquots (100-300 µl) were injected into the reaction mixture by gas-tight Hamilton syringes.

For nitrosated (S-nitroso and N-nitroso) products (RXNO), the sample was transferred into a new clean Eppendorf tube (minimum 100 µl), and sulfanilamide was added in the ratio of 1:10 (v:v). The role of sulfanilamide is to consume free nitrite forming an azo compound allowing the measurement of RXNO levels specifically. Incubation was done for 15 minutes at Rt.

Peak integration was accomplished with the software PowerChrom (eDAQ, Colorado Spring, USA) after signal smoothing to eliminate high-frequency noise and baseline correction. The software operates by converting the voltage signal from the CLD into signal intensity (usually ppb) and forms the chromatograms.

3.12 Statistical Analyses

Sample size was calculated a priori by using G-Power V.3.1 (Heinrich Heine University of Düsseldorf). Statistical analysis was carried out with GraphPad Prism 9 for MacOS (Version 9.1.1(223)); GraphPad Software, San Diego, CA, USA). Normal distribution was tested by the D'Agostino-Pearson test. Comparisons among multiple groups were performed using 1-way and 2-way analysis of variance (ANOVA), as appropriate, followed by Tukey's or Sidak's post-hoc analysis, as indicated. Where indicated, unpaired Student's t-test with Welch correction was used to determine if two groups of data were significantly different. The Mann-Whitney test was carried out when data were not normally distributed. $p < 0.05$ was considered statistically significant. Unless stated otherwise, the results are reported as means \pm standard deviation (SD).

4. Results

4.1 Analysis of eNOS and AE-1 localization on RBC membrane

Immunostaining was performed to confirm whether eNOS is expressed in the RBCs and to study its localization on the RBC membrane. Localization of eNOS on the membrane of RBCs was determined by visualizing the co-localization with the transmembrane protein AE-1.

As shown in figures 9A and 9B, staining was carried out with anti-eNOS and anti-AE-1 antibodies that were highly specific for the proteins and showed overlapping signals between eNOS (yellow) and AE-1 (red). The signals of eNOS and AE-1 appeared to be co-localized on the membrane of the RBCs. Control staining of IgG from mouse, IgG from rabbit, and secondary antibodies only was performed in parallel with real experiments (Figure 9C).

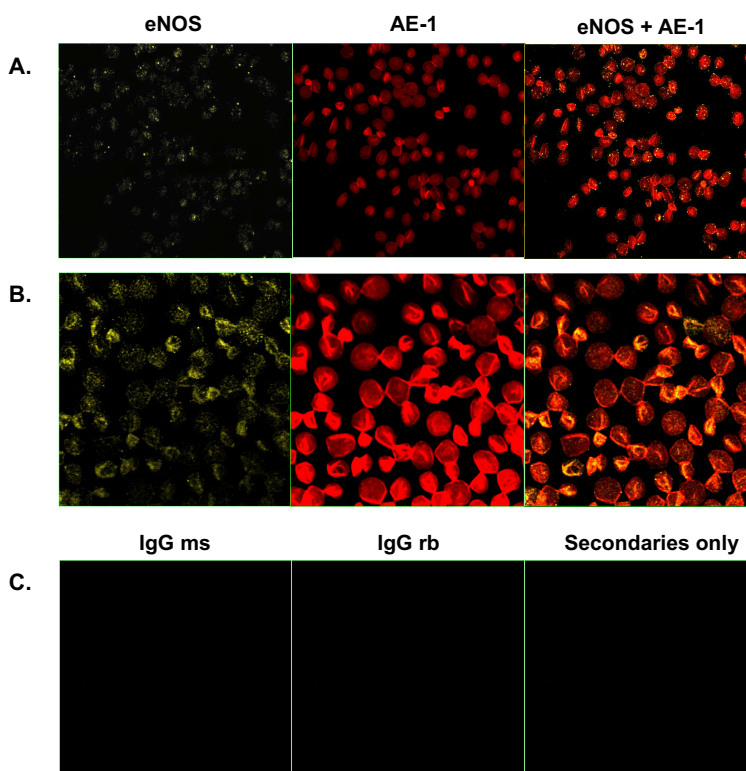


Figure 9 – Immunohistochemistry staining of RBCs from WT mice for eNOS and AE-1 identification

Confocal immunofluorescence microscopy of RBCs using anti-mouse eNOS (yellow) and anti-rabbit AE-1 (red) antibodies shows co-expression of eNOS and AE-1 on the RBC surface. **(A)** immunostaining of 1:200 diluted RBCs with eNOS and AE-1 antibodies, 100x objective without zooming in. **(B)** Immunostaining images of 1:200 diluted RBCs with eNOS and AE-1 antibodies using a 100x objective and increased the zoom. **(C)** Control staining after RBCs incubation with IgG from mouse (ms), IgG from rabbit (rb), and secondary antibodies only. Representation of n = 3 pictures.

In addition, to observe microstructural features inside RBC samples, TEM was carried out. RBCs were dehydrated in ethanol and embedded for sectioning. As a control staining, IgG from mouse, IgG from rabbit, and secondary antibodies only were used in parallel with real experiments. No signal was detected, which demonstrates the specificity of the antibodies used (Figure 10A).

eNOS and AE-1 antibodies were also used in the single staining procedure. Both proteins have been localized along the surface of RBCs, and no signal was detected in the cytoplasm (Figure 10B). For AE-1, the secondary antibody used presented a 25 nm size, while a 15 nm was used for eNOS. The last panel represents the staining with both eNOS and AE-1 antibodies. As can be seen, the proteins are localized on the borders of RBCs, and there is significant proximity of eNOS and AE-1 on the RBC membrane, as shown by dots of different sizes (Figure 10C).

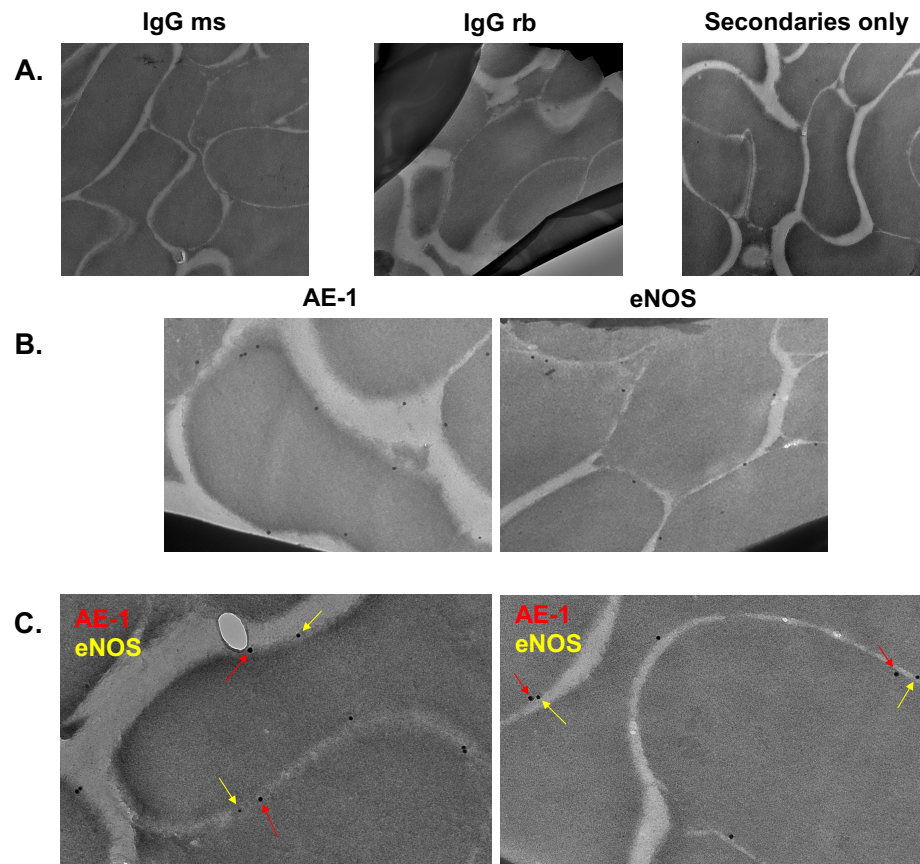


Figure 10 – Transmission electron microscopy on isolated RBCs of WT mice

TEM on washed isolated RBCs evidenced co-expression and proximity of eNOS and AE-1 on RBC membrane. (A) Control staining with IgG from mouse (ms), IgG from rabbit (rb), and secondary antibodies only. No signal was detected. (B) Immunostaining with eNOS or AE-1 shows a specific membrane localization of the proteins. (C) Double staining with eNOS and AE-1 antibodies confirmed the membrane localization of the proteins and evidenced the different sizes of the secondary antibodies (yellow eNOS - red AE-1).

4.2 Generation of tissue-specific conditional eNOS KO mice

This section aimed to create tissue-specific transgenic eNOS mice to investigate the role of vascular eNOS and RBC eNOS in regulating vascular tone and blood pressure.

To dissect the role of eNOS expressed in different compartments, we created different models of tissue-specific eNOS KO mice using the Cre-loxP system (Figure 11).

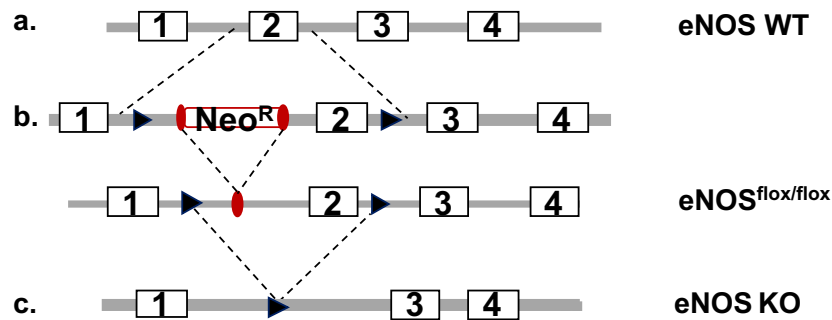


Figure 11 – Genomic construct for gene deletion of eNOS

Scheme describing the gene targeting strategy showing the position of the loxP sequences (black) within the gene targeting construct before and after exon 2 of *Nos3* used to generate the founder eNOS^{flox/flox} mice.

To generate eNOS^{flox/flox} mice, an orphan loxP site and a FRT-neo-FRT-loxP resistance cassette were simultaneously inserted into the eNOS genomic locus to target exon 2 of eNOS for Cre-mediated excision.

To generate EC eNOS KO mice, eNOS^{flox/flox} mice were crossed with *Cdh5*Cre/ERT2^{pos} mice, expressing an ERT2/Cre recombinase fusion protein under the control of a *Cadherin5* (*Cdh5*) promoter.

To induce Cre-mediated excision, a five-day treatment with TAM (75 mg/kg) was necessary via i.p. injections to guarantee the complete absence of eNOS from the ECs (Figure 12A).

To create erythroid-specific eNOS KO mice (RBC eNOS KO), eNOS^{flox/flox} mice were crossed with mice constitutively expressing Cre recombinase in erythroid cells under the control of the promoter for the hemoglobin beta chain (*Hbb*-Cre^{pos}) (Figure 12B).

To generate global eNOS KO mice, eNOS^{flox/flox} mice were crossed with *Deleter*Cre^{pos} mice expressing Cre in all their tissues, promoting a complete ablation of eNOS from the genome (Figure 12C).

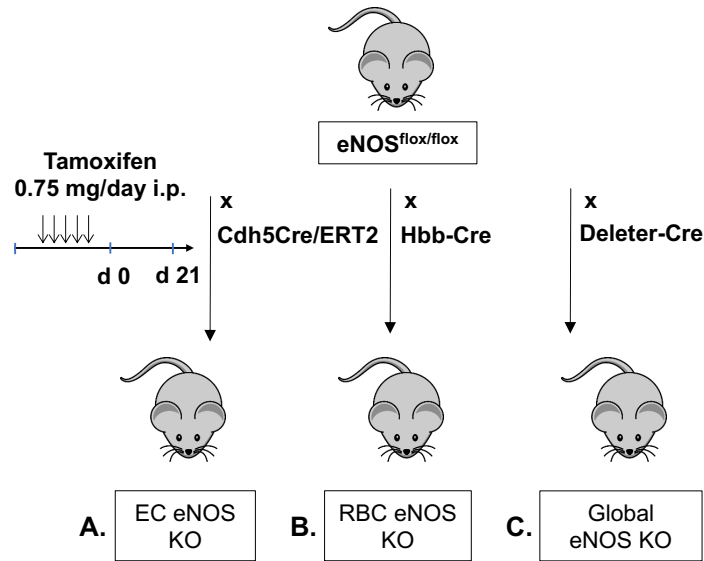


Figure 12 – Crossing strategies for the generation of eNOS KO mice

(A) To generate EC eNOS KO mice and their respective WT control ($eNOS^{flox/flox} Cdh5-Cre/ERT2^{neg}$), the founder $eNOS^{flox/flox}$ mice were crossed with endothelial-specific TAM-inducible $Cdh5-Cre/ERT2^{pos}$ mice to obtain $eNOS^{flox/flox} Cdh5-Cre/ERT2^{pos/neg}$ mice; these were treated with TAM for five days and analyzed after 21 days. (B) To create RBC eNOS KO mice and their respective WT littermate controls, the founder $eNOS^{flox/flox}$ was crossed with erythroid-specific ($HbbCre^{pos}$). (C) The founder $eNOS^{flox/flox}$ mice were crossed with $DeleterCre^{pos}$ mice (expressing Cre in all tissues) to generate global eNOS KO mice and their respective WT littermate controls.

4.3 Determination of eNOS protein expression levels to characterize global eNOS KO and EC eNOS KO and RBC eNOS KO

Next, the aim was to characterize tissue-specific eNOS KO mice to demonstrate the validity of the models.

4.3.1 Characterization of EC eNOS KO mice

qPCR analysis was conducted to analyze the DNA recombination events in the mice genome induced by Cre recombinase. For the qPCR analysis based on gDNA, a probe detecting the exon 2 allele floxed by LoxP sites (FL) and a probe detecting the lack of exon 2 allele (EX) were used.

The primer pairs and a TaqMan probe detected the floxed allele (FL) or detected the excised allele (EX). Analysis with the FL probe showed that EC eNOS KO, RBC eNOS KO, and controls contain the LoxP sequences in their genome in the proper position.

In EC eNOS KO mice and respective WT controls, DNA recombination was evaluated in aorta and BM and showed a signal exclusively in the aortic tissue of EC eNOS KO mice (Figure 13A, blue).

To verify that lack of eNOS leads to decreased eNOS expression, expression levels of eNOS mRNA were first tested with RT qPCR on aortic tissues. eNOS expression was significantly decreased compared to WT littermate controls. On the other hand, Cre expression was detected exclusively in the aorta of EC eNOS KO and not on littermate WT controls (Figure 13B).

To confirm cell-specific ablation, eNOS and Cre expression were also studied in isolated ECs extracted from the lungs of the mice. As assessed by qPCR, this resulted in a lack of eNOS expression in lung ECs (CD31⁺ CD45⁻). No Cre recombinase was detected in tissues from WT control mice, but Cre recombinase expression was detected in EC eNOS KOs (Figure 13C).

Immunoblotting (IB) of aortic lysates of EC eNOS KO and controls confirmed the absence of eNOS in the endothelium of EC eNOS KO mice (Figure 13D).

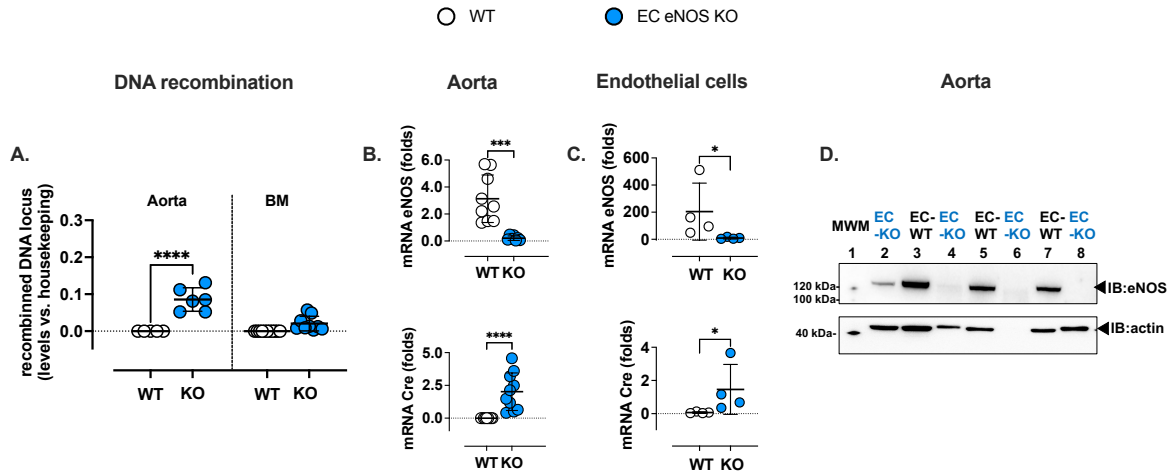


Figure 13 – Characterization of EC eNOS KO mice

(A) Real-time PCR analysis shows that tissue-specific DNA recombination occurs in the aorta of EC eNOS KO mice. No recombination is observed in WT littermate control mice (white). 1-way ANOVA ****p<0.0001; Tukey's multiple comparison test **p<0.01, vs. respective WT control. (B) RT qPCR analysis shows loss of eNOS expression and Cre recombinase expression in the aorta of EC eNOS KO (blue) but not in WT littermate control mice (white). Mann-Whitney t-test; ***p<0.001, ****p<0.0001 vs. respective WT controls. (C) RT qPCR analysis shows that endothelial cells (CD31⁺ CD45⁻) extracted from the lung of EC eNOS KO mice lack eNOS expression as compared to WT controls. * Mann-Whitney test, p = 0.0286. Cre recombinase is expressed in lung endothelial cells from EC eNOS KO, but not in endothelial cells from WT (white) * Mann-Whitney test, p = 0.0286. Data were collected by Sophia Heuser. (D) Immunoblot (IB) analysis shows loss of eNOS (135 kDa) expression in the aorta of EC eNOS KO (eNOS^{fllox/fllox}Chd5CreERT2^{pos} + TAM) mice but not in littermate controls (eNOS^{fllox/fllox}Chd5-CreERT2^{neg} + TAM) after treatment with TAM. Loading control actin (45 kDa). Note: Sample in the first lane shows a residue of eNOS expression in that particular mouse as knockdown efficiency of this model is around 90-95%. Western blot by Lukas Vornholtz.

4.3.2 Characterization of RBC eNOS KO mice

In RBC eNOS KO mice, recombination occurred exclusively in the BM, with a significant difference as compared to WT control mice. In addition, Cre-dependent deletion of exon 2 was confirmed by qPCR in DNA extracted from the bone marrow of RBC eNOS KO mice but was not found in the aorta of the mice (Figure 14A).

eNOS mRNA levels were tested with RT qPCR in aortic tissues. No differences in eNOS expression nor Cre recombinase were detected as compared to WT littermate controls (Figure 14B).

Analysis of isolated CD31⁺ ECs extracted from lung tissue showed that eNOS expression was fully preserved in lung ECs of RBC eNOS KO, with no differences as compared to littermate WT controls (Figure 14C).

To characterize RBC eNOS KO, erythroid cells were isolated from BM. RT qPCR analysis showed that Cre recombinase was expressed in the BM of RBC eNOS KO mice but not in WT controls (Figure 13D,

bottom panel). IB of aortic lysates of RBC eNOS KO and controls showed no differences of eNOS expression in RBC eNOS KO mice (Figure 14E, 14F). IP of RBC lysates showed eNOS expression in WT mice and lack of eNOS in global eNOS KO mice (gKO) and RBC eNOS KO mice.

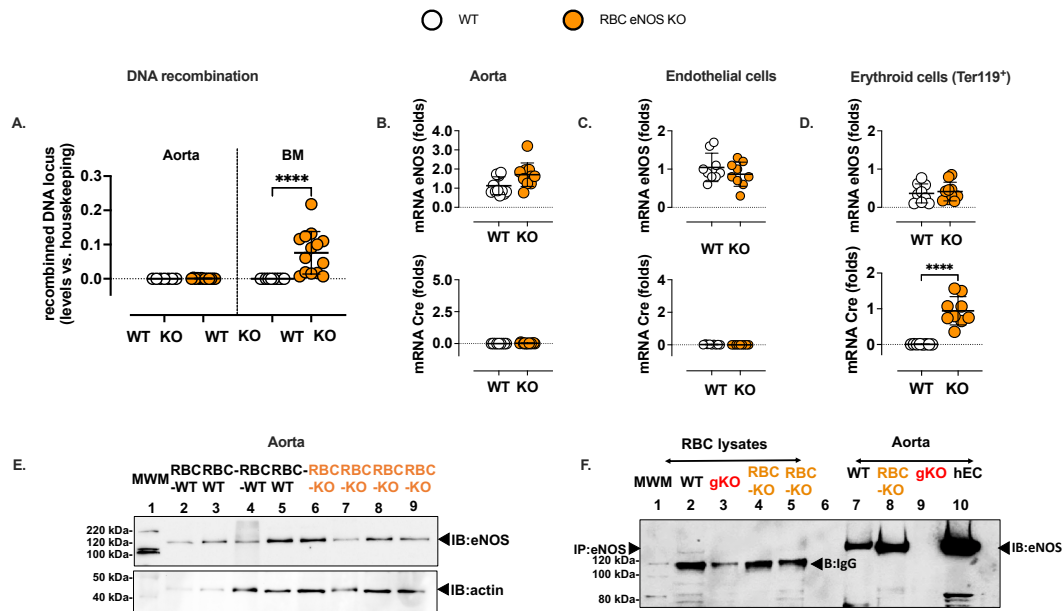


Figure 14 – Characterization of RBC eNOS KO mice

(A) qPCR analysis shows that tissue-specific DNA recombination occurs in the BM of RBC eNOS KO mice (0.08 ± 0.06 for RBC eNOS KO; $n = 14$). No recombination is observed in WT littermate control mice (white). 1-way ANOVA **** $p < 0.0001$; Tukey's multiple comparison test ** $p < 0.01$, **** $p < 0.0001$ vs. respective WT control. (B) RT qPCR analysis shows no significant changes in eNOS expression in the aorta of RBC eNOS KO. No Cre is expressed in the aorta of RBC eNOS KO nor WT controls. Mann-Whitney t-test. (C) Expression of eNOS in lung EC (CD31⁺ CD45⁺) from RBC eNOS KO is not different from WT control. Cre recombinase is not expressed in lung endothelial cells from RBC eNOS KO and WT mice. Mann-Whitney t-test. Data collected by Sophia Heuser. (D) Real-time RT PCR analysis shows eNOS expression and Cre recombinase expression in the bone marrow of RBC eNOS KO mice. Cre-recombinase is expressed in the bone marrow of RBC eNOS KO mice but not in the BM of WT littermate controls. Similar levels of eNOS expression were detected in the BM of RBC eNOS KO, and WT controls due to the high abundance of endothelial cells in the bone marrow. **** $p < 0.0001$ Mann-Whitney test vs. WT mice. (E) Immunoblot of the aorta of RBC eNOS KO mice and WT littermate controls, showing that eNOS expression is not different in these two groups. Western blot by Lukas Vornholtz. (F) Immunoprecipitation (IP) of eNOS (135 kDa) from RBC lysates show eNOS expression in WT mice and lack of eNOS in global eNOS KO mice (gKO) and RBC eNOS KO mice. The IgG (120 kDa) is seen in the IP samples. Western blot by Sivatharsini Thasian-Sivarajah.

To summarize, tissue-specific eNOS KO mice were generated and characterized by different molecular biology techniques. EC eNOS KO mice were characterized by specific deletion of eNOS from the vascular compartment; RBC eNOS KO mice showed DNA recombination exclusively in the BM and were characterized by specific removal of eNOS from erythroid cells.

4.4 Blood count

Blood count analysis was carried out to investigate possible changes in the hematology of EC eNOS KO and RBC eNOS KO upon specific eNOS deletion.

Blood parameters were analyzed (Table 12). EC eNOS KO were compared with WT controls (eNOS^{flx/flx} Cdh5Cre/ERT2^{neg} + TAM); RBC eNOS KO mice were compared with the founder line eNOS^{flx/flx}.

The analysis showed no significant differences and thus unaltered hematology in mice lacking eNOS, specifically in ECs or RBCs.

Table 12 – Blood count parameters evaluated in EC eNOS KO and RBC eNOS KO mice

The table summarizes the blood count parameters measured in EC eNOS KO, RBC eNOS KO mice, and WT controls. Abbreviations: RBC, red blood cells; HCT, hematocrit; HGB, hemoglobin; RDW, RBC distribution width; MCHC, mean corpuscular hemoglobin concentration; MCH, mean corpuscular hemoglobin; MCV, mean corpuscular volume; WBC, white blood cells; Lymph, lymphocytes; Mo, monocytes; and Gra, granulocytes; PLT, platelet count; MPV, mean platelet volume. All data are expressed as mean \pm SD. T-test.

	WT	EC eNOS KO		WT	RBC eNOS KO	
	eNOS ^{flx/flx} Cdh5Cre/E RT2 ^{neg} +TAM	eNOS ^{flx/flx} Cdh5Cre/E RT2 ^{pos} +TAM	P	eNOS ^{flx/flx}	eNOS ^{flx/flx} HbbCre ^{pos}	P
n	9	15		6	12	
Red blood cell count						
RBC (10⁶/μl)	9.93 \pm 1.94	11.29 \pm 1.60	0.0745	9.26 \pm 1.65	9.64 \pm 1.58	0.6477
HCT (%)	50.78 \pm 10.11	56.93 \pm 8.87	0.1324	47.95 \pm 7.79	47.51 \pm 5.20	0.8902
HGB (g/dl)	14.90 \pm 3.50	16.75 \pm 2.75	0.1639	15.03 \pm 2.85	14.99 \pm 3.06	0.9782
Red blood cell indexes						
RDW (%)	15.10 \pm 0.88	14.87 \pm 0.37	0.3720	16.06 \pm 1.46	15.14 \pm 0.61	0.2625
MCHC (g/dl)	29.19 \pm 2.18	29.41 \pm 1.34	0.7568	31.25 \pm 1.21	30.05 \pm 1.83	0.0613
MCH (pg)	14.91 \pm 1.24	14.87 \pm 0.67	0.9234	16.22 \pm 0.44	15.49 \pm 0.93	0.0907
MCV (μm³)	51.22 \pm 1.86	50.67 \pm 0.72	0.3068	52.00 \pm 0.89	51.50 \pm 1.57	0.4829
White blood cell count						
WBC (10³/μl)	9.73 \pm 2.20	6.70 \pm 0.85	0.1727	7.93 \pm 2.35	6.91 \pm 2.77	0.4498
Lymph (10³/μl)	5.14 \pm 1.76	4.04 \pm 1.49	0.1231	5.13 \pm 2.05	4.34 \pm 1.71	0.3974
Lymph (%)	70.63 \pm 7.74	70.80 \pm 11.64	0.9700	65.15 \pm 12.82	65.36 \pm 13.90	0.9759
Mo (10³/μl)	0.32 \pm 0.16	0.29 \pm 0.07	0.6504	0.40 \pm 0.25	0.31 \pm 0.24	0.4671
Mo (%)	5.00 \pm 1.78	5.97 \pm 1.74	0.2045	5.73 \pm 3.27	4.95 \pm 1.85	0.5212
Gra (10³/μl)	2.27 \pm 0.81	1.99 \pm 0.61	0.4893	2.40 \pm 0.98	2.23 \pm 1.50	0.8097
Gra (%)	24.33 \pm 8.41	23.24 \pm 11.11	0.8018	28.95 \pm 9.80	29.69 \pm 103.18	0.9084
Platelet count						
PLT (10³/μl)	1134.90 \pm 479.51	1144.07 \pm 334.80	0.9575	1770.67 \pm 13.18	1570.00 \pm 348.28	0.1957
MPV (μm³)	5.11 \pm 0.25	5.34 \pm 0.33	0.1257	5.78 \pm 0.34	5.78 \pm 0.61	0.9956

4.5 Evaluation of the impact of the absence of EC eNOS and RBC eNOS on cardiovascular homeostasis and systemic hemodynamics

To analyze the specific role of vascular eNOS and red cell eNOS in the regulation of vascular function, cardiovascular hemodynamics, and blood pressure, analysis of flow-mediated dilation (FMD), echocardiography, and blood pressure *in vivo*, and aortic rings relaxation *ex vivo* were evaluated.

4.5.1 Vascular endothelial function is lost in EC eNOS KO and preserved in RBC eNOS KO mice

Ex vivo measurements of vascular endothelial function in aortas of eNOS KO and WT mice were executed. Aortic rings of EC eNOS KO and RBC eNOS KO mice and their respective WT littermate controls were mounted on the organ bath system, and measurements were started after injections of acetylcholine (ACh), phenylephrine (PE), and sodium nitroprusside (SNP).

The selective removal of eNOS from the endothelium caused a complete loss of NO-dependent vascular endothelial function in EC eNOS KO mice, as demonstrated by the lack of ACh-induced vasodilation of aortic rings *ex vivo* (Figure 15A). On the other hand, RBC eNOS KO mice showed no changes in ACh-mediated vasodilation of aortic rings (Figure 15D).

The responses to the constrictor PE and the NO donor SNP were fully preserved in the aorta of both mouse strains (Figure 15B, 15C, 15E, 15F). In EC eNOS KO, we observed a significant leftward shift in the SNP-mediated response, which indicates an increased sensitivity to NO donors; this response has been observed upon inhibition of NOS activity and in different strains of global eNOS KO mice [133-135].

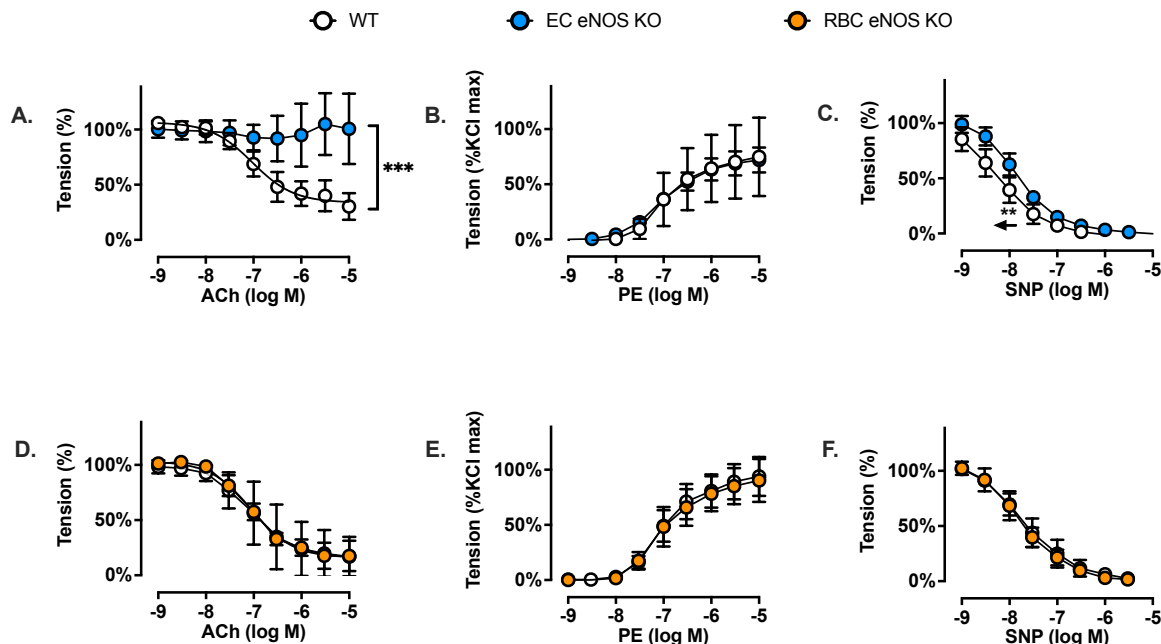


Figure 15 – Vascular endothelial dilator function is lost in EC eNOS KO and preserved in RBC eNOS KO

NO-dependent vascular endothelial function is fully abolished in EC eNOS KO and fully preserved in RBC eNOS KO. (A) Pre-constricted aortic rings from EC eNOS KO lacks acetylcholine (ACh)-induced vasodilation (2-way repeated measurement (RM)-ANOVA $p < 0.0001$; Sidak's *** $p < 0.001$ vs. WT control for concentrations of ACh $> 10^{-6.5}$ M ($n = 6$ per group). (B) The contractile response of aortic rings to increasing phenylephrine (PE) concentrations is not different in EC eNOS KO. (C) The vasodilatory response of aortic rings to increasing sodium nitroprusside (SNP) concentrations is increased in EC eNOS KO. (D) In aortic rings from RBC eNOS, KO (orange) ACh-induced vasodilation was not different from WT littermates (white). 2-way RM-ANOVA $p < 0.0001$. $n = 5$ per group. (E) The contractile response of aortic rings to increasing PE concentrations is not different in RBC eNOS KO. (F) The vasodilatory response of aortic rings to increasing concentrations of the NO donor sodium nitroprusside (SNP) is fully preserved in RBC eNOS KO mice, as compared to their littermate WT controls. 2-way-ANOVA $p < 0.0001$; Sidak's ** $p < 0.01$ $10^{-9} > \text{SNP} > 10^{-7.5}$ M. Data collected in collaboration with Lukas Vornholtz.

4.5.2 FMD is lost in EC eNOS KO and preserved in RBC eNOS KO mice

FMD was evaluated in EC eNOS KO mice before and after TAM treatment. Before TAM injection, EC eNOS KO had an FMD profile comparable to WT littermate controls (Figure 16A). TAM treatment induced a loss of eNOS in the ECs. This is accompanied by an abrogated FMD response in the iliac artery as determined by ultrasound *in vivo* compared to WT littermate controls (Figure 16B).

RBC eNOS KO mice, on the other hand, showed a normal FMD, with no significant differences, as compared to WT littermate controls (Figure 16C).

These results are consistent with fully preserved eNOS expression and activity in the vasculature. Furthermore, preservation of eNOS activity and function in conductance vessels of RBC eNOS KO mice indicates no off-target effects of genetic knockdown in vascular tissue.

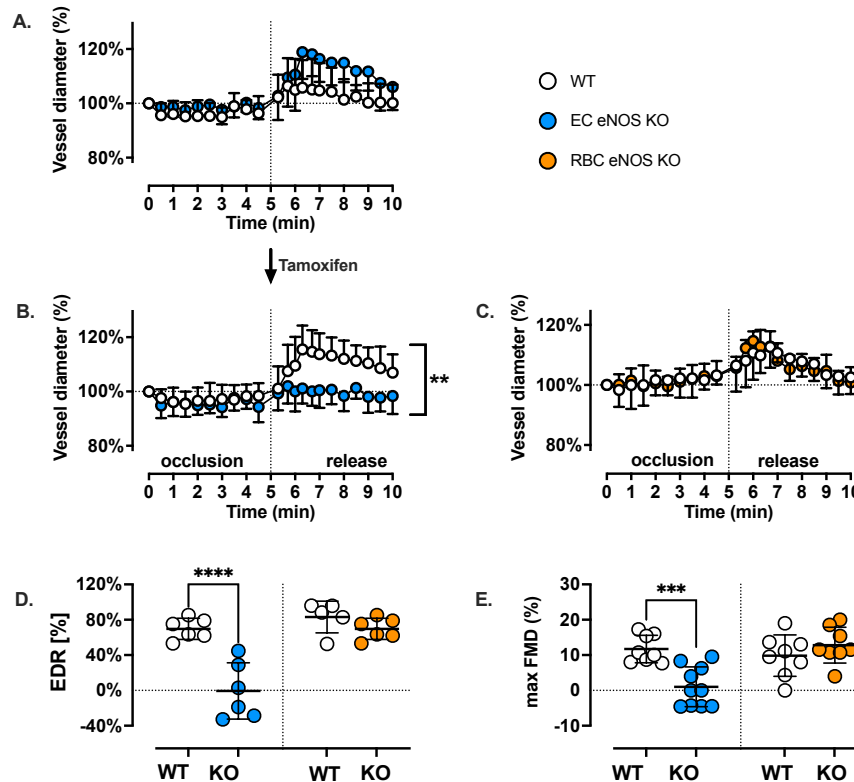


Figure 16 – Flow-mediated dilation evaluation in EC eNOS KO and RBC eNOS KO mice

(A) FMD of the iliac artery assessed *in vivo* by ultrasound before TAM treatment is fully functional in EC eNOS KO (n = 13) and WT controls (n = 6). (B) After TAM, flow-mediated dilation (FMD) of the iliac artery assessed *in vivo* by ultrasound is abolished in EC eNOS KO (blue) (2-way RM-ANOVA $p < 0.0001$; Sidak's $** p < 0.01$ vs. WT control (white) for $t > 6.3$ min; n = 10 per group). (C) FMD of the iliac artery is fully preserved in RBC eNOS KO mice (2-way RM-ANOVA $p < 0.0001$, n = 8 per group). (D) Endothelium-dependent relaxation in response to ACh (calculated as the percentage of the maximal ACh response) is significantly impaired in EC eNOS KO and fully preserved in RBC eNOS KO compared to their respective WT controls. (E) Maximal FMD (corresponding to the percentage of maximal flow-mediated dilator response) is significantly decreased in EC eNOS KO mice and fully preserved in RBC eNOS KO mice compared to their respective WT controls. Lines represent means \pm standard deviation (SD).

To conclude, eNOS expressed in the endothelium plays a major role in modulating vascular endothelial function. FMD was completely lost in EC eNOS KO as well as ACh response of aortic rings.

On the other hand, FMD and vascular function were fully preserved in RBC eNOS KO as compared to WT littermate controls.

4.5.3 EC eNOS KO mice and RBC eNOS KO mice are hypertensive

To evaluate the role of EC eNOS and RBC eNOS in the modulation of BP, Millar catheterization of the right carotid artery was performed (Figure 17).

Global eNOS KO (gKO) mice were used as control, HbbCre mice were used to evaluate a possible effect of Cre on mean arterial pressure (MAP). HbbCre^{neg} and HbbCre^{pos} mice showed no difference in MAP, indicating that the presence/absence of Cre was not affecting blood pressure measurements. HbbCre^{pos} mice were compared to WT mice (C57BL/6J), and no differences were detected (Figure 17A).

Measurements of BP using a pressure catheter demonstrated that EC eNOS KO mice have a significantly higher MAP (Figure 17B, blue) as compared to their WT littermates, and it was characterized by a difference of 15-18 mmHg in both systolic blood pressure (SBP) and diastolic blood pressure (DBP). However, neither difference in heart rate (HR) was detected in both groups (Table 13).

MAP was also significantly increased in RBC eNOS KO mice as compared to their WT littermates (figure 17B, orange), and it was characterized by a 14 mmHg increase in SBP, 8 mmHg increase in DBP, and no differences in HR (Table 13).

gKO mice were generated from the founder line eNOS^{flx/flx} crossed with DeleterCre^{pos}. An increase of 17-23 mmHg in SBP and DBP was detected as compared to WT mice (Figure 17B, gKO, red).

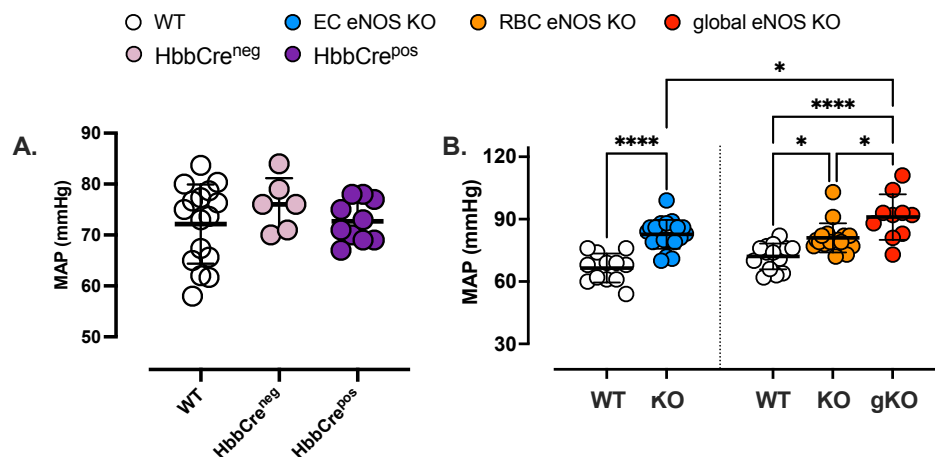


Figure 17 – Red cell eNOS and endothelial eNOS both contribute to blood pressure homeostasis

(A) Invasive measurements of blood pressure (BP) in anesthetized mice show that HbbCre^{neg} mice (76 ± 5 mmHg, $n = 6$) and HbbCre^{pos} mice (73 ± 4 mmHg, $n = 10$) have blood pressure comparable with the one observed in WT control mice (74 ± 5 mmHg, $n = 8$). 1-way ANOVA $p < 0.001$; Tukey $*p < 0.05$; $****p < 0.0001$. (B) Invasive measurements of blood pressure (BP) in anesthetized mice show that both EC eNOS KO (MAP = 83 ± 7 mmHg, $n = 19$) and RBC eNOS KO mice (MAP = 80 ± 8 mmHg, $n = 16$) have increased MAP as compared to their respective WT littermate controls. Global eNOS KO mice (gKO = eNOS^{flx/flx} DeleterCre) are hypertensive and show significantly higher MAP (91 ± 1 mmHg; $n = 10$) as compared to EC eNOS KO and RBC eNOS KO. 1-way ANOVA $p < 0.001$; Tukey $*p < 0.05$; $****p < 0.0001$.

Table 13 – Blood pressure and heart rate in all the eNOS KO strains investigated

Abbreviations: SBP, systolic blood pressure; DBP, diastolic blood pressure; MAP, mean arterial pressure; SVR, systemic vascular resistance; RPP, rate pressure product.

	Strain	Genotype	Litter size	Body weight (g)	SBP (mmHg)	DBP (mmHg)	MAP (mmHg)	HR (bpm)	RPP (mmHg*bpm)	n
1	WT	C57BL/6J	6±3	29.7±1.9	92±9.4	59±10	74±5.2	504±51	46 144±6 027	8
2	HbbCre ^{neg}	HbbCre ^{neg}	6±3	33.0±2.1	95±5	67±5	76±5	563±35	53 320±5 405	6
	HbbCre ^{pos}	HbbCre ^{pos}		33.3±3.2	91±5	64±4	73±4	575±48	52 093±5 266	10
3	WT	eNOS ^{flx/flx}	7±2	30.3±2.5	92±8	62±9	71±1	543±67	49 591±5 512	14
4	WT	eNOS ^{flx/flx} Cdh5Cre/ERT2 neg +TAM	6±2	29.3±3.6	86±5	57±8	67±7	564±53	48 413±5 018	12
	EC eNOS KO	eNOS ^{flx/flx} Cdh5Cre/ERT2 pos +TAM		29.4±3.1	104±8	72±7	83±7	535±58	55 696±6 929	19
5	WT	eNOS ^{flx/flx} HbbCre ^{neg}	6±2	29.1±2.1	89±9	61±1	70±1	528±56	46 622±5 306	15
	RBC eNOS KO	eNOS ^{flx/flx} HbbCre ^{pos}		29.7±2.6	103±1	69±7	80±8	476±93	48 506±9 392	16
6	gKO	eNOS ^{flx/flx} DeleterCre ^{pos}	4±2	30.2±2.6	115±1	79±1	91±1	516±76	56 275±20 504	10

4.5.4 No differences are detected in cardiac parameters in EC eNOS KO and RBC eNOS KO mice but significant increase in systemic vascular resistance

To evaluate the impact of the absence of eNOS from the ECs or the RBCs, respectively, echocardiography was performed in a sub-cohort of mice.

Cardiac function and BP were evaluated in parallel in the same mouse.

No changes in cardiac output (CO) or HR were observed in EC eNOS KO or RBC eNOS KO mice as assessed by echocardiography (Figure 18A, 18B), as well as for stroke volume (SV), ejection fraction (EF), end-diastolic volume (EDV), and end-systolic volume (ESV). HR assessed invasively by a Millar catheter was also not different between the groups (Table 14).

Systemic vascular resistance (SVR), estimated as the ratio between MAP and CO, was higher in both strains than their respective WT controls (Figure 18C).

These results demonstrated that EC eNOS and red cell eNOS contribute independently to BP homeostasis.

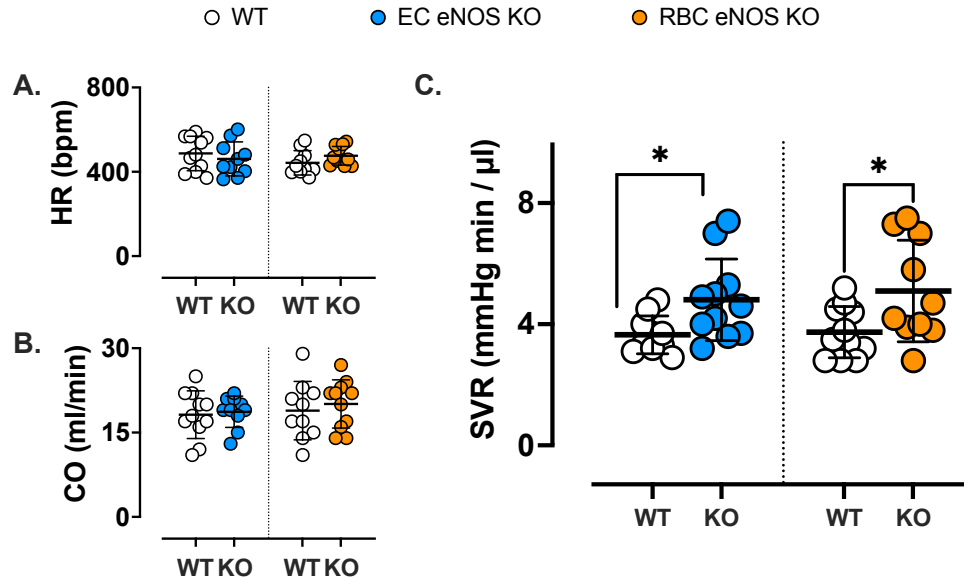


Figure 18 – RBC eNOS has an impact on SVR

SVR was estimated in a sub-cohort of mice by measuring MAP and cardiac output (CO) by ultrasound in the same animal ($SVR \approx MAP/CO$) and was significantly increased in both EC eNOS KO and RBC eNOS KO as compared to their respective controls. 1-way-ANOVA * $p = 0.0149$; T-test Welch * $p < 0.05$. **A:** The heart rate depicted here represents the values measured by cardiac ultrasound. **B:** Cardiac output. See also Table 12 for other cardiac parameters.

Table 14 – Systemic hemodynamics assessed in a sub-cohort of mice by measurements of echocardiography and Millar in the same individual

T-test vs. respective control group. *p<0.05; **p<0.01; ***p<0.001; ****p<0.0001 Abbreviations: HR, heart rate; CO, cardiac output; SV, stroke volume; EDV, end diastolic volume; ESV, end systolic volume; Millar: SBP, systolic blood pressure; DBP, diastolic blood pressure; MAP, mean arterial pressure; SVR, systemic vascular resistance; RPP, rate pressure product.

	WT	EC eNOS KO		WT	RBC eNOS KO	
	eNOS ^{fllox/fllox} Cdh5Cre/ERT2 ^{neg} +TAM	eNOS ^{fllox/fllox} Cdh5Cre/ERT2 ^{pos} +TAM	p	eNOS ^{fllox/fllox} HbbCre ^{neg}	eNOS ^{fllox/fllox} HbbCre ^{pos}	p
n	10	11		11	9	
Echocardiography						
HR (bpm)	461±8	487±82	0.4743	476±44	448±59	0.2514
CO (ml/min)	19±3	18±4	0.7426	20±4	19±5	0.4979
SV (μl)	41±8	37±5	0.1274	42±7	41±11	0.8748
EDV (μl)	64±2	66±14	0.8169	79±17	83±33	0.7287
ESV (μl)	23±1	29±15	0.3386	37±16	42±25	0.6154
EF (%)	67±1	58±15	0.1740	55±14	52±11	0.5152
Millar						
HR (bpm)	555±55	537±56	0.4586	511±53	487±101	0.5381
SBP (mmHg)	86±4	103±10	<0.0001* ***	91±6	105±13	0.0107 *
DBP (mmHg)	57±7	71±9	0.0007 ***	63±8	71±8	0.0464 *
MAP (mmHg)	67±6	82±9	0.0002 ***	73±7	82±9	0.0176 *
SVR (mmHg/ml/min)	3.7±0.6	4.8±1.3	0.0220*	3.7±0.8	4.8±1.5	0.0797
RPP (mmHg*bpm)	47 418±4 152	55 248±7 061	0.0063**	46 302±4 099	50 951±10 560	0.2412

To summarize, this set of experiments demonstrated that EC eNOS KO mice had impaired FMD and vascular endothelial function caused by an efficient KO of the eNOS protein.

On the other hand, RBC eNOS KO mice showed a fully preserved FMD and vascular functionality following ACh administration.

Interestingly both EC eNOS KO and RBC eNOS KO mice showed significantly increased MAP as compared to the respective WT controls, but no differences in cardiac parameters were detected.

These results indicate an independent role of vascular eNOS and red cell eNOS in the modulation of vascular tone and blood pressure.

4.6 Generation of tissue-specific conditional eNOS KI mice

Conditional tissue-specific eNOS KI mice were generated to analyze the effect of reactivation of eNOS in ECs or RBCs in an otherwise global eNOS KO construct.

4.6.1 Test of the efficiency of the gene reactivation construct

A Cre-inducible eNOS knock-in (KI) gene construct (eNOS^{inv/inv}) was generated by inserting an inverted exon 2 and two additional LoxP511 sites in the eNOS genomic construct. These mice are conditional eNOS KO mice (CondKO), and the construct allows Cre-induced activation of eNOS in the tissue of interest (Figure 19).

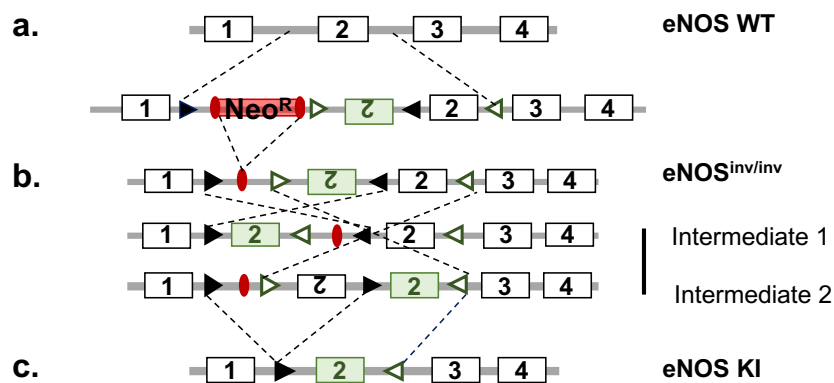


Figure 19 – Genomic construct for gene reactivation of eNOS

Scheme describing the gene targeting strategy showing the position of a loxP (black) and loxP511 (green) sequences within the gene targeting construct used to generate eNOS^{inv/inv} mice, which are conditional eNOS KO mice (CondKO).

To test the efficiency of the construct *in vivo*, CondKO mice were crossed with DeleterCre^{pos} mice (Figure 20).



Figure 20 – Test efficiency of the gene reactivation construct

To test the efficiency of the eNOS gene reactivation construct, CondKO mice were crossed with DeleterCre mice, and global eNOS KI mice were generated.

The generation of global eNOS KI mice as proof of concept for the efficiency of the gene reactivation model required different crossing steps. A specific crossing strategy was necessary to generate the inv/inv allele (-), the WT allele (+), and the flipped allele (FL) (Figure 21).

The different generations obtained also comprised heterozygous mice for the FL allele, indicated as fl/-. Heterozygous mice served to evaluate a possible gene dosage behavior of eNOS as compared to CondKO controls and homozygous fl/fl mice. Four different generations were created to get fl/fl and fl/- mice, as shown in table 15. P3 and P4 were the final necessary progenitor lines crossed to generate the lines of interest in a high percentage (Table 15).

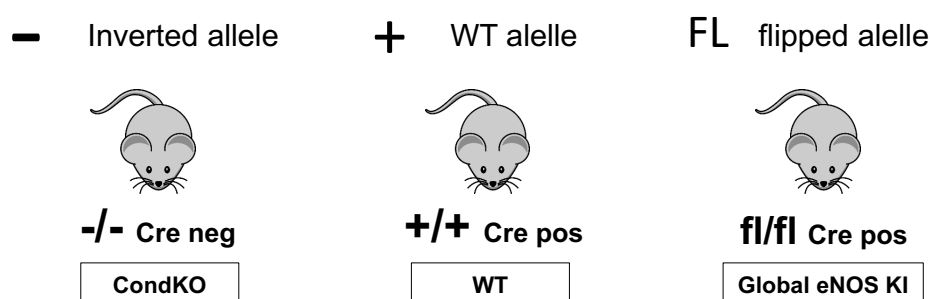


Figure 21 – Representation of the three alleles used to test the generation of the KI model

The inverted allele is represented as a “-“ and homozygous -/- mice represent the CondKO mice. The “+” symbol represents the WT allele, and the “FL” represents the flipped allele. fl/fl Cre positive mice are global eNOS KI mice.

Table 15 – Generation of heterozygous and homozygous global eNOS KI

eNOS^{inv/inv} Cre^{neg} were crossed with different murine lines generated from three different progenitor lines (P1, P3, P4) to generate the lines of interest: heterozygous (fl/-) and homozygous global eNOS KI (fl/fl). When Cre is present, the negative allele (-) is flipped.

Progenitor line	Crossing	Final line	Resulting generation
P1	-/- Cre neg X +/+ Cre pos	F1	-/+ Cre pos = fl/+ Cre pos -/+ Cre neg = -/+ Cre neg
P2	-/- Cre neg X fl/+ Cre pos	F2	fl/- Cre pos = fl/fl Cre pos fl/- Cre neg = fl/- Cre neg +/- Cre pos = +/fl Cre pos +/- Cre neg = +/- Cre neg
P3	-/- Cre neg X fl/fl Cre pos	F3	fl/- Cre pos = fl/fl Cre pos fl/- Cre neg = fl/- Cre neg
P4	-/- Cre neg X fl/- Cre pos	F4	fl/- Cre pos = fl/fl Cre pos fl/- Cre neg = fl/- Cre neg -/- Cre neg = -/- Cre neg

4.6.2 eNOS gene dosage effect in global eNOS KI mice

qPCR analysis was conducted to analyze Cre-induced recombination of the eNOS gene. Two different probes were used for the qPCR analysis based on gDNA to detect recombination events: an Inv-probe (INV) that recognized the inverted allele and a Flip-probe (FLIP) to recognize the flipped allele. Aortic samples were collected and analyzed.

The global eNOS KI line was analyzed to identify a correlation between the genotype of the mice and eNOS expression levels. The efficiency of the mice model to induce a global eNOS reintroduction from the founder line eNOS^{inv/inv} was evaluated by RT qPCR. eNOS expression was studied in the aorta of the mice of interest (Figure 22A). Heterozygous fl/- and homozygous fl/fl were analyzed. 1-way ANOVA, multiple comparisons evaluated statistical significance among the groups. A significant difference was detected in fl/- heterozygous mice (n = 4) compared to the eNOS^{inv/inv} founder line. However, because only an n of 1 was analyzed for fl/fl mice, no statistical difference could be evaluated between fl/- and fl/fl mice, even if a tendency of increased values can be speculated (Figure 22A).

To further confirm the exclusive presence of eNOS on protein level in the endothelium of global eNOS KI mice after TAM treatment, the aorta of the mice was collected and lysed, and western blot experiments were performed. Figure 22B shows the representative western blot for eNOS protein in the aortic tissue of global eNOS KI and eNOS^{inv/inv} controls. In the aorta of the founder line, no eNOS protein was expressed (position 3, 4, 5), while clear bands were detected in global eNOS KI mice (well 6, 7, 8) and WT controls (well 1, 2). Actin served as a loading control (Figure 22B).

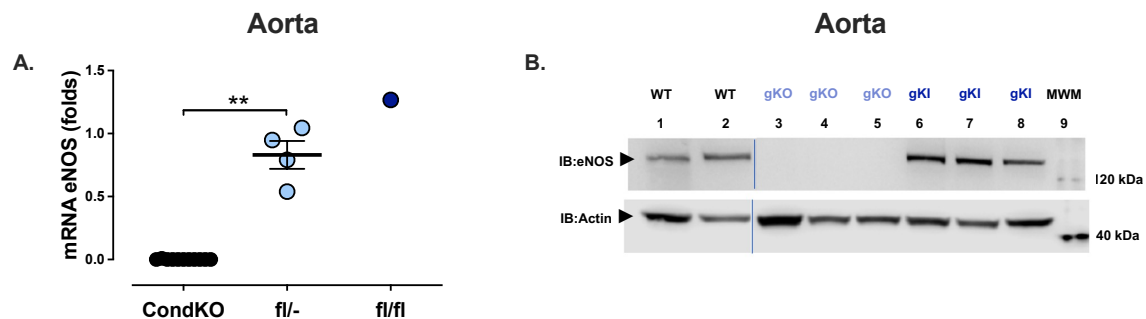


Figure 22 – Characterization of global eNOS KI mice

(A) eNOS expression levels were analyzed in the aorta of global eNOS KI. Heterozygous fl/- mice (0.83 ± 0.22 ; n = 4) and fl/fl (1.27, n = 1), showing a tendency to a gradual reintroduction of eNOS in heterozygous fl/- and homozygous fl/fl. A significant difference is detected in fl/- heterozygous mice (n=4) as compared to eNOS^{inv/inv} founder line; **p=0.0036. Because of a reduced number of samples, only speculations are possible. T-test, *p<0.05, **p<0.01, ***p<0.0001. (B) Western blot analysis demonstrating eNOS expression after Cre-dependent reactivation of eNOS expression. Wells 3-5 and 6-8 are representatives of 3 independent analyses. Western blot by Wiebke Lückstädt.

4.6.3 Tissue-specific eNOS KI mice

To generate endothelial-specific eNOS KI mice, $eNOS^{inv/inv}$ mice were crossed with $Cdh5Cre/ERT2^{pos}$ mice to obtain $eNOS^{inv/inv} Cdh5Cre/ERT2^{pos}$ and $eNOS^{inv/inv} Cdh5Cre/ERT2^{neg}$ mice (CondKO). To induce endothelial-specific activation of the Cre recombinase, TAM was injected for five days at the dose of 75 mg/kg/day (Figure 23A).

Homozygous $eNOS^{inv/inv}$ mice were crossed with erythroid-specific $HbbCre^{pos}$ mice, to obtain erythroid-specific eNOS KI mice ($eNOS^{inv/inv} HbbCre^{pos}$; RBC eNOS KI) and their CondKO littermate controls ($eNOS^{inv/inv} HbbCre^{neg}$) (Figure 23B).

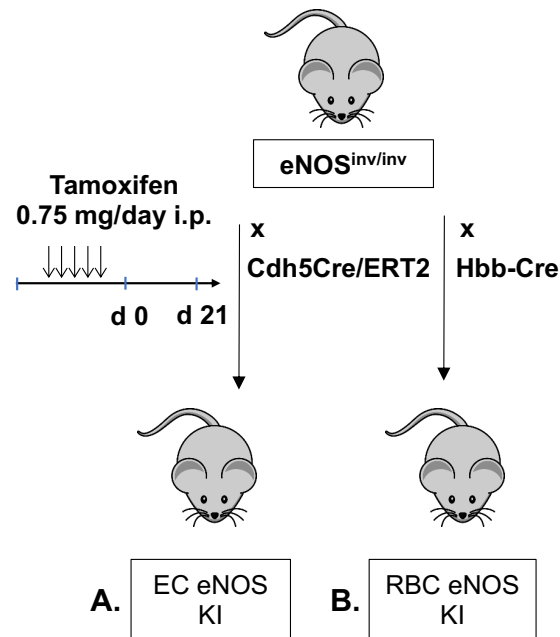


Figure 23 – Generation of tissue-specific eNOS KI mice

Schematic representation of the crossing strategy. (A) To create EC eNOS KI mice, $eNOS^{inv/inv}$ mice were crossed with endothelial-specific TAM-inducible Cre mouse ($Cdh5Cre/ERT2^{pos}$) and treated with TAM for five days and analyzed after 21 days. (B) To create RBC eNOS KI mice, $eNOS^{inv/inv}$ mice were crossed with erythroid-specific ($HbbCre^{pos}$) mice.

4.7 Determination of eNOS protein expression levels in EC eNOS KI and RBC eNOS KI mice

The next aim was to characterize tissue-specific eNOS KI mice to demonstrate the validity of the models.

4.7.1 Characterization of tissue-specific eNOS KI mice

Significant DNA recombination was detected in the aorta and BM of EC eNOS KI as compared to CondKO littermate controls (Figure 24A).

Organs were harvested 21 days after TAM treatment, and eNOS and Cre mRNA levels were evaluated with RT qPCR in the aorta of EC eNOS KI after RNA isolation (Figure 24B, upper panel). No Cre was detected in the tissues from CondKO control mice, but significantly higher eNOS levels were detected in EC eNOS KI. eNOS expression was significantly higher in EC eNOS KI as compared to the respective CondKO littermate controls, where no eNOS was detected (Figure 24B, bottom panel).

To analyze eNOS protein expression, IB was performed. As shown, eNOS reintroduction occurred exclusively in the aortic tissue of EC eNOS KI (well 2), while no eNOS was expressed in the aorta of CondKO controls (well 3). WT mice and tissue-specific eNOS KO mice were loaded on the same blot; actin served as loading control (Figure 24C).

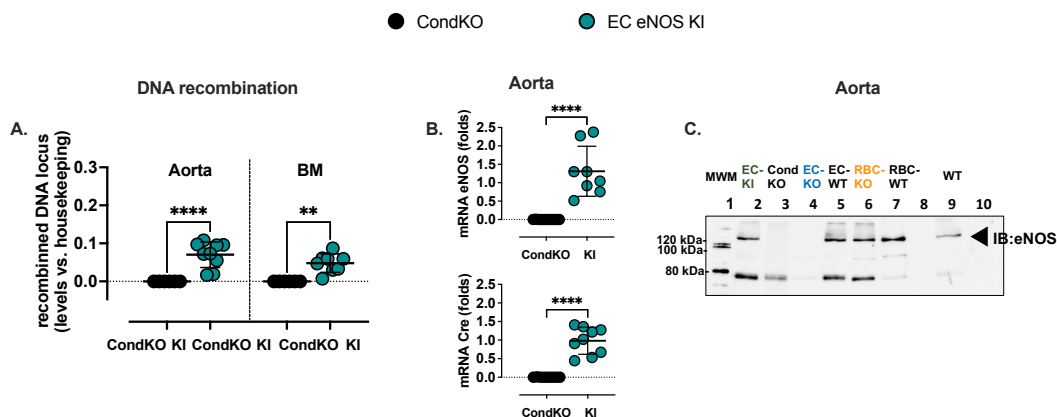


Figure 24 – Characterization of EC eNOS KI mice

(A) qPCR analysis shows that tissue-specific DNA recombination occurs in the aorta (0.07 ± 0.03 , $n = 9$) and BM (0.05 ± 0.02 , $n = 8$) of EC eNOS KI mice (green). No recombination is observed in CondKO littermate control mice (black). 1-way ANOVA $p < 0.0001$; Tukey's multiple comparison test $*p < 0.05$, $****p < 0.0001$ vs. respective CondKO control. (B) RT qPCR analysis shows eNOS (1.31 ± 0.68 , $n = 11$) and Cre (0.98 ± 0.36 , $n = 9$) expression in the aorta of EC eNOS KI mice, but not in CondKO littermate control mice. Mann-Whitney t-test. (C) Representative immunoblot analysis demonstrating eNOS expression after Cre-dependent reactivation of eNOS in aorta EC eNOS KI mice compared to CondKO, EC eNOS KO RBC eNOS KO, and WT controls. Actin was used as loading control (45 kDa).

No recombination was observed in aortic tissue when evaluating DNA recombination in RBC eNOS KO and CondKO controls. On the other hand, a significant difference was detected in the BM of RBC eNOS KI and the respective CondKO littermate controls (Figure 25A).

eNOS mRNA levels were evaluated with RT qPCR in the aorta of the mice after RNA isolation, and no eNOS was expressed in RBC eNOS KI and CondKO controls (Figure 25B).

Erythroid cells were isolated from BM. RT qPCR analysis showed that eNOS was expressed in the BM of RBC eNOS KI mice but not in CondKO controls (Figure 25C).

IB of aortic lysates of RBC eNOS KI and CondKO controls showed a lack of eNOS expression (Figure 25D), EC eNOS KI mice were used as positive control. IP of RBC lysates showed eNOS expression in RBC eNOS KI mice and lack of eNOS in gKO mice and CondKO control mice (Figure 25E).

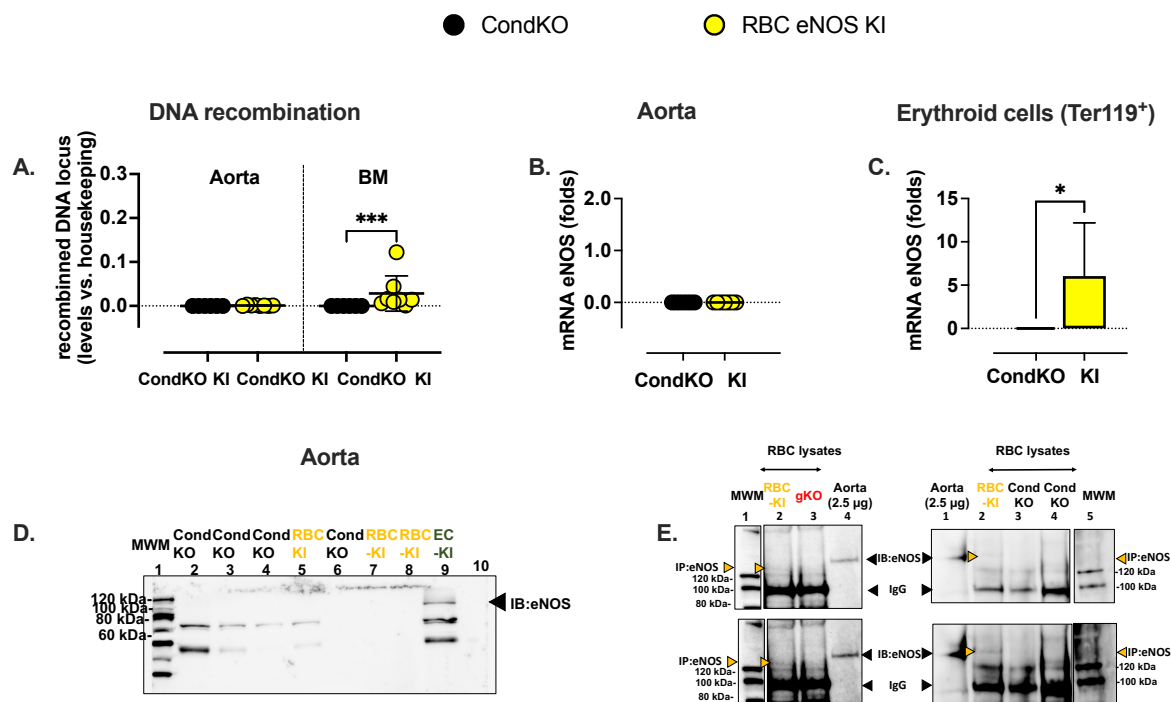


Figure 25 – Characterization of EC eNOS KI and RBC eNOS KI mice

(A) DNA recombination occurred in BM of RBC eNOS KI (0.03 ± 0.04 , $n = 8$). 1-way ANOVA $p < 0.0001$; Tukey's multiple comparison test $*p < 0.05$, $****p < 0.0001$ vs. respective CondKO control. (B) Real-time RT PCR analysis shows lack of eNOS expression in the aorta of RBC eNOS KI mice and CondKO controls. (C) RT qPCR analysis shows that erythroid cells (Ter119⁺ CD71⁺ CD45⁻) extracted from the bone marrow of RBC eNOS KI mice ($n = 3$) express eNOS mRNA as compared to CondKO controls, where we could not detect any eNOS mRNA ($n = 3$) $*p = 0.05$ (exact) Mann-Whitney test. Data collected by Sophia Heuser. (D) Representative immunoblot analysis demonstrates eNOS absence in aorta RBC eNOS KI mice compared to CondKO. EC eNOS KI mice were used as positive control. Western blots were performed by Anthea Lo Bue. (E) Representative western blot analysis demonstrating lack of eNOS expression in the aorta of RBC eNOS KI mice and CondKO mice. Western blots were performed by Anthea Lo Bue.

To summarize, tissue-specific eNOS KI mice were generated and characterized by different molecular biology techniques. Global eNOS KI mice were used as a proof of concept to verify the functionality of the models, and EC eNOS KI mice were characterized by the specific reintroduction of eNOS in the ECs. RBC eNOS KI mice showed DNA recombination exclusively in the BM and were characterized by the specific reintroduction of eNOS in erythroid cells.

4.8 Blood count

Blood count analysis was carried out to investigate any possible changes in the hematology of EC eNOS KI and RBC eNOS KI after eNOS reintroduction in the different compartments.

EC eNOS KI were compared with CondKO controls (eNOS^{inv/inv} Cdh5Cre/ERT2^{neg} + TAM) and no differences were detected.

RBC eNOS KI mice were compared with the founder line eNOS^{inv/inv}. Significant differences were detected in platelet number (PLT), granulocytes percentages (Gra%), and RBC distribution width (RDW), indicating an increased variability in the dimension of RBCs (Table 16).

Table 16 – Blood count parameters evaluated in EC eNOS KI and RBC eNOS KI mice

The table summarizes the blood count parameters measured in EC eNOS KO, RBC eNOS KO mice, and WT controls. All data are expressed as mean \pm SD.

	WT	EC eNOS KI		WT	RBC eNOS KI	
	eNOS ^{inv/inv} Chd5/ERT2Cre ^{neg} +TAM	eNOS ^{inv/inv} Chd5Cre/ERT2 ^{pos} +TAM	p	eNOS ^{inv/inv}	eNOS ^{inv/inv} HbbCre ^{pos}	p
n	4	5		10	4	
<u>Red blood cell count</u>						
RBC (10 ⁶ /μl)	5.3 \pm 1.0	5.1 \pm 1.7	0.8507	9.9 \pm 1.6	9.3 \pm 0.5	0.4809
HCT (%)	25.9 \pm 4.4	25.4 \pm 8.6	0.9234	47.7 \pm 8.4	45.9 \pm 3.0	0.6922
HGB (g/dl)	7.8 \pm 1.3	7.3 \pm 2.9	0.7445	14.4 \pm 2.4	13.9 \pm 0.9	0.6947
<u>Red blood cell indexes</u>						
RDW (%)	14.9 \pm 0.6	14.8 \pm 0.5	0.8258	13.9 \pm 0.7	15.4 \pm 0.4	0.0022**
MCHC (g/dl)	30.5 \pm 0.5	50.2 \pm 0.8	0.0969	30.2 \pm 0.8	30.2 \pm 0.2	>0.9999
MCH (pg)	15.1 \pm 0.5	14.3 \pm 1.2	0.2207	14.5 \pm 0.4	15.0 \pm 0.3	0.0830
MCV (μm ³)	51.8 \pm 3.5	50.2 \pm 0.8	0.3634	48.2 \pm 1.1	49.5 \pm 0.6	0.0532
<u>White blood cell count</u>						
WBC (10 ³ /μl)	2.1 \pm 0.5	2.1 \pm 0.7	0.9914	4.9 \pm 2.9	8.2 \pm 5.1	0.1341
Lymph (10 ³ /μl)	1.8 \pm 0.4	1.9 \pm 0.6	0.8823	3.5 \pm 2.1	3.7 \pm 0.8	0.9259
Lymph (%)	87.6 \pm 4.4	89.4 \pm 4.3	0.5350	74.0 \pm 13.1	56.4 \pm 27.9	0.8453
Mo (10 ³ /μl)	0.1 \pm 0.1	0.1 \pm 0.1	0.5113	0.3 \pm 0.3	0.7 \pm 0.7	0.0517
Mo (%)	6.0 \pm 2.5	4.6 \pm 2.0	0.3803	6.8 \pm 2.9	7.7 \pm 3.6	0.3244
Gra (10 ³ /μl)	0.2 \pm 0.1	0.2 \pm 0.1	0.7524	1.1 \pm 1.1	3.9 \pm 3.9	0.0538
Gra (%)	6.4 \pm 2.0	5.9 \pm 2.5	0.7524	19.3 \pm 10.3	36.0 \pm 24.3	0.0451*
<u>Platelet count</u>						
PLT (10 ³ /μl)	1012.0 \pm 590.7	647.2 \pm 61.4	0.2053	1330.0 \pm 363.5	2003.3 \pm 103.1	0.0039**
MPV (μm ³)	5.4 \pm 0.2	5.3 \pm 0.3	0.3934	5.5 \pm 0.4	5.9 \pm 0.1	0.0853

4.9 Evaluation of the impact of eNOS on cardiovascular homeostasis and systemic hemodynamics after tissue-specific eNOS reactivation

This section aimed to investigate the role of vascular eNOS and red cell eNOS in regulating vascular function, cardiovascular homeostasis, and blood pressure.

4.9.1 Vascular endothelial dilation to acetylcholine is reestablished in EC eNOS KI mice

Ex vivo measurements of vascular endothelial function in aortic rings of EC eNOS KI and CondKO control mice were performed. Different cohorts were analyzed in order to have information about vascular functionality before and after TAM treatment.

Before TAM treatment, all mice were gKO as they did not express eNOS in any tissue. In this case, treatment with ACh or PE showed no vascular relaxation/contraction of aortic rings (Figure 26A, 26B). On the other hand, SNP administration promoted vasodilation by downstream stimulation of sGC, bypassing the eNOS step (Figure 26C).

A second cohort of mice was subjected to a five-day treatment with TAM and 21 days after the measurements were performed. Of note, TAM treatment of EC eNOS KI mice induced a fully restored vascular endothelial dilator response to ACh as determined *ex vivo*, indicating reactivation of eNOS specifically in ECs (Figure 26D). Furthermore, the vascular contraction was decreased after PE treatment (Figure 26E). In addition, the vasodilatory response of aortic rings to increasing concentrations of the NO donor SNP was not significantly different in EC eNOS KI mice from the response in littermate CondKO mice (Figure 26F).

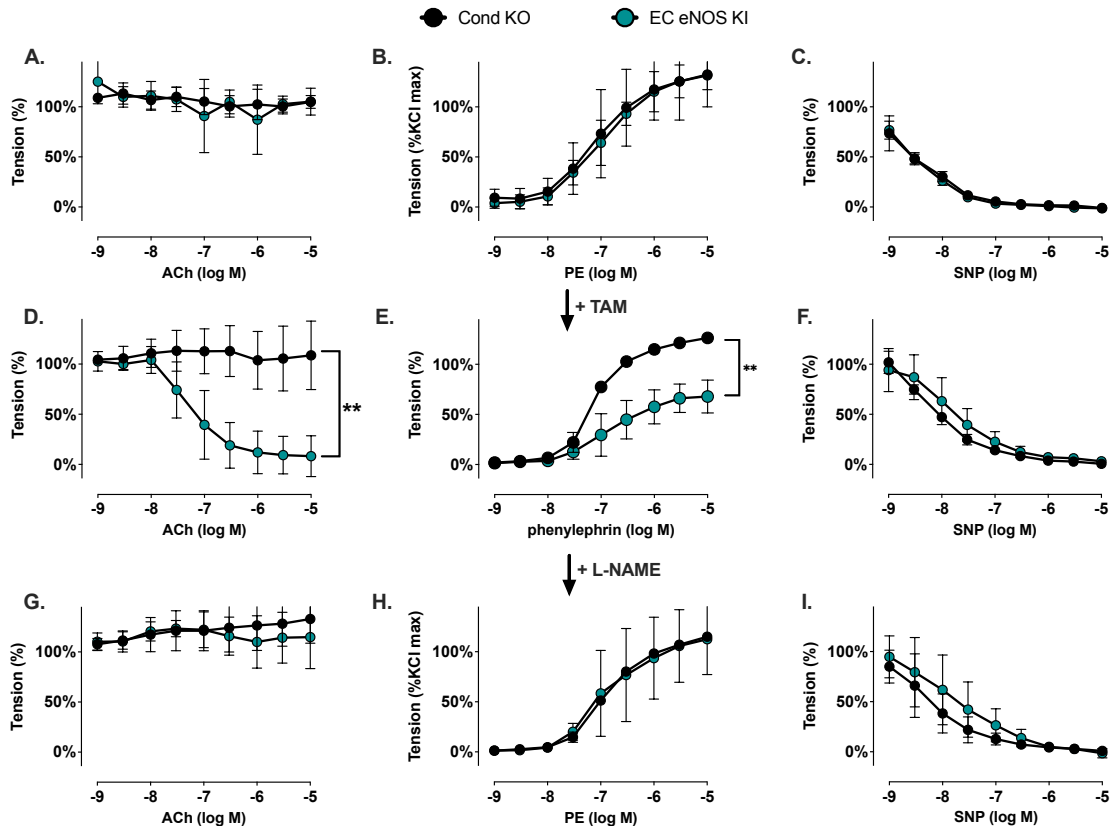


Figure 26 – Vascular endothelial function is restored in EC eNOS KI mice after TAM treatment

(A, B, C) The vascular function of EC eNOS KI is completely absent before TAM injections. (D) Pre-constricted aortic rings from CondKO mice (black, n = 2) lacks acetylcholine (ACh)-induced vasodilation, while reactivation of eNOS fully restore ACh response in EC eNOS KI (green, n = 3). 2-way (RM)-ANOVA concentration $p < 0.0001$; KI vs. KO $p = 0.0461$; Sidak's $** p < 0.01$ vs. CondKO control for concentrations of ACh $> 10^{-7}$ M. (E) The contractile response of aortic rings to increasing concentrations of phenylephrine (PE) is decreased in EC eNOS KI mice as compared to CondKO mice. 2-way-ANOVA $p < 0.0001$; Sidak's $** p < 0.01$ PE $> 10^{-7.5}$ M. (F) The vasodilatory response of aortic rings to increasing concentrations of the NO donor sodium nitroprusside (SNP) is not significantly different from the response in littermate CondKO mice. (G) The administration of the NOS inhibitor L-NAME fully blocks the ACh-induced vasorelaxation in EC eNOS KI mice (green). (H) The administration of the NOS inhibitor L-NAME increase PE-induced contractile response in EC eNOS KI to the level of the CondKO mice. (I) No difference in SNP-dependent relaxation between CondKO and EC eNOS KI after L-NAME administration. Data were collected by Lukas Vornholtz.

4.9.2 FMD is restored in EC eNOS KI mice

To test the vascular function of EC eNOS KI and CondKO controls, FMD was evaluated *in vivo* before and after TAM treatment.

Before TAM injection, EC eNOS KI mice had a phenotype comparable to the respective CondKO mice. No FMD was detected, indicating the iliac artery's inability to overcome the temporary occlusion of the vessel (Figure 27A). eNOS reactivation in the endothelium fully restored FMD (Figure 27B).

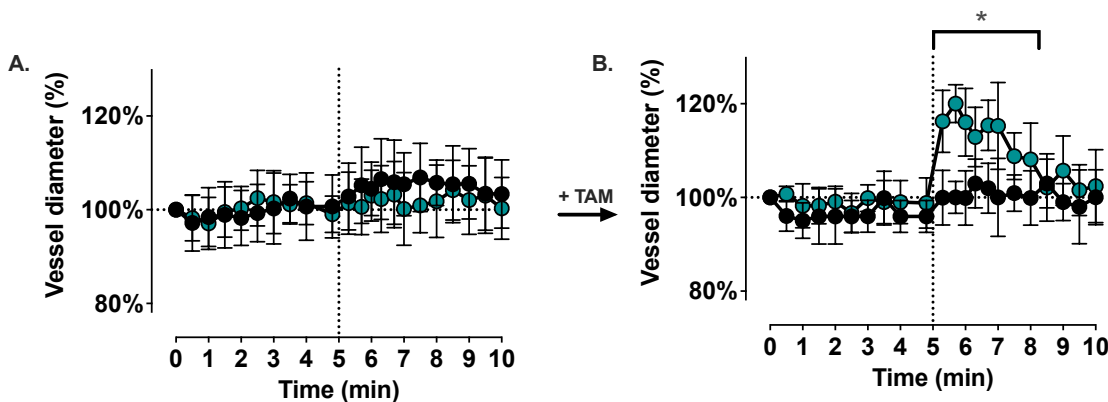


Figure 27 – FMD is restored in EC eNOS KI after tamoxifen treatment

(A) FMD of the iliac artery assessed *in vivo* by ultrasound is abolished in CondKO mice (n = 9, black) as well as EC eNOS KI (n = 11, green) before tamoxifen treatment. (B) Flow-mediated dilation (FMD) of the iliac artery assessed *in vivo* by ultrasound is abolished in CondKO mice (2-way RM-ANOVA time p = 0.0007 KI vs. KO p = 0.329; Fisher's Test ** p < 0.01 vs. CondKO control for t > 6.3 min); and restored in EC eNOS KI mice (green).

To summarize this set of experiments, vascular eNOS plays an important role in the modulation of vascular endothelial function. FMD was completely restored after TAM treatment and EC-specific eNOS reintroduction. ACh response of aortic rings was also fully restored in EC eNOS KI and, administration of a NOS inhibitor showed a complete loss of vascular function.

4.9.3 EC eNOS KI mice and RBC eNOS KI show decreased BP

To evaluate the role of reactivation of vascular eNOS and red cell eNOS in the modulation of the blood pressure, Millar catheterization of the right carotid artery was performed.

In EC eNOS KI mice, reactivation of eNOS specifically in ECs decreased BP by 23-28 mmHg (Table 17) as compared to CondKO littermate controls (Figure 28, green). However, HR was not significantly different (Table 17).

An important finding was that reactivation of eNOS specifically in erythroid cells fully rescued the global eNOS KO (eNOS^{inv/inv}) from hypertension with a significant decrease in BP of 19-24 mmHg in the RBC eNOS KI as compared to their CondKO littermate controls (Figure 28, yellow, Table 17).

These data provided additional evidence for an independent role of vascular eNOS and red cell eNOS to BP homeostasis.

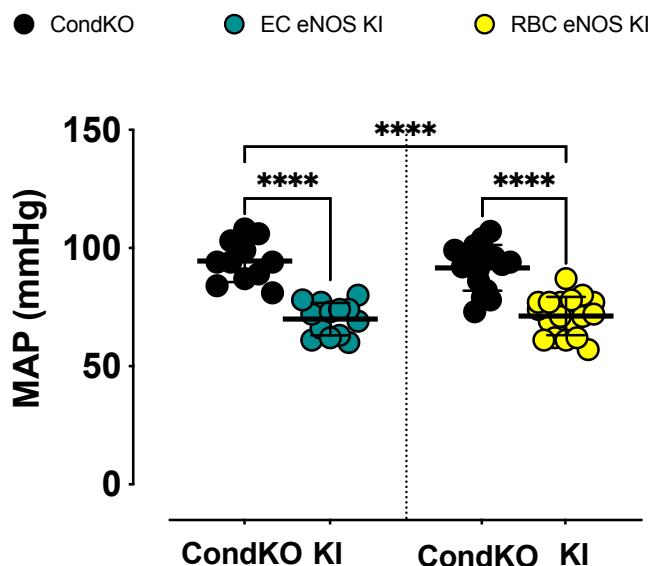


Figure 28 – Red cell eNOS and endothelial eNOS both contribute to blood pressure homeostasis

Invasive BP analysis in anesthetized mice shows that reactivation of eNOS expression significantly decrease MAP in EC eNOS KI (MAP = 70 ± 7 mmHg, n = 13), and RBC eNOS KI (MAP = 69 ± 8 mmHg, n = 10), mice as compared to their littermate CondKO. 1-way ANOVA p<0.001; Tukey's ****p<0.0001.

Table 17 – Blood pressure and heart rate in all the eNOS KI strains investigated

The table summarizes the litter size, body weight, SBP, DBP, MAP, HR, and RPP of global eNOS KI, EC eNOS KI, RBC eNOS KI and respective CondKO littermate controls. All data are expressed as mean ± SD.

	Strain	Genotype	Litter size	Body weight (g)	SBP (mmHg)	DBP (mmHg)	MAP (mmHg)	HR (bpm)	RPP (mmHg*bpm)	n
1	CondKO	eNOS ^{inv/inv}	5±3	27.8±1.8	127±1	84±1	98±1	465±44	59 046±8 299	11
2	fl/- (het)	eNOS ^{inv/inv} DeleterCre	4±2	29.9±1.5	106±6	73±7	84±6	466±65	49 546±7 555	20
	fl/fl (homo)	eNOS ^{inv/inv} DeleterCre		28.8±2.8	100±6	68±6	79±5	498±72	49 724±7 308	11
3	CondKO	eNOS ^{inv/inv} Cdh5Cre/ ERT2 ^{neg} +TAM	4±2	28.7±2.2	122±6	81±1	94±9	547±49	66 562±5 285	11
	EC eNOS KI	eNOS ^{inv/inv} Cdh5Cre/ ERT2 ^{pos} +TAM		28.3±2.2	94±7	58±8	70±7	540±48	50 849±5 346	13
4	CondKO	eNOS ^{inv/inv} HbbCre ^{neg}	4±2	28.7±1.2	119±1	75±1	90±1	494±45	58 845±5 542	18
	RBC eNOS KI	eNOS ^{inv/inv} HbbCre ^{pos}		31.1±2.5	95±8	56±9	69±8	469±67	47 022±7 322	10

4.9.4 No differences are detected in cardiac parameters and systemic vascular resistance in EC eNOS KO and RBC eNOS KO mice

To evaluate the impact of vascular eNOS and red cell eNOS in cardiac function, echocardiography was performed in a sub-cohort of mice.

Systemic hemodynamics and cardiac parameters were evaluated in parallel on the same mouse.

No changes in CO or HR were observed in EC eNOS KI and RBC eNOS KI mice as assessed by echocardiography (Figure 29A, 29B), as well as in SV, EF, EDV, and ESV. HR assessed invasively by Millar catheter was also not different between the groups (Table 18). In addition, no significant differences were observed in the SVR of EC eNOS KI and RBC eNOS KI mice as compared to CondKO controls (Figure 29C).

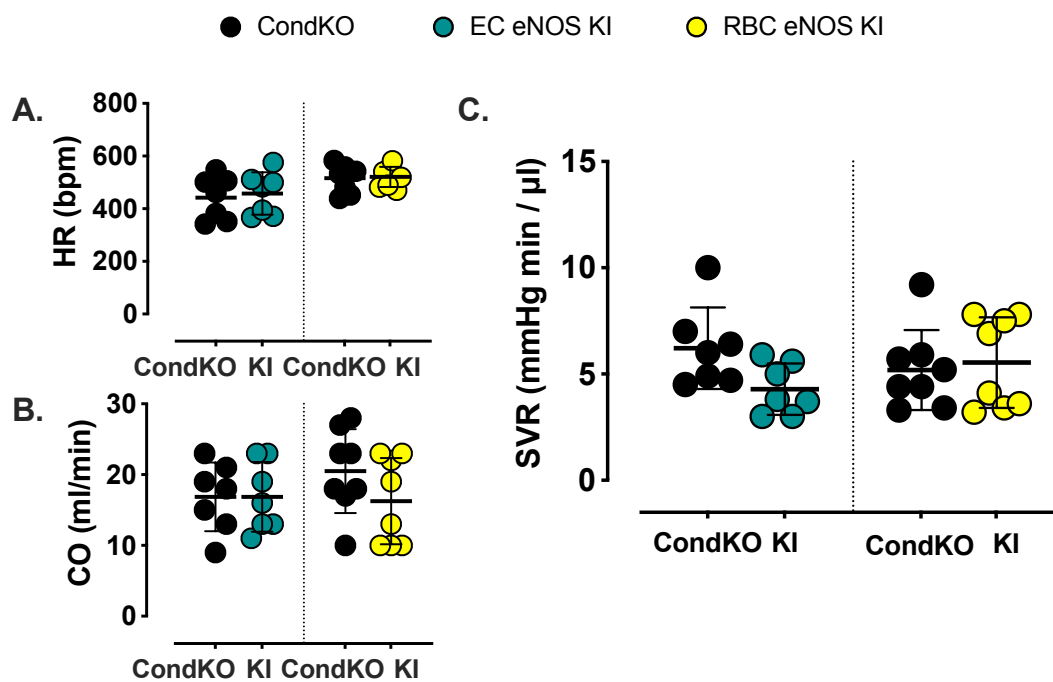


Figure 29 – No differences in SVR are detected after tissue-specific eNOS reintroduction

SVR was estimated in a sub-cohort of mice by measuring MAP and CO by ultrasound in the same animal ($SVR \approx MAP/CO$). The heart rate depicted here represents the values measured by cardiac ultrasound. SVR is decreased in EC eNOS KI compared to CondKO mice; t-test Welch * $p < 0.05$. See also Table 3 for other cardiac parameters. Refer to table 15 for additional values.

Table 18 – Systemic hemodynamics as assessed in a sub-cohort of mice by measurements of echocardiography and Millar in the same individual

The table summarizes cardiac parameters and blood pressure of EC eNOS KI, RBC eNOS KI, and respective CondKO controls. All data are expressed as mean \pm SD. T-test vs. respective control group. *p<0.05, **p<0.001.

	CondKO	EC eNOS KI		CondKO	RBC eNOS KI	
	eNOS ^{inv/inv} Cdh5Cre/ERT2 ^{neg}	eNOS ^{inv/inv} Cdh5Cre/ERT2 ^{pos}	P	eNOS ^{inv/inv} HbbCre ^{neg}	eNOS ^{inv/inv} HbbCre ^{pos}	P
n	7	7		8	8	
Echocardiography						
HR (bpm)	442 \pm 83	458 \pm 81	0.7227	516 \pm 52	521 \pm 38	0.8430
CO (ml/min)	17 \pm 5	17 \pm 5	0.9999	21 \pm 6	16 \pm 6	0.1791
SV (μ l)	38 \pm 8	37 \pm 7	0.8177	40 \pm 1	31 \pm 1	0.1368
EDV (μ l)	59 \pm 1	64 \pm 1	0.5246	62 \pm 2	51 \pm 2	0.2668
ESV (μ l)	21 \pm 1	27 \pm 1	0.4061	22 \pm 1	20 \pm 1	0.7158
EF (%)	67 \pm 2	59 \pm 1	0.3514	67 \pm 2	63 \pm 1	0.6033
Millar						
HR (bpm)	531 \pm 56	514 \pm 55	0.5795	508 \pm 40	507 \pm 80	0.9663
SBP (mmHg)	125 \pm 4	95 \pm 8	<0.0001****	120 \pm 7	98 \pm 5	<0.0001****
DBP (mmHg)	84 \pm 1	57 \pm 8	0.0009***	85 \pm 5	67 \pm 6	<0.0001****
MAP (mmHg)	98 \pm 9	70 \pm 8	<0.0001****	97 \pm 5	77 \pm 5	<0.0001****
SVR (mmHg/ml/min)	6.2 \pm 2	4.3 \pm 1.2	0.0475*	5.2 \pm 1.9	5.5 \pm 2.1	0.7331
RPP (mmHg bpm)	66 292 \pm 6 396	48 793 \pm 6 236	0.0002***	60 589 \pm 4 805	49 439 \pm 6 941	0.0027**

4.10 Summary

Taken together, tissue-specific mouse models for vascular eNOS and red cell eNOS were successfully generated and tested for their endothelial function, blood pressure, and cardiovascular hemodynamics.

Removal of eNOS from the vascular compartment (EC eNOS KO) determined a complete loss of ACh dilator response and PE vascular constriction that was instead fully preserved in RBC eNOS KO mice. FMD was also completely lost in EC eNOS KO, and no differences were detected in RBC eNOS KO mice. Hemodynamic measurements evidenced an increased BP in both lines, and cardiac function was not altered in EC eNOS KO and RBC eNOS KO mice.

On the other hand, EC eNOS KI mice demonstrated a fully restored vascular endothelial function after *ex vivo* treatment with ACh and PE. In addition, FMD was also completely restored. Moreover, reintroducing eNOS specifically in ECs or RBCs determined a decrease in BP as compared to CondKO littermate controls that showed a significant hypertensive phenotype.

In conclusion, it was demonstrated that vascular eNOS and red cell eNOS play an important and independent role in the modulation of vascular tone and blood pressure.

4.11 Evaluation of NO metabolites concentration in blood and tissues

To analyze the impact of cell-specific eNOS deletion/reintroduction on the concentration of NO metabolites, blood, and tissues of EC eNOS KO/KI and RBC eNOS KO/KI were collected and analyzed by CLD 77AM sp (Eco Physics).

4.11.1 Circulating nitrite decreases in EC eNOS KO and RBC eNOS KO, and NO-heme levels change in RBC eNOS KO/KI mice.

Analysis of EC eNOS KO mice showed a decrease in circulating nitrite and nitrate levels in plasma (Figure 30A, blue, Table 19), and no significant changes were detected in circulating RXNO levels in all the different compartments, except for RBCs, where a significant decrease of RXNO was detected (Figure 30C, blue, Table 19).

Moreover, total NO species, evaluated as the sum of all NO species (RSNO + RNNO) in a specific compartment, were decreased in all the tissues of EC eNOS KO mice as compared with their WT littermate controls, but not in the liver (Table 19), where a significant increase was instead detected. However, the decrease in total NO species was statistically significant only in the lung of EC eNOS KO mice.

RBC eNOS KO mice showed decreases in nitrite and nitrate concentrations in plasma together with an increase in nitroso species (Figure 30A, 30C, orange, Table 19), and a significant decrease of nitrite levels was also detected in the aorta (Table 19) as compared to WT littermate controls. Total NO species were significantly decreased in plasma and liver of RBC eNOS KO mice, but no changes were detected in other tissues (Table 19).

NO metabolites measured in CondKO mice showed an overall decrease in the different compartments as compared to WT mice (compare Table 19, WT with Table 20, Cond KO), with a decrease in circulating nitrite levels of almost 50% (compare figure 30A, white with figure 30B, black). However, no significant difference was detected in nitrite and RXNO levels in the plasma of EC eNOS KI or RBC eNOS KI as compared with their respective littermate CondKO controls (Figure 30B, 30D, green and yellow).

Interestingly, NO-heme levels measured in RBCs were fully preserved in EC eNOS KO mice and EC eNOS KI mice (Figure 30E, blue and figure 30F, green).

Moreover, levels of NO-heme significantly decreased in RBCs from RBC eNOS KO mice as compared to WT controls (Figure 30F, orange) and significantly increased in RBCs from RBC eNOS KI mice (Figure 30F, yellow) as compared to the respective CondKO littermates.

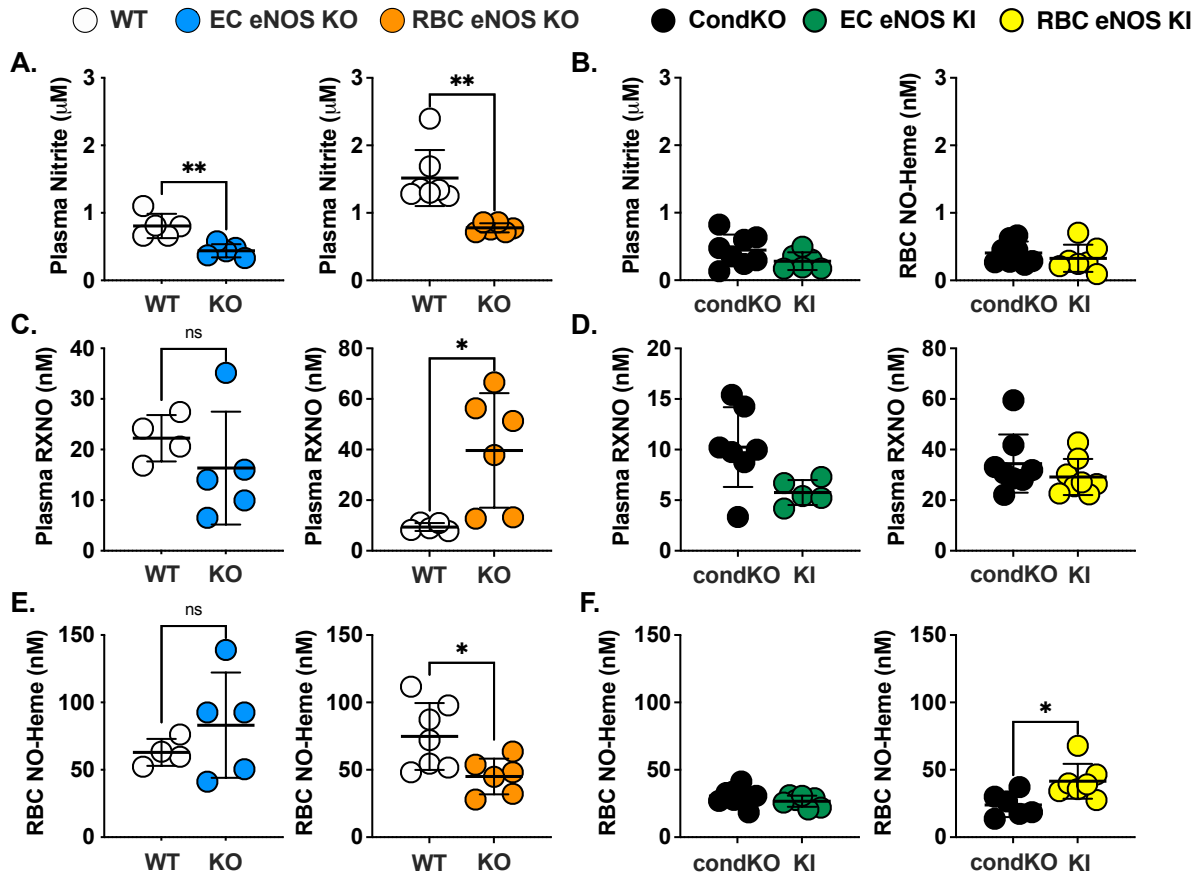


Figure 30 – Red cell eNOS and endothelial eNOS both contribute to plasma nitrite, but red cell eNOS is the major determinant of circulating NO-heme

(A) A significant decrease in plasma nitrite is observed in EC eNOS KO (blue) and RBC eNOS KO (orange), as compared to their respective WT controls (white). Welch's t-test * $p < 0.05$ ** $p < 0.01$. (B) Plasma nitrite in EC eNOS KI (green) or RBC eNOS KI (yellow) is not different from CondKO mice (black), but CondKO mice show lower plasma nitrite levels compared to WT mice (white, see also Table 21 and Table 22). (C) The levels of nitroso species (RXNO = RSNO + RNNO) were unchanged in EC eNOS KO (blue) and significantly higher in the plasma of RBC eNOS KO mice (orange) as compared to their respective WT controls (white). Welch's t-test * $p < 0.05$. (D) RXNO levels in the plasma of EC eNOS KI, RBC eNOS KI, and CondKO mice are not different. (E) NO-heme concentrations in RBCs were unchanged in EC eNOS KO mice (blue) and decreased in RBC eNOS KO mice (orange). Welch's t-test * $p < 0.05$ (F) Concentrations of NO-Heme were unchanged in EC eNOS KI mice (green) but higher in RBC eNOS KI mice (yellow) as compared to CondKO control mice (black), indicating that RBC eNOS is the major determinant of circulating NO-heme. Welch's t-test * $p < 0.05$.

Table 19 – NO metabolites in blood and organs of EC eNOS KO, RBC eNOS KO, and corresponding WT littermate controls
 t-test between the groups. *p<0.05, **p<0.01m ***p<0.001. † one value excluded as outlier according to Tuckey's test or not determined/available. ‡two values were not determined/available, or one was excluded as an outlier according to Tuckey's test.

		WT	EC eNOS KO		WT	RBC eNOS KO	
Metabolite		eNOS ^{flx/flx} Cdh5/ERT2Cre ^{neg}	eNOS ^{flx/flx} Cdh5/ERT2Cre ^{pos}	P	eNOS ^{flx/flx} HbbCre ^{neg}	eNOS ^{flx/flx} HbbCre ^{pos}	P
n		5	5		7	6	
Heart							
Nitrite	μM	1.10±0.30	1.27±0.25	0.3557	0.69±0.15	0.92±0.60†	0.4463
Nitrate	μM	93.86±26.51	77.84±14.97	0.2818	65.16±19.11	86.82±54.70	0.3914
RXNO	nM	81.94±26.31	102.74±37.20	0.3406	54.00±19.06	43.81±10.47	0.2528
NO-heme	nM	475.21±320.85	97.74±24.20	0.0579*	125.04±37.83	38.82±20.11	0.0005** *
Total NO species	μM	95.09±26.43	79.31±14.91	0.2871	66.02±19.14	87.66±54.33	0.3890
Lung							
Nitrite	μM	0.88±0.51†	0.71±0.11	0.5100	0.71±0.24	0.50±0.13†	0.0801
Nitrate	μM	35.62±6.74†	19.49±5.52	0.0035**	44.01±13.20	40.10±22.66	0.7202
RXNO	nM	94.01±19.94†	79.43±20.31	0.3173	62.99±29.43	122.80±106.3	0.2331
NO-heme	nM	228.44±92.18†	463.51±121.30	0.0131*	282.16±166.87	104.77±61.72	0.0316*
Total NO species	μM	34.25±5.57†	20.74±5.62	0.0096**	45.06±13.40	33.78±16.50†	0.2450
Liver							
Nitrite	μM	0.63±0.34	0.83±0.15	0.2798	0.20±0.06	0.16±0.04†	0.2483
Nitrate	μM	38.47±22.34	71.02±20.84	0.0445*	57.69±17.70	33.88±7.05†	0.0116*
RXNO	nM	1378.28±749.29	1038.64±283.33	0.3857	366.42±71.71	1836.38±1541.77	0.0666
NO-heme	nM	1190.08±722.98	310.85±104.09	0.0523	1149.31±323.81	494.14±573.76	0.0396*
Total NO species	μM	40.65±22.39	73.20±21.08	0.0456*	59.41±17.54	36.68±8.85†	0.0159*
Aorta							
Nitrite	μM	138.12±62.10	141.36±39.21	0.9243	57.57±16.44†	118.71±42.34	0.0147*
Nitrate	μM	10191.95±7764.94	5473.15±4015.51	0.2730	2931.00±1184.00†	3408.00±1888.00	0.6357
RXNO	nM	2058.42±1653.39	1870.34±1002.49	0.8344	2103.00±980.10†	3067.00±1737.00	0.2712
Total NO species	μM	10331.13±7805.42	5616.38±4052.67	0.2758	3020.34±1181.83†	2455.27±1651.94	0.5126
Plasma							
Nitrite	μM	0.81±0.18	0.44±0.10	0.0065**	1.52±0.42	0.78±0.07	0.0031**
Nitrate	μM	41.35±15.75	20.65±4.25	0.0402*	57.63±9.22	25.40±10.93	0.0002** *
RXNO	nM	22.24±4.58	16.34±11.15	0.3268	9.39±1.57‡	39.65±22.64	0.0220*
Total NO species	μM	36.66±11.28	21.11±4.30	0.0642	59.96±9.07‡	26.22±10.91	0.0003** *
RBCs							
Nitrite	μM	0.49±0.16	0.43±0.16	0.6088	0.94±0.14†	1.09±0.35†	0.4063
Nitrate	μM	35.23±14.27	17.64±3.14	0.0880	67.95±15.61	68.43±29.82	0.9727
RXNO	nM	475.06±158.27	225.04±76.99	0.0201*	196.32±123.29	125.32±28.68	0.1846
NO-heme	nM	62.92±9.99†	83.12±39.12	0.3209	74.76±24.84	45.06±13.31	0.0220*
Total NO species	μM	32.02±21.79†	18.38±3.33	0.2999	56.34±31.65†	75.91±28.53†	0.3097

Table 20 – NO metabolites in blood and organs of EC eNOS KI, RBC eNOS KI, and corresponding CondKO littermate controls

t-test between the groups *p<0.05, **p<0.01. †one value excluded as outlier according to Tuckey's test, or not determined/available.

‡two values were not determined/available, or one was excluded as an outlier according to Tuckey's test. N.D. non-determined.

		CondKO	EC eNOS KI		WT	RBC eNOS KI	
Metabolite		eNOS ^{inv/inv} Cdh5/ERT2Cre ^{neg}	eNOS ^{inv/inv} Cdh5/ERT2Cre ^{pos}	P	eNOS ^{inv/inv} HbbCre ^{neg}	eNOS ^{inv/inv} HbbCre ^{pos}	P
n		8	7		8	8	
Heart							
Nitrite	μM	2.27±0.14†	2.24±0.48	0.8745	0.64±0.23	0.67±0.18‡	0.7817
Nitrate	μM	N.D.	N.D.		13.86±6.27	13.98±6.08‡	0.9715
RXNO	nM	34.86±16.40	32.50±3.38	0.7043	15.54±4.38	20.65±6.23	0.0810
NO-heme	nM	26.57±12.00	32.67±8.46	0.2865	6.94±1.49	8.40±2.09	0.1303
Total NO species	μM	N.D.	N.D.		14.52±6.31	14.68±6.09‡	0.9628
Lung							
Nitrite	μM	2.42±0.52†	3.05±0.62	0.0626	0.70±0.26	0.70±0.65‡	0.9796
Nitrate	μM	N.D.	N.D.		28.75±14.78	21.31±9.03‡	0.2674
RXNO	nM	71.73±35.40	54.26±12.34	0.2237	3783.51±2023.74‡	3666.83±2476.96	0.9244
NO-heme	nM	27.62±14.30	29.86±7.76	0.7090	425.90±238.14†‡	443.89±88.30‡	0.8792
Total NO species	μM	N.D.	N.D.		39.21±16.11†‡	25.28±9.53‡	0.1378
Liver							
Nitrite	μM	3.32±1.44	2.72±0.36†	0.2921	0.65±0.52	0.31±0.08	0.1050
Nitrate	μM	N.D.	N.D.		17.56±9.23	14.68±5.38	0.4606
RXNO	nM	617.11±336.52	496.28±193.14	0.4046	672.09±412.26	377.99±47.68‡	0.0842
NO-heme	nM	118.74±46.90†	79.44±3.42‡	0.0686	342.06±207.87	353.56±136.61	0.8981
Total NO species	μM	N.D.	N.D.		19.23±9.47	14.52±4.20‡	0.2389
Aorta							
Nitrite	μM	9.56±4.74	6.20±2.06	0.0995	2.90±1.05	2.28±1.21‡	0.3407
Nitrate	μM	N.D.	N.D.		126.67±104.88	100.97±97.25‡	0.6451
RXNO	nM	79.10±46.81	55.80±47.50	0.3579	141.72±106.74	191.45±106.22†	0.3834
NO-heme	nM	11.49±3.97‡	21.28±5.55	0.0037**	129.71±105.59	67.44±48.22‡	0.1780
Total NO species	μM	N.D.	N.D.		N.D.	N.D.	
Plasma							
Nitrite	μM	0.45±0.23	0.28±0.13†	0.1218	0.32±0.12	0.24±0.09†	0.1542
Nitrate	μM	N.D.	N.D.		55.72±48.50	43.47±21.12	0.5279
RXNO	nM	15.67±15.77	12.89±13.12	0.7160	34.46±11.52	29.16±7.14	0.2909
Total NO species	μM	N.D.	N.D.		56.06±48.53	44.71±22.62†	0.5668
RBCs							
Nitrite	μM	0.15±0.04	0.21±0.10	0.2011	3.29±1.24†	2.94±1.51†	0.6435
RXNO	nM	88.78±47.89	103.57±72.60	0.6562	1.26±0.52	0.72±0.25	0.0253*
NO-heme	nM	3.06±0.66	2.67±0.41	0.1904	23.89±8.89‡	41.54±12.94†	0.0150*
Total NO species	μM	N.D.	N.D.		4.66±1.43†	3.78±1.72‡	0.3425

To summarize, circulating plasma nitrite levels were significantly decreased in EC eNOS KO and RBC eNOS KO mice than WT littermate controls. However, no differences were detected in EC eNOS KI, RBC eNOS KI, and CondKO mice. Moreover, CondKO mice showed significantly reduced plasma nitrite levels as compared to WT mice, of approximately 50%.

Total NO species were significantly decreased in all the different EC eNOS KO mice tissues, but a statistical significance was observed only in the lung. On the other hand, nitrate levels were found to significantly increase in the liver of EC eNOS KO mice, contributing to an overall increase in total NO species.

RBC eNOS KO mice showed a significant decrease of total NO species in liver and plasma, while no significant differences were detected in EC- and RBC eNOS KI mice.

Of particular interest, no differences in NO-heme levels were detected in RBCs of EC eNOS KO and EC eNOS KI mice, but a significant increase of NO-heme was observed in RBCs of RBCs eNOS KO. On the other hand, RBC eNOS KI mice showed a significant decrease in NO-heme levels in RBCs.

These data show that the levels of NO-heme in RBCs depend on the presence/absence of eNOS in RBCs.

4.12 Effects of nitrate supplementation on systemic hemodynamics

Mice were given tap water ad libitum directly from the sink of the laboratory (nitrate around 230 μM) except when indicated. In specific experiments, mice were given different nitrate concentrations dissolved in drinking water:

- 1- Water containing low nitrate amount (Vittel water, source: Vittel, Vogesen, France);
- 2- A prepared solution containing 200 μM of nitrate, comparable to the amount present in the tap water. Considering that an average mouse weighs 30 mg and drinks around 6 ml of water/day, the dose of nitrate assumed with the prepared solution is 0.074 mg, corresponding to a concentration of 2.48 mg/kg.

Mice received the water for 24 hours, and then BP was measured via Millar catheterization (Figure 8).

4.12.1 Blood pressure and NO metabolites in EC- and RBC eNOS KO after nitrate supplementation

The amount of nitrate in the drinking water of the mice was detected by ENO-20. Vittel water contains a very low nitrate amount and represented the control within the cohorts; tap water contains around 230 μM nitrate ($237 \pm 36 \mu\text{M}$) (Figure 31).

These results indicated that one mouse assumed a dose of around 0.088 mg/day by drinking tap water, corresponding to a concentration of 2.93 mg/kg/day.

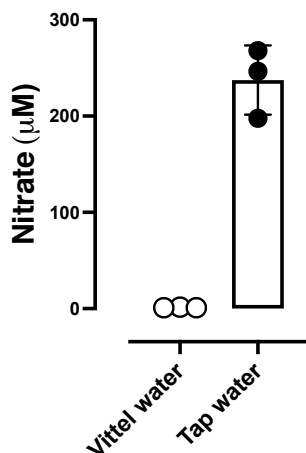


Figure 31 – Measurement of nitrate concentration in Tap water and Vittel water

Nitrate content was measured in different water solutions by ENO-20. Tap water contains an amount of $237.46 \pm 36.00 \mu\text{M}$ ($n = 3$). The amount of nitrate evaluated in Vittel water is $1.11 \pm 0.35 \mu\text{M}$ ($n = 3$). Data were collected by Carina Nihlén (Karolinska Institute, Stockholm, Sweden).

To verify whether the dose of nitrate in tap water might affect systemic hemodynamics, mice were treated with water containing 200 μM nitrate, with a similar dose to the amount of nitrate in tap water.

- low-nitrate water ($\sim 0 \mu\text{M}$);
- tap water ($\sim 200 \mu\text{M}$);
- Vittel + nitrate (200 μM).

As already shown, EC eNOS KO and RBC eNOS KO mice drinking tap water had a hypertensive phenotype as compared to their respective WT controls (Figure 32A, 32B, Table 21).

Administration of low-nitrate water to EC eNOS KO and WT mice induced an increase of MAP, to a significant extent in EC eNOS KO mice. However, no significant differences were detected in RBC eNOS KO mice when drinking low-nitrate water as compared to tap water.

To verify whether the lower BP observed in WT and EC eNOS KO mice drinking tap water as compared to low-nitrate water was attributable to the dose of nitrate contained in the tap water, mice were supplemented with a prepared solution of the low-nitrate water with the addition of nitrate, to a final concentration of 200 μM , with a comparable dose of nitrate to the amount of nitrate in tap water.

Administration of the nitrate-enriched water to WT mice and EC eNOS KO mice caused a significant BP decrease (Figure 32A, 32B).

On the other hand, the high BP in RBC eNOS KO mice was confirmed after administration of nitrate-enriched water, showing no differences as compared to mice drinking tap water or low-nitrate water (Figure 32B, Table 21).

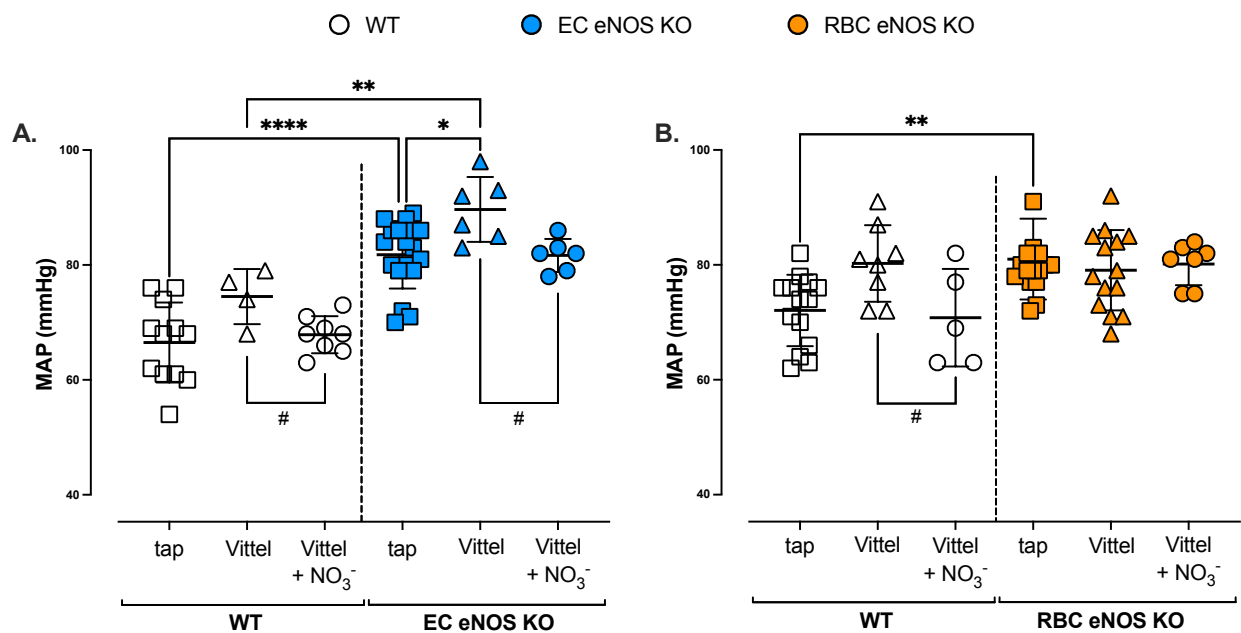


Figure 32 – The nitrate concentration in the tap water affects BP in WT and EC eNOS KO but not in RBC eNOS KO mice

(A) Invasive BP measurements in anesthetized mice show that nitrate supplementation causes a decrease in BP in control mice and EC eNOS KO mice. Tap water administration shows the hypertensive phenotype of EC eNOS KO mice as compared to WT littermate controls. Low-nitrite water (Vittel) determines an increased MAP in WT and EC eNOS KOs as compared to mice drinking tap water. To verify if the lower BP detected after tap water administration was caused by the dose of nitrate in the tap water, mice were administered with a solution of Vittel water with the addition of nitrate, to a final concentration of 200 μ M, similar to the dose of nitrate in the tap water. After administering the nitrate-enriched water (Vittel + nitrate), BP decreases, and no differences are detected between mice treated with tap water and those drinking the Vittel + nitrate solution. All data are expressed as mean \pm SD. 1-way ANOVA $p < 0.001$; Tukey's **** $p < 0.0001$. t-test # $p < 0.05$. (B) WT controls for RBC eNOS KO, drinking low-nitrate water, showed a significant increase of MAP as compared to mice drinking tap water. A decrease in MAP is detected when nitrate-enriched water is administered. When eNOS is not expressed in the RBCs, no differences are detected when different nitrate concentrations are supplemented in the drinking water. All data are expressed as mean \pm SD. 1-way ANOVA $p < 0.001$; Tukey's **** $p < 0.0001$. t-test # $p < 0.05$. Refer to table 17 for additional information.

Table 21 – Blood pressure parameters and heart rate measured by Millar catheterization after supplementation of different nitrate concentrations to tissue-specific eNOS KO mice

Summary of all hemodynamic parameters evaluated by Millar catheterization of tissue-specific eNOS KO mice. All data are expressed as mean \pm SD.

Strain	Genotype	Drinking water	SBP	DBP	MAP	HR	PP	n
WT	eNOS ^{flx/flx} Cdh5Cre/ERT2 ^{neg} +TAM							
		Tap	86 \pm 5	57 \pm 8	67 \pm 7	564 \pm 53	48 413 \pm 5 018	12
		Vittel	94 \pm 3	65 \pm 6	75 \pm 5	549 \pm 53	51 379 \pm 3 418	4
		Vittel + nitrate	87 \pm 5	58 \pm 3	68 \pm 3	574 \pm 75	50 127 \pm 8 230	8
EC eNOS KO	eNOS ^{flx/flx} Cdh5Cre/ERT2 ^{pos} +TAM							
		Tap	104 \pm 8	72 \pm 7	83 \pm 7	535 \pm 58	55 696 \pm 6 929	19
		Vittel	111 \pm 6	79 \pm 6	90 \pm 6	549 \pm 58	60 993 \pm 8 198	6
		Vittel + nitrate	101 \pm 6	72 \pm 5	82 \pm 3	545 \pm 53	55 156 \pm 6 012	6
WT	eNOS ^{flx/flx} HbbCre ^{neg}							
		Tap	89 \pm 9	61 \pm 1	70 \pm 1	528 \pm 56	46 622 \pm 5 306	15
		Vittel	100 \pm 6	70 \pm 7	80 \pm 7	525 \pm 67	52 957 \pm 9 271	8
		Vittel + nitrate	98 \pm 6	57 \pm 10	71 \pm 8	581 \pm 61	57 016 \pm 8 414	5
RBC eNOS KO	eNOS ^{flx/flx} HbbCre ^{pos}							
		Tap	103 \pm 1	69 \pm 7	80 \pm 8	476 \pm 93	48 506 \pm 9 392	16
		Vittel	100 \pm 8	69 \pm 7	79 \pm 7	525 \pm 77	52 196 \pm 6 022	14
		Vittel + nitrate	104 \pm 3	68 \pm 5	80 \pm 4	608 \pm 68	63 406 \pm 8 347	7

4.12.2 Plasma nitrite levels are increased in EC eNOS KO and WT controls but not in RBC eNOS KO mice after nitrate supplementation

To investigate the effect of nitrate supplementation in the drinking water on circulating nitrite levels, mice were treated with nitrate dissolved in drinking water (at low nitrate concentration), and organs and plasma were collected.

Plasma nitrite levels of EC eNOS KO mice, RBC eNOS KO mice, and WT controls were analyzed, and as can be seen in figure 33, administration of nitrate caused a significant increase in circulating nitrite levels in EC eNOS KO (blue) and WT mice (grey) (Figure 33A).

Interestingly RBC eNOS KO mice showed a slight increase in circulating nitrite levels after nitrate administration, but not in a significant way (Figure 33A, orange; Table 22).

The heatmap graph of plasma nitrite levels (Figure 33B) also shows that nitrate administration increased circulating plasma nitrite levels in WT controls and EC eNOS KOs, with a lower extent in RBC eNOS KOs, indicated by a brighter shade of grey (Figure 33B).

No differences were detected between RBC eNOS KO mice and WT controls when drinking the same water (low-nitrate water or low-nitrate + nitrate water) and between EC eNOS KO mice and WT littermate controls in the same conditions (Figure 33B; Table 22).

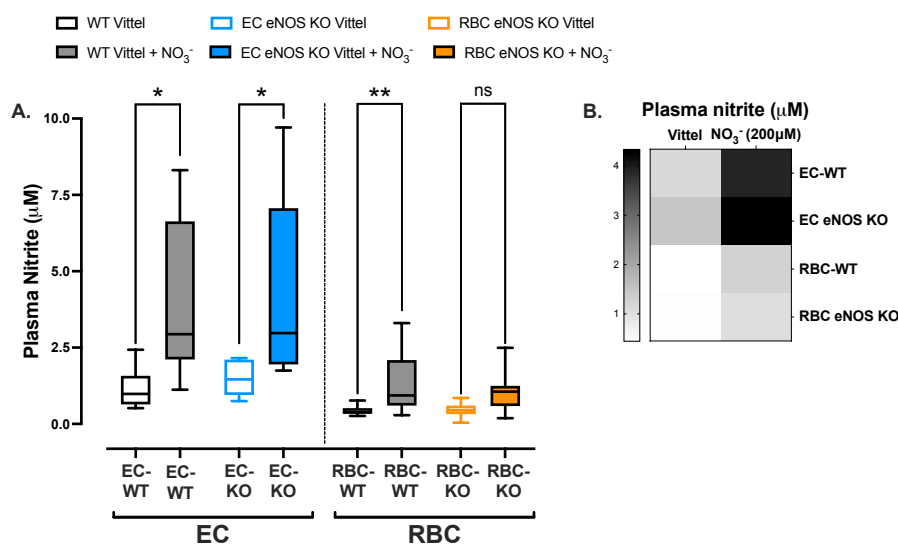


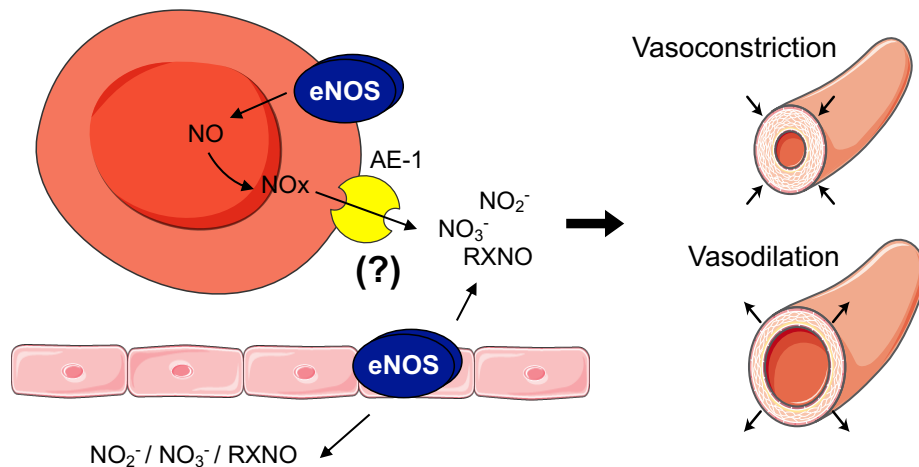
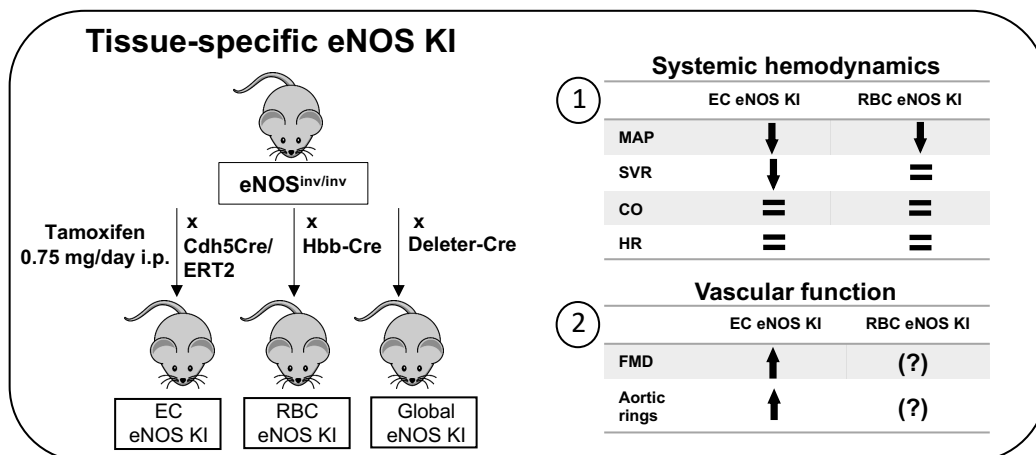
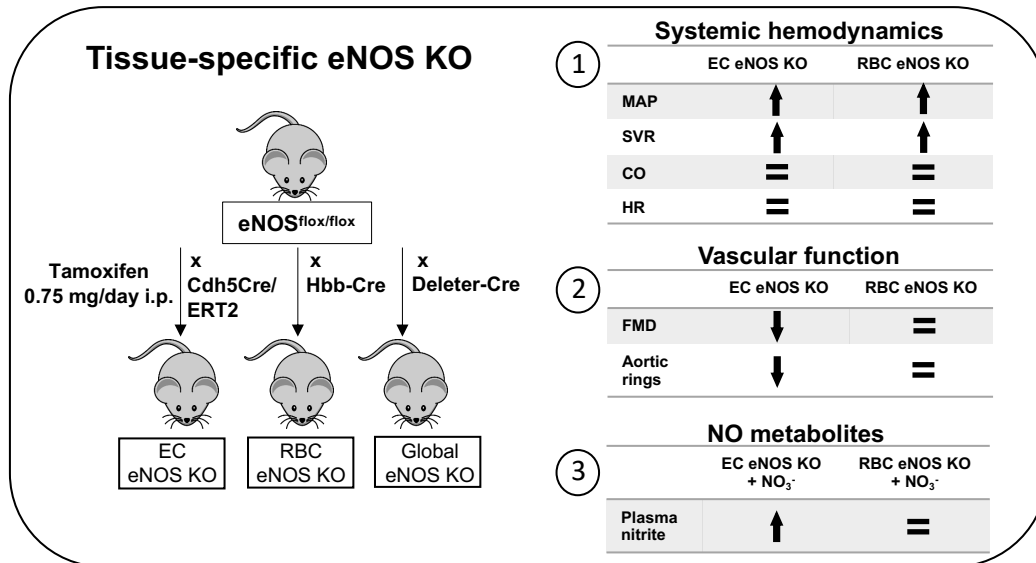
Figure 33 – Plasma nitrite is increased in EC eNOS KO and WT mice. No differences are detected in RBC eNOS KO mice
(A) A significant increase in plasma nitrite levels is observed in WT mice (grey) and EC eNOS KO mice (blue). RBC eNOS KOs represent the only group where external nitrate administration does not affect circulating nitrite levels. All data are expressed as mean ± SD. t-test *p<0.05, **p<0.01. **(B)** Correlation heatmap of plasma nitrite in RBC eNOS KO, EC eNOS KO, and respective littermate controls. Administration of external nitrate determines a significant increase in plasma nitrite levels, with a lower extent in RBC eNOS KOs. All data are expressed as mean ± SD.

Table 22 – Plasma circulating nitrite levels and MAP of EC eNOS KO, RBC eNOS KO, and corresponding WT littermate controls before and after nitrate supplementation

The table gives an overview of the circulating nitrite levels and MAP of EC eNOS KO, RBC eNOS KO, and WT littermate controls before and after nitrate supplementation in the drinking water. All data are expressed as mean \pm SD. t-test * $p < 0.05$, ** $p < 0.01$, *** $p < 0.0001$.

	Vittel						Nitrate (200 μ M)					
	WT	EC eNOS KO	p	WT	RBC eNOS KO	p	WT	EC eNOS KO	p	WT	RBC eNOS KO	p
n	8	9		15	23		4	6		15	16	
Nitrite (μM)	1.17 \pm 0.63	1.49 \pm 0.57	0.2892	0.45 \pm 0.16	0.48 \pm 0.26	0.6655	3.92 \pm 2.61	4.33 \pm 3.03	0.7673	1.26 \pm 0.88	1.56 \pm 2.08	0.6056
n	4	6		8	14		8	6		5	7	
MAP (mmHg)	75 \pm 5	90 \pm 6	0.0023**	80 \pm 7	79 \pm 7	0.7032	68 \pm 3	82 \pm 3	<0.0001****	71 \pm 8	80 \pm 4	0.0254*

5. Discussion



The aim of this study was to elucidate the functional significance and specific role of red cell eNOS directly compared to endothelial eNOS in controlling vascular hemodynamics and systemic NO metabolism.

The initial hypothesis of this study was that red cell eNOS contributes to the regulation of NO metabolites, vascular tone, and BP.

It was possible to determine the independent contribution of vascular eNOS and red cell eNOS in controlling vascular hemodynamics and systemic NO metabolism by creating and comparing tissue-specific eNOS KO and eNOS KI mice with targeted mutations specifically in the endothelium or in the erythroid cells.

The main findings are the following: (1) knock-out (KO) and knock-in (KI) models for eNOS in the ECs and RBCs have been successfully generated, and the functionality of the model has been demonstrated; (2) removal of eNOS from ECs and RBCs determines increased BP and no changes in cardiac parameters. Vascular function is lost only in EC eNOS KO mice and fully preserved in RBC eNOS KO. Reactivation of eNOS in the endothelium or RBCs fully rescues the CondKO from hypertension. (3) Nitrate administration determines an increase in circulating nitrite levels and a BP decrease in EC eNOS KO and control mice, but no changes in the BP of RBC eNOS KO are detected.

Therefore, it can be concluded that red cell eNOS plays an important role in the modulation of BP and systemic hemodynamics, which is independent of the role of vascular eNOS.

5.1 New functional models of tissue-specific eNOS KO and eNOS KI mice were generated

It is well known that eNOS is a protein constitutively expressed in the vascular endothelial cells of the blood vessels and is responsible for NO production and modulation of the vascular tone [12]. NO produced by eNOS in ECs is considered the central regulator of vascular tone and systemic hemodynamics [22]. An active eNOS has also been recognized in the RBCs [77].

To investigate the role of vascular eNOS and red cell eNOS in the modulation of vascular tone, BP, and cardiac hemodynamics, eNOS^{flox/flox} and eNOS^{inv/inv} mice were crossed with Cdh5Cre/ERT2^{pos} mice and HbbCre^{pos} mice, resulting in EC eNOS KO/KI, RBC eNOS KO/KI mice, respectively, and controls.

To confirm the functionality of the loxP-Cre reintroduction model, eNOS^{inv/inv} mice were crossed with ubiquitous expressing Cre mice (DeleterCre^{pos}).

EC eNOS KO mice showed specific deletion of eNOS from the endothelium, EC eNOS KI mice were characterized by the specific reintroduction of eNOS in the ECs.

RBC eNOS KO and RBC eNOS KI mice showed DNA recombination exclusively in the BM and were characterized by specific absence/presence of eNOS in erythroid cells, respectively.

Western blot analysis further confirmed the absence/presence of eNOS in the tissues of interest.

Blood count analyses were also carried out to evaluate whether eNOS signaling in erythroid and endothelial bone marrow cells plays a role in controlling the differentiation of erythroid cells and hematopoiesis [136].

No changes were observed in the hematological phenotype of the mice: RBC count, HCT, and RBC deformability were not significantly different in EC eNOS KO nor RBC eNOS KO mice, limiting the role of rheological changes in BP phenotype in those mice.

Hematological parameters were also evaluated in EC eNOS KI mice and respective CondKO controls. The values detected were lower than those observed for EC eNOS KO and WT mice. In particular, significantly lower values were observed in parameters related to the RBC count: RBC, HCT, and HGB. These results could be attributed to the different genomic construct that characterizes the KI models: the CondKO controls used in this case are global eNOS KO mice, and the absence of eNOS from all the tissues, coupled with TAM treatment, could have determined changes in the hematological phenotype of these mice.

However, eNOS reintroduction specifically in the endothelium did not show any difference in blood parameters in EC eNOS KI mice as compared to CondKO controls.

Furthermore, blood count was carried out on RBC eNOS KI mice that were compared in this case to the founder line eNOS^{inv/inv}. The parameters evaluated in eNOS^{inv/inv} mice were not as low as the values observed in the CondKO controls for EC eNOS KI mice.

Blood count analysis of eNOS^{inv/inv} mice showed values comparable to those observed for WT controls of the tissue-specific eNOS KO strains. Moreover, the parameters observed were not significantly different from those detected in EC eNOS KO and RBC eNOS KO.

Both CondKO and eNOS^{inv/inv} mice are born as global eNOS KO mice. For this reason, the difference between hematological parameters observed in CondKO and eNOS^{inv/inv} mice could be attributed to TAM treatment, which was performed exclusively in CondKO controls for the EC eNOS KI model and not in the founder line eNOS^{inv/inv}. However, only speculations are possible, and further investigations on the blood properties of the lines of interest need to be done.

Analysis of blood parameters of RBC eNOS KI mice showed a significant increase of RDW, PLT count, and granulocytes percentage as compared to eNOS^{inv/inv}. Moreover, a tendency of decreased monocyte percentage was detected.

High RDW values indicate that RBCs are produced in different sizes, and there is some issue with RBC production or survival. However, no significant differences were observed in RBC number or HTC. Moreover, the tendency of an increase in monocytes percentage and the significant thrombocytosis and granulocytosis could be related to an inflammatory process taking place in RBC eNOS KI mice.

Further investigations are needed to investigate the hematological phenotype observed in RBC eNOS KI mice and the physiological mechanisms that take place following eNOS reintroduction in the RBCs.

5.2 Reintroduction of eNOS in the endothelium rescues from hypertension and restores vascular endothelial function and FMD. Circulating nitrite levels are decreased in EC eNOS KO mice

As shown in this study, removing eNOS specifically from the endothelium induced a complete loss of vascular endothelial function, as demonstrated by the lack of ACh dilator response of aortic rings.

Numerous studies have demonstrated the critical role of eNOS in the endothelium in the modulation of vascular tone [13, 25, 137, 138]. Thus, it was not surprising to find a blunted reactivity of aortic rings of EC eNOS KO mice towards ACh.

The contractile response of aortic rings to increasing concentration of the α 1-adrenergic receptor agonist PE was not different in EC eNOS KO mice as compared to their WT littermate controls.

According to previous studies, the administration of vasoconstrictors determines a signaling cascade that ultimately leads to the increase of intracellular Ca²⁺ levels in the ECs and consequently the eNOS-dependent release of NO (myoendothelial feedback response). Lack of eNOS from the endothelium would impair the

functionality of this pathway and lead to a stronger response towards the application of vasoconstrictors like PE [139].

Moreover, treatment with the NO-donor SNP led to a significant leftward shift in the response of the aortic rings in EC eNOS KO mice, indicating an increased sensitivity to NO donors. This response had already been observed upon inhibition of NOS activity and in different global eNOS KO mice [133-135, 140]; however, the mechanisms responsible for shifting the curve towards higher sensitivity to NO donors are not understood yet.

A proposed theory that other research groups did not support relied on the up-regulation of sGC expression levels as a compensatory mechanism to counteract the decreased sensitivity of sGC itself [133].

However, Brandes and colleagues did not find any alteration in the expression of sGC subunits and proposed a decreased sensitivity of sGC towards NO donors after exposure to NO [134].

Another hypothesis was based on possible mutations on critical cysteines in the sGC structure (S-nitrosation) that were causing an inhibition of the enzyme itself, serving as a negative feedback mechanism for NO signaling [141].

These findings applied to the EC eNOS KO model would allow the conclusion that a baseline S-nitrosation of the sGC protein is necessary to avoid the leftward shift of the dose-response curve to SNP due to higher sensitivity to NO donors.

In vivo measurements were also carried out, and FMD was evaluated on the iliac artery after vascular occlusion. Following the lack of eNOS from the vascular compartment, an expected complete loss of FMD was detected in EC eNOS KO mice as compared to WT littermate controls, confirming the critical role of endothelial eNOS in the regulation of vascular tone and vascular function.

To make visible the unbiased effects of eNOS expressed in the endothelium, a “gain-of-function” model was generated by the reintroduction of eNOS in the endothelium of global eNOS KO mice to generate EC eNOS KI mice.

EC eNOS KI mice showed a completely restored vascular endothelial function after TAM treatment. At baseline (before TAM treatment), the aortic rings of EC eNOS KI mice behaved as aortic rings of global eNOS KO mice since TAM treatment was necessary to induce the gene sequence of interest inversion and generate the functional KI model. After TAM treatment, endothelium-dependent vasorelaxation to ACh was reestablished.

Moreover, treatment with PE determined a decreased contractile response of aortic rings in EC eNOS KI mice as compared to CondKO controls, indicating a reestablished eNOS-dependent feedback mechanism. Administration of the NOS inhibitor L-NAME showed a further loss of vascular function, indicating eNOS as the primary responsible for the vascular response.

Endothelium-independent dilation of aortic rings of EC eNOS KI mice was evaluated after treatment with the NO donor SNP and showed a signal shifted towards higher concentrations, as compared to respective CondKO controls, indicating, in this case, a decreased sensitivity to NO donors.

Furthermore, reintroduction of eNOS specifically in the endothelium completely restored FMD in EC eNOS KI mice *in vivo* as compared to CondKO control mice.

The results observed after FMD measurements of EC eNOS KO and EC eNOS KI mice confirm the predominant role of vascular eNOS as a key endogenous source of NO and its role in preserving vascular functionality following alterations of the blood flow and hypoxic stimuli. Moreover, these data confirm the role of EC eNOS in controlling the flow-mediated diameter of conduit vessels [27, 51].

The analysis of EC eNOS in vascular functionality and integrity confirms and strongly contributes to advancing previous findings, underlying the pivotal role of EC eNOS in preserving vascular endothelial function and its essential role in overcoming changes in vascular function that may result from the deletion of other proteins such as Nrf2 [131].

To investigate the role of EC eNOS in modulating BP and NO metabolism, hemodynamic measurements were carried out invasively, and NO metabolites distribution was evaluated in tissues of EC eNOS KO and EC eNOS KI mice.

Fitting to impaired vascular endothelial function findings, mice lacking eNOS specifically in the endothelium exhibited increased levels of DBP and SBP.

Although an increased BP was detected, these changes were not accompanied by changes in HR and CO as compared to WT littermate controls. However, SVR was significantly increased in EC eNOS KO mice. The finding of an increased BP is in line with previous findings on the three global eNOS KO lines investigated by Gödecke, Huang, and Shesely [25-27]. However, in contrast, global eNOS KO mice showed significantly decreased HR, but the mechanisms behind them are yet unknown.

One suggestion on this observation was that the decreased HR resulted from a compensatory response to the increased BP [26].

In EC eNOS KO mice, the lack of eNOS from the ECs is induced only a few weeks before carrying out the analysis; thus, it is reasonable to think that long-term adaptive mechanisms might not have occurred yet.

An interesting finding was that eNOS reintroduction into ECs of CondKO mice successfully rescued the hypertensive phenotype of these mice, strongly confirming the essential role of eNOS expressed in the endothelium as a regulator of systemic hemodynamics.

As previously observed in EC eNOS KO mice, also in this case, no changes in HR were detected. The HR observed in EC eNOS KI mice, and respective CondKO controls is comparable to the one observed in EC eNOS KO and WT mice. Because of TAM treatment, eNOS reintroduction in the endothelium is induced

few weeks before carrying out the analysis, excluding also in this case adaptive mechanisms that could have promoted a decrease of HR, according to Shesely hypothesis [26].

The measurement of NO metabolites on EC eNOS KO mice showed a significant decrease of circulating plasma nitrite levels as compared to WT littermate controls, demonstrating the contribution of endothelial eNOS to the circulating pool of active NO metabolites. Total NO species were significantly decreased in all the different EC eNOS KO mice tissues, but a statistical significance was observed only in the lung tissue. Nitrate levels were significantly increased in the liver of EC eNOS KO mice, contributing to an overall increase of total NO species. On the other hand, CondKO controls for EC eNOS KI mice showed significantly reduced plasma nitrite levels as compared to WT mice, of approximately 50%, indicating a profound deficiency of circulating nitrite levels upon eNOS removal.

The rescue of eNOS exclusively in the ECs was not enough to restore circulating nitrite levels in these models. Indeed, EC eNOS KI mice did not show any significant changes in circulating nitrite levels as compared to CondKO controls. These findings suggest that in global eNOS KO mice, the mechanism governing the regulation of plasma nitrite is only in part dependent on vascular/red cell eNOS-derived NO production.

RXNO levels in plasma and RBCs of EC eNOS KO and EC eNOS KI mice showed some variability and no correlation with the presence/absence of eNOS in the endothelium, conversely to what was previously reported by Stamler and colleagues. Their hypothesis was that S-nitrosylation of peptides and proteins largely mediates NO biological effects to produce bioactive nitroso species, RXNO [142-145]. After the identification of an S-nitrosoglutathione (GSNO) reductase (GSNOR) [146, 147], they generated GSNOR KO mice to distinguish *in vivo* the activity of RXNO from NO (or other reactive nitrogen species). GSNOR deficiency led to increases in basal SNO and predisposed mice to dysregulation of BP [144]. Moreover, they demonstrated that in cultured arterial ECS, stimulation of eNOS by ionophore-mediated Ca^{2+} influx is coupled to increased protein S-nitrosylation. On the other hand, inhibition of red cell eNOS with the NOS inhibitor L-NMMA eliminates RSNO levels [145].

Of particular interest are RBC levels of NO-heme, an intermediate molecule formed in the RBCs after the reaction of NO with the iron of the heme group of the Hb (Fe^{2+} -NO). NO-heme has been for a long time considered a good indicator of NO derived from the eNOS expressed in the endothelium and of systemic NO bioavailability [148].

The analysis of NO-heme levels in the RBCs of EC eNOS KO and EC eNOS KI mice surprisingly indicates that removal/reintroduction of eNOS from the endothelium does not affect NO-heme levels, questioning the theory mentioned above [148] and opening new possibilities on the role of NO-heme expressed in the RBCs.

Mice lacking the endothelial eNOS have been previously described in different global eNOS KO models [25-27], but not confirmed in other eNOS KO strains, with the hypothesis of a potential contribution of a compensatory increase of COX-mediated prostaglandins [149] or by other NOS isoforms like nNOS or iNOS [150].

Because of these new EC-specific tamoxifen-inducible models (EC eNOS KO and EC eNOS KI mice), it was possible to confirm the suggested central role of ECs in eNOS-mediated control of BP and cardiovascular hemodynamics, as initially proposed when EDRF was discovered. The advantage of these models is that the KO/KI is induced shortly before carrying out the analysis (21 days), thus avoiding the possibility that long-term compensatory mechanisms occurred, as observed in all the global eNOS KO strains [25-27].

5.3 Red cell eNOS modulates blood pressure independently from vascular eNOS. Circulating nitrite is decreased in RBC eNOS KO mice, and the levels of NO-heme are changed in RBC eNOS KO/KI mice

As already mentioned, a functional eNOS is also expressed in the RBCs [77, 78].

The role of red cell eNOS in the modulation of vascular function, systemic hemodynamics, and NO metabolism was evaluated here on RBC eNOS KO and RBC eNOS KI mouse models.

RBC eNOS KO mice did not show any changes in vascular endothelial dilator function in response to ACh, or after treatment with PE or SNP. These findings are in accordance with previous studies on chimeric mice models generated by BM transplantation from global eNOS KO mice into irradiated WT mice and *vice versa* [67].

The fully preserved vascular function of RBC eNOS KO mice upon ACh treatment of aortic rings indicates that the genetic knockdown of eNOS in the RBCs does not cause any off-target effect in the vascular tissue. FMD was also evaluated *in vivo* and showed a fully preserved vascular functionality in RBC eNOS KO mice as compared to WT littermate controls.

Hemodynamic measurements demonstrated that the lack of eNOS in the RBCs significantly increased DBP, SBP, and SVR without affecting cardiac parameters *in vivo*. These data indicate a role of red cell eNOS in regulating SVR and/or function of resistant arteries *in vivo* via the regulation of circulating NO metabolites, and it indicates the limited role of red cell eNOS in regulating cardiac performance under basal conditions. The fact that mice lacking eNOS in the RBCs were hypertensive was surprising.

A role for a circulating blood cell-eNOS in BP regulation had already been postulated in chimera mice [67], which showed an increased BP and decreased circulating nitrite levels.

HR of RBC eNOS KO mice showed a tendency to decreased values as compared to WT littermate controls, and this result was different from what was observed in EC eNOS KO mice. The reason behind this difference may be that RBC eNOS KO mice were born with this mutation and developed high BP early on. This would support the theory proposed by Shesely that lower HR in global eNOS KO mice is an adaptive mechanism in response to high BP [26].

NO metabolites distribution of RBC eNOS KO mice showed a significant decrease of total NO species in the liver and plasma.

NO-heme levels were significantly increased in RBCs of RBC eNOS KO mice as compared to WT controls. These results could indicate a paracrine role of nitrite and, in general, NO metabolites in the regulation of BP [104] and demonstrate a central role of eNOS-dependent signaling in RBCs.

An important finding was that reactivation of eNOS specifically in RBCs fully rescued the CondKO controls from hypertension, and the HR of RBC eNOS KI mice was not different from the respective CondKO controls. Conversely to what was observed for RBC eNOS KO mice, RBC eNOS KI mice showed significantly decreased levels of NO-heme in the RBCs.

The results observed in NO-heme levels in the RBCs of RBC eNOS KO and RBC eNOS KI mice are fascinating and suggest that eNOS in the RBCs is one crucial source of NO-heme and indicate red cell eNOS as the major contributor to eNOS-derived NO and systemic NO bioavailability. Moreover, it appears that NO-heme levels in RBCs depend on the presence/absence of eNOS in RBCs.

5.4 Administration of nitrate in the drinking water affects BP of WT and EC eNOS KO mice and has no effects on BP and plasma nitrite levels of RBC eNOS KO mice

Further conducted experiments focused on the possible role of RBCs in utilizing dietary nitrate to modulate NO metabolism and systemic hemodynamics.

Tissue-specific eNOS KO mice were supplemented with low-nitrate water (Vittel) vs. nitrate-enriched water (Vittel + nitrate, 200 μ M), and BP was measured invasively by catheterization of the coronary artery to evaluate the effects of nitrate intake on systemic hemodynamics.

Moreover, circulating nitrite levels were analyzed in EC eNOS KO and RBC eNOS KO mice to investigate the role of vascular eNOS and red cell eNOS on NO metabolism after nitrate administration.

Addition of dietary nitrate in the drinking water induced a significant decrease in BP in WT controls and EC eNOS KO mice. In detail, a significant decreased MAP was observed in mice drinking nitrate-enriched water as compared to MAP levels measured after drinking the low-nitrate water. The decrease in BP was

accompanied by a significant increase in circulating nitrite levels, suggesting that the organism used the exogenous nitrate to produce nitrite, which promoted a decrease in MAP after its release into the circulation, according to the following literature [39, 151].

In RBC eNOS KO mice, nitrate addition to the drinking water had no effects on MAP, and no differences were detected as compared to RBC eNOS KO mice drinking tap water or water with low-nitrate concentration. No differences were detected when nitrate was added to the drinking water when analyzing the plasma nitrite levels.

These results may suggest that when eNOS is not expressed in the RBCs, there is no correlation among nitrate administration, nitrite levels in the plasma, and BP.

These experiments speculate that red cell eNOS plays a key role in the modulation of BP by using an exogenous source of nitrate to modulate NO metabolism and systemic hemodynamics.

However, the mechanisms underlying the role of red cell eNOS in modulating BP upon nitrate administration in the drinking water remain still unknown, and further investigations will be necessary for future studies. With this purpose, RBC eNOS KI mice might be a valuable tool in these investigations to reveal the distinct role of red cell eNOS, specifically in the modulation of blood pressure upon nitrate administration.

5.5 How does red cell eNOS regulate BP?

As observed by results on vascular function, BP measurements, and analysis of NO metabolites, we demonstrated that endothelial eNOS and red cell eNOS both play a pivotal but independent role in the modulation of systemic hemodynamics and contribute to the levels of systemic NO metabolites in different ways. Moreover, red cell eNOS rather than EC eNOS was shown as the primary contributor of NO-heme levels, as clearly demonstrated by comparing the levels of NO-heme in the four mouse lines analyzed.

However, the mechanisms by which RBCs modulate BP are unclear yet, and there are different theories.

Although it was hypothesized, a direct effect of eNOS-derived-NO on the vascular wall seems rather difficult to achieve since this would need NO to diffuse from RBCs to the plasma avoiding the scavenging of Hb, and then it should stimulate sGC in the SMCs through ECs. A possible mechanism to avoid Hb inhibition of NO signaling could be the mediation by NO metabolites, and candidates include SNO-hemoglobin [72-74], NO-heme [71], and nitrite [75, 76]. Moreover, under normoxic conditions, the compartmentalization of NO synthesis in RBCs could mediate the direct diffusion of NO through the membrane to escape the fast scavenging reaction with Hb [103].

As already mentioned, Hb is a tetramer composed of two α and two β subunits containing a prosthetic heme group with a central Fe^{2+} ion that can reversibly bind oxygen in the lungs and transport it to the tissues. At the same time, NO can interact with heme groups or thiols of Hb, serving as a paradigm for NO function in biology [73, 152-154].

The reaction of NO with thiols (cysteine-93) of the Hb β -chain leads to the formation of SNO-Hb and the further release of NO in the form of S-nitrosoglutathione [73]. This reaction is regulated by conformational changes of Hb tetramer structure from the oxygenated relaxed (R)-state to the tensed (T)-state, and it is proposed that SNO-Hb formation is disfavored under deoxygenated conditions in the T structure [154]. However, multiple findings have challenged these proposed mechanisms postulating that SNO-Hb is not stable in RBCs [155] and that NO binds to the R- or T-state of Hb independently, with the same constant rates [110]. Another opinion is that NO is degraded by Hb rather than preserved [82]. Taken all these observations together, the formation of SNO-Hb seems unlikely a mediator of red cell eNOS-derived NO signaling. Moreover, we did not find changes in RXNO levels in the plasma of tissue-specific eNOS KO/KI mice.

On the other hand, we observed that RBC eNOS KO had decreased NO-heme levels in RBCs, indicating red cell eNOS one crucial source of NO-heme and pointing at NO-heme as a good indicator of NO derived from the eNOS expressed in the RBCs rather than the one expressed in the endothelium.

NO-heme is an intermediate formed from the reaction of NO in the RBCs with the Fe^{2+} ion of the heme groups of Hb, and it is also considered a candidate for NO signaling.

Several physiological and experimental observations have suggested that NO-heme is not stable under oxidizing conditions; in fact, NO-heme and nitrite are forming in the pulmonary vasculature during NO gas inhalation and are further consumed, creating an artery-to-vein gradient, as observed by reductive chemiluminescence and electron paramagnetic resonance (EPR) spectroscopy in humans breathing NO gas. This experiment suggested a rapid *in vivo* dissociation of NO from the heme group under these conditions [156-158].

Stamler and colleagues attributed the rapid disappearance of NO-heme to an allosteric transition of NO in the Hb from heme groups to acceptor thiols on cysteine-93, such as glutathione [73, 159] or those in the RBC membranes that transduce NO bioactivity [47, 159]. This transfer is favored under oxygenated conditions, in oxygenated R-state molecules, and in the presence of high nitrite concentrations [154, 160]. On the other hand, Grubina and colleagues demonstrated that NO-heme degradation was observed exclusively in the presence of nitrite, suggesting that the oxidative denitrosylation of NO-heme is required for the release of NO from NO-heme [161].

The findings of this work indicate the fundamental role of NO-heme in the RBCs as an indicator of NO derived from the eNOS expressed in the RBCs rather than the one expressed in the endothelium.

Interestingly, a further mechanism for bioactivity related to NO-heme was proposed recently. The “NO-heme signaling hypothesis” assumes that NO-heme is a reservoir of NO and the release of the entire complex in the circulation as a signaling entity [162]. According to this theory, the NO-heme complex could operate as an sGC receptor agonist and promote sGC activation. A major *in vivo* product of constitutive eNOS is the exchangeable NO-(Fe²⁺)heme that in the physiological environment can be reversibly converted to its redox sibling, NO-(Fe³⁺)heme. A carrier-bound NO-(Fe³⁺)heme has the potential to mediate the selective S- (N-) nitrosation of proteins and, thus, regulate numerous signaling pathways [162]. However, its functional significance is still under investigation.

According to our findings, the possibility that RBCs export NO-heme cannot be excluded. However, Hb-bound-NO is more likely to be extruded from the RBCs through membrane channels. We hypothesize the escape of NO or its metabolites from the RBCs through the anion exchanger AE-1, which could provide the optimal pathway for NO export through the formation of a direct complex with Hb. According to our results, eNOS and AE-1 are co-localized on the RBC membrane, and further investigations are necessary to evaluate the possibility of interactions between Hb and AE-1 following NO production by red cell eNOS. eNOS expressed in the RBCs contributes to the overall pool of circulating nitrite [63, 103]. This is in accordance with Wood, who observed eNOS deficiency in the blood cells of chimera mice and a decrease in the circulating nitrite levels [67]. As previously shown, we also found a significant decrease in circulating nitrite levels upon eNOS removal from both the endothelium and RBCs.

Nitrite has been demonstrated to actively participate in the modulation of vascular tone and BP in different tissues [39, 151, 163]. Nitrite is reduced to NO by several mechanisms, including enzymatic reduction by xanthine oxidase [164-166], NOS [167], components of the mitochondrial electron transport chain [168], and by nonenzymatic acidic disproportionation [58]. However, these mechanisms require low pH and oxygen saturation and, thus, do not occur under physiological hypoxia.

Under low oxygen tension conditions, RBCs have been shown to reduce nitrite to NO by reaction with deoxyHb that exerts a nitrite reductase activity, producing NO from nitrite and promoting NO-dependent vasorelaxation [48, 77, 78, 104, 105]. This reaction has been demonstrated to be implicated in nitrite- and deoxyHb-dependent vasodilation *in vivo* [104, 169] and *in vitro* [104, 106], as well as in nitrite-mediated protection after I/R injury [103, 170, 171]. In particular, studies of NO gas inhalation in humans have demonstrated increases in red cell NO-heme and plasma nitrite concentrations associated with peripheral NO-dependent vasodilation [104, 169].

In support of these findings, RBCs were proposed to store high nitrite concentrations, but we cannot confirm this [76]. Moreover, a gradient of nitrite from arterial to venous plasma could support the theory that nitrite is used for hypoxic vasodilation [112].

To conclude, we observed a decrease of nitrite levels in RBC eNOS KO mice, which is not recovered in RBC eNOS KI, and there is a correlation between NO-heme levels in the RBCs and red cell eNOS expression. Nitrite and NO-heme are likely candidates to mediate BP regulation. However, future investigations are needed to evaluate how eventually NO, or its metabolites can be released in the circulation and how RBCs can modulate systemic hemodynamics.

5.6 Summary and perspective

In summary, in this study, we generated and characterized a series of novel mouse models for tissue-specific gene targeting of eNOS.

The comparison of mouse models where eNOS was specifically removed or reintroduced in the endothelium or erythroid cells demonstrates that eNOS plays independent roles in these two cellular compartments in the modulation of systemic hemodynamics and NO metabolism.

Importantly, for the first time, compelling evidence are presented, demonstrating that red cell eNOS directly contributes to systemic NO bioavailability and BP homeostasis independently of vascular endothelial eNOS. Specifically, removing eNOS from the RBCs leads to a surprisingly significant increase in BP, and eNOS reintroduction in the RBCs restores the hypertensive phenotype of global eNOS KO mice, demonstrating a direct link between eNOS signaling in RBCs and BP homeostasis.

Moreover, analysis of NO metabolites indicates red cell eNOS rather than EC eNOS as the primary contributor of NO-heme levels, as clearly demonstrated by comparing the levels of NO-heme in the mouse lines analyzed. These data suggest that eNOS in the RBCs is functional and is one crucial source of NO-heme in RBCs.

From a future perspective, these mouse models might be essential to investigate what tissue is important for effects attributed to eNOS and will allow a better understanding of the specific role of red cell eNOS in pathophysiological conditions, including AMI, CAD, and chronic kidney disease, as well as hematological diseases and hemoglobinopathies, which are characterized by a systemic decrease in NO bioavailability and/or defects in eNOS signaling (like sickle cell disease) [172].

The expression of eNOS might play a protective role after ischemia/reperfusion (I/R) injury [173, 174]. Moreover, these data and models may also help understanding how red cell eNOS signaling may affect RBC function and integrity (e.g., as oxygen transporters) and may enable us to refine the criteria for blood banking and transfusion [175].

6. References

1. Virani, S.S., Alonso, C.A., Benjamin, E.J., Bittencourt, M.S., Callaway, C.W., Carson, A.P., Chamberlain, A.M., Chang, A.R., Cheng, S., Delling, F.N., Djousse, L., Elkind, M.S.V., Ferguson, J.F., Fornage, M., Khan, S.S., Kissela, B.M., Knutson, K.L., Kwan, T.W., Lackland, D.T., Lewis, T.T., Lichtman, J.H., Longenecker, C.T., Loop, M.S., Lutsey, P.L., Martin, S.S., Matsushita, K., Moran, A.E., Mussolino, M.E., Perak, A.M., Rosamond, W.D., Roth, G.A., Sampson, U.K.A., Satou, G.M., Schroeder, E.B., Shah, S.H., Shay, C.M., Spartano, N.L., Stokes, A., Tirschwell, D.L., VanWagner, L.B., Tsao, C.W., *Heart Disease and Stroke Statistics—2020 Update: A Report From the American Heart Association*. *Circulation*, 2020. **141**: p. 139-596.
2. Staessen, J.A., Wang, J., Bianchi, G., Birkenhäger, W.H., *Essential hypertension*. *The Lancet*, 2003. **361**(9369): p. 1629-1641.
3. Yusuf, S., Hawken, S., Ôunpuu, S., Dans, T., Avezum, A., Lanas, F., McQueen, M., Budaj, A., Pais, P., Varigos, J., Lisheng, L.,, *Effect of potentially modifiable risk factors associated with myocardial infarction in 52 countries (the INTERHEART study): case-control study*. *The Lancet*, 2004. **364**(9438): p. 937-952.
4. Mahmood, S.S., Levy, D., Vasan, R.S., Wang, T.J., *The Framingham Heart Study and the epidemiology of cardiovascular disease: a historical perspective*. *The Lancet*, 2014. **383**(9921): p. 999-1008.
5. Daiber, A., Steven, S., Weber, A., Shuvaev, V.V., Muzykantov, V.R., Laher, I., Li, H., Lamas, S., Munzel, T., *Targeting vascular (endothelial) dysfunction*. *Br J Pharmacol*, 2017. **174**(12): p. 1591-1619.
6. Committee, G., *2003 European Society of Hypertension–European Society of Cardiology guidelines for the management of arterial hypertension*. *Journal of Hypertension*, 2003. **21**(6): p. 1011-1053.
7. Tennant, M., McGeachie, J.K., *Blood vessel structure and function: a brief update on recent advances*. *National Library of Medicine*, 1990. **60**(10): p. 747-753.
8. Mulvany, M.J., *Vascular remodelling of resistance vessels: can we define this?* . *Cardiovasc Res*, 1999. **41**(1): p. 9-13.
9. Taddei, S., Virdis, A., Mattei, P., Ghiadoni, L., Sudano, I., Salvetti, A., *Defective L-arginine-nitric oxide pathway in offspring of essential hypertensive patients*. *Circulation*, 1996. **94**(6): p. 1298-303.

10. Widlansky, M.E., Gokce, N., Keaney Jr., J.F., Vita, J.A., *The clinical implications of endothelial dysfunction*. J Am Coll Cardiol, 2003. **42**(7): p. 1149-60.
11. Lekakis, J., Abraham, P., Balbarini, A., Blann, A., Boulanger, C.M., Cockcroft, J., Cosentino, F., Deanfield, J., Gallino, A., Ikonomidis I., Kremasinos, D., Landmesser, U., Protogerou, A., Stefanadis, C., Tousoulis, D., Vassalli, G., Vink, H., Werner, N., Wilkinson, I., Vlachopoulos, C., *Methods for evaluating endothelial function: a position statement from the European Society of Cardiology Working Group on Peripheral Circulation*. European Journal of Preventive Cardiology, 2011. **18**(6): p. 775-789.
12. Moncada, S., Palmer, R.M., Higgs, E.A., *Nitric oxide: physiology, pathophysiology, and pharmacology*. Pharmacol Rev, 1991. **43**(2): p. 109-42.
13. Furchgott, R.F., Zawadzki, J.V., *The obligatory role of endothelial cells in the relaxation of arterial smooth muscle by acetylcholine*. Nature, 1980. **288**: p. 373-376.
14. Ignarro, L.J., *Biological actions and properties of endothelium-derived nitric oxide formed and released from artery and vein*. Circ Res, 1989. **65**: p. 1-21.
15. Hill, B.G., Dranka, B.P., Bailey, S.M., Lancaster, J.R., Jr., Darley-Usmar, V.M., *What part of NO don't you understand? Some answers to the cardinal questions in nitric oxide biology*. J Biol Chem, 2010. **285**(26): p. 19699-704.
16. Vallance, P., Collier, J., Moncada, S., *Effects of endothelium-derived nitric oxide on peripheral arteriolar tone in man*. The Lancet, 1989. **2**: p. 997-1000.
17. Brecht, D.S., Snyder, S.H., *Nitric oxide: a physiologic messenger molecule*. Annu. Rev. Biochem., 1994. **63**: p. 175-195.
18. Nathan, C., *Points of control in inflammation*. Nature, 2002. **420**: p. 846-852.
19. Forstermann, U., Sessa, W.C., *Nitric oxide synthases: regulation and function*. Eur Heart J, 2012. **33**(7): p. 829-37, 837a-837d.
20. Balligand, J.L., Feron, O., Dessy, C., *eNOS activation by physical forces: from short-term regulation of contraction to chronic remodeling of cardiovascular tissues*. Physiol Rev., 2009. **89**: p. 481-534.
21. Erkens, R., Suvorava, T., Kramer, C.M., Diederich, L.D., Kelm, M., Cortese-Krott, M.M., *Modulation of Local and Systemic Heterocellular Communication by Mechanical Forces: A Role of Endothelial Nitric Oxide Synthase*. Antioxid Redox Signal, 2017. **26**(16): p. 917-935.
22. Farah, C., Michel, L.Y.M., Balligand, J.-L., *Nitric oxide signalling in cardiovascular health and disease*. Nature Reviews Cardiology, 2018. **15**(5): p. 292.

23. Straub, A.C., Lohman, A.W., Billaud, M., Johnstone, S.R., Dwyer, S.T., Lee, M.Y., Bortz, P.S., Best, A.K., Columbus, L., Gaston, B., Isakson, B.E., *Endothelial cell expression of haemoglobin α regulates nitric oxide signalling*. Nature, 2012. **491**(7424): p. 473-7.
24. Biwer, L.A., Taddeo, E. P., Kenwood, B. M., Hoehn, K. L., Straub, A. C., Isakson, B. E., *Two functionally distinct pools of eNOS in endothelium are facilitated by myoendothelial junction lipid composition*. Biochim Biophys Acta, 2016. **1861**(7): p. 671-9.
25. Huang, P.L., Huang, Z., Mashimo, H., Bloch, K.D., Moskowitz, M.A., Bevan, J.A., Fishman, M.C., *Hypertension in mice lacking the gene for endothelial nitric oxide synthase*. Nature, 1995. **377**(6546): p. 239-42.
26. Shesely, E.G., Maeda, N., Kim, H.S., Desai, K.M., Kregel, J.H., Laubach, V.E., Sherman, P.A., Sessa, W.C., Smithies, O., *Elevated blood pressures in mice lacking endothelial nitric oxide synthase*. Proc Natl Acad Sci U S A, 1996. **93**(23): p. 13176-81.
27. Godecke, A., Decking, U.K., Ding, Z., Hirchenhain, J., Bidmon, H. J., Godecke, S., Schrader, J., *Coronary hemodynamics in endothelial NO synthase knockout mice*. Circ Res, 1998. **82**(2): p. 186-94.
28. Cortese-Krott, M.M., Kelm, M., *Endothelial nitric oxide synthase in red blood cells: key to a new erythrocrine function?* Redox Biol, 2014. **2**: p. 251-8.
29. Rapoport, R.M., Draznin, M.B., Murad, F., *Endothelium-dependent vasodilator- and nitrovasodilator-induced relaxation may be mediated through cyclic GMP formation and cyclic GMP-dependent protein phosphorylation*. Trans Assoc Am Physicians, 1983. **96**: p. 19-30.
30. Raj, U., Shimoda, L., *Oxygen-dependent signaling in pulmonary vascular smooth muscle*. Am J Physiol Lung Cell Mol Physiol, 2002. **283**(4): p. L671-7.
31. Somlyo, A.P., Somlyo, A.V., *Signal transduction and regulation in smooth muscle*. Nature, 1994. **372**: p. 231-236.
32. Surks, H.K., Mochizuki, N., Kasai, Y., Georgescu, S.P., Tang, K.M., Ito, M., Lincoln, T.M., Mendelsohn, M.E., *Regulation of Myosin Phosphatase by a Specific Interaction with cGMP-Dependent Protein Kinase Ia*. Science, 1999. **286**(5444): p. 1583-1587.
33. Mergia, E., Friebe, A., Dangel, O., Russwurm, M., Koesling, D., *Spare guanylyl cyclase NO receptors ensure high NO sensitivity in the vascular system*. J Clin Invest, 2006. **116**(6): p. 1731-7.
34. Durante, W., Johnson, F.K., Johnson, R.A., *Arginase: A critical regulator of nitric oxide synthesis and vascular function*. Clin Exp Pharmacol Physiol, 2007. **34**(9): p. 906-911.
35. Pernow, J., Jung, C., *Arginase as a potential target in the treatment of cardiovascular disease: Reversal of arginine steal?* Cardiovasc Res, 2013. **98**(3): p. 334-343.

36. Ryoo, S., Gupta, G., Benjo, A., Lim, H.K., Camara, A., Sikka, G., Lim, H.K., Sohi, J., Santhanam, L., Soucy, K., Taday, E., Baraban, E., Ilies, M., Gerstenblith, G., Nyhan, D., Shoukas, A., Christianson, D.W., Alp, N.J., Champion, H.C., Huso, D., Berkowitz, D.E., *Endothelial arginase II: A novel target for the treatment of atherosclerosis*. *Circ Res*, 2008. **102**(8): p. 923-932.
37. Shemyakin, A., Kövamees, O., Rafnsson, A., Böhm, F., Svenarud, P., Settergren, M., Jung, C., Pernow, J., *Arginase Inhibition Improves Endothelial Function in Patients With Coronary Artery Disease and Type 2 Diabetes Mellitus*. *Circulation*, 2012. **126**(25): p. 2943-2950.
38. Bryan, N.S., Rassaf, T., Maloney, R.E., Rodriguez, C.M., Saijo, F., Rodriguez, J.R., Feelisch, M., *Cellular targets and mechanisms of nitrosylation: an insight into their nature and kinetics in vivo*. *Proceedings of the National Academy of Sciences*, 2004. **101**(12): p. 4308-4313.
39. Lundberg, J.O., Carlsson, S., Engstrand, L., Morcos, E., Wiklund, N.P., Weitzberg, E., Gladwin, M. T., *The nitrate-nitrite-nitric oxide pathway in physiology and therapeutics*. *Nat Rev Drug Discov*, 2008. **7**(2): p. 156-67.
40. Jansson, E.A., Huang, L., Malkey, R., Govoni, M., Nihlen, C., Olsson, A., Stensdotter, M., Petersson, J., Holm, L., Weitzberg, E., Lundberg, J.O., *A mammalian functional nitrate reductase that regulates nitrite and nitric oxide homeostasis*. *Nat Chem Biol*, 2008. **4**(7): p. 411-7.
41. Kleinbongard, P., Dejam, A., Lauer, T., Rassaf, T., Schindler, A., Picker, O., Scheeren, T., Gödecke, A., Schrader, J., Schulz, R., Heusch, G., Schaub, G.A., Bryan, N. S., Feelisch, M., Kelm, M., *Plasma nitrite reflects constitutive nitric oxide synthase activity in mammals*. *Free Radic Biol Med*, 2003. **35**(7): p. 790-6.
42. Milsom, A.B., Fernandez, B.O., Garcia-Saura, M.F., Rodriguez, J., Feelisch, M., *Contributions of nitric oxide synthases, dietary nitrite/nitrate, and other sources to the formation of NO signaling products*. *Antioxid Redox Signal*, 2012. **17**(3): p. 422-32.
43. Tannenbaum, S.R., Correa, P., *Nitrate and gastric cancer risks*. *Nature*, 1985. **317**: p. 675-676.
44. Mirvish, S.S., *Role of N-nitroso compounds (NOC) and N-nitrosation in etiology of gastric, esophageal, nasopharyngeal and bladder cancer and contribution to cancer of known exposures to NOC*. *Cancer Letters*, 1995. **93**(1): p. 17-48.
45. Lundberg, J.O., Govoni, M., *Inorganic nitrate is a possible source for systemic generation of nitric oxide*. *Free Radic Biol Med*, 2004. **37**(3): p. 395-400.
46. Cooper, C.E., *Nitric oxide and iron proteins*. *Biochim Biophys Acta*, 1999. **1411**(2-3): p. 290-309.
47. Pawloski, J.R., Hess, D.T., Stamler, J.S., *Export by red blood cells of nitric oxide bioactivity*. *Nature*, 2001. **409**(6820): p. 622-626.

48. Bryan, N.S., Fernandez, B.O., Bauer, S.M., Garcia-Saura, M.F., Milsom, A.B., Rassaf, T., Maloney, R.E., Bharti, A., Rodriguez, J., Feelisch, M., *Nitrite is a signaling molecule and regulator of gene expression in mammalian tissues*. *Nature Chemical Biology*, 2005. **1**: p. 290–297.
49. Govoni, M., Jansson, E.Å., Weitzberg, E., Lundberg, J.O., *The increase in plasma nitrite after a dietary nitrate load is markedly attenuated by an antibacterial mouthwash*. *Nitric Oxide*, 2008. **19**(4): p. 333-337.
50. Petersson, J., Carlström, M., Schreiber, O., Phillipson, M., Christoffersson, G., Jägare, A., Roos, S., Jansson, S.Å., Persson, A.E.G., Lundberg, J.O., Holm, L., *Gastroprotective and blood pressure lowering effects of dietary nitrate are abolished by an antiseptic mouthwash*. *Free Radic Biol Med*, 2009. **46**(18): p. 1068-1075.
51. Kapil, V., Milsom, A.B., Okorie, M., Maleki-Toyserkani, S., Akram, F., Rehman, F., Arghandawi, S., Pearl, V., Benjamin, N., Loukogeorgakis, S., MacAllister, R., Hobbs, A.J., Webb, A.J., Ahluwalia, A., *Inorganic Nitrate Supplementation Lowers Blood Pressure in Humans: role for Nitrite-Derived NO*. *Hypertension*, 2010. **56**: p. 274-281.
52. Böhmer, A., Beckmann, B., Sandmann, J., Tsikas, D., *Doubts concerning functional endothelial nitric oxide synthase in human erythrocytes*. *Blood*, 2012. **119**(5): p. 1322-3.
53. Doel, J.J., Benjamin, N., Pritchard, M., Rogers, H.M., Allaker, R.P., *Evaluation of bacterial nitrate reduction in the human oral cavity*. *Eur J Oral Sci*, 2005. **113**(1): p. 14-19.
54. Cortese-Krott, M.M., *Response to commentary*. *Redox Biol*, 2015. **5**: p. 411-2.
55. Spiegelhalder, B., Eisenbrand, G., Preussmann, R., *Influence of dietary nitrate on nitrite content of human saliva: Possible relevance to in vivo formation of N-nitroso compounds*. *Food and Cosmetics Toxicology*, 1976. **14**(6): p. 545/548.
56. Lundberg, J.O., Weitzberg, E., Cole, J.A., Benjamin, N., *Nitrate, bacteria and human health*. *Nat Rev Microbiology*, 2004. **2**: p. 593-602.
57. Benjamin, N., O'Driscoll, F., Dougall, H., Duncan, C., Smith, L., Golden, M., McKenzie, H., *Stomach NO synthesis*. *Nature*, 1994. **368**: p. 502.
58. Lundberg, J.O., Weitzberg, E., Lundberg, J.M., Alving, K., *Intragastric nitric oxide production in humans: measurements in expelled air*. *Gut*, 1994. **35**(11): p. 1543-1546.
59. Weller, R., Pattullo, S., Smith, L., Golden, M., Ormerod, A., Benjamin, N., *Nitric Oxide Is Generated on the Skin Surface by Reduction of Sweat Nitrate*. *Journal of Investigative Dermatology*, 1996. **107**(3): p. 327-331.
60. Lundberg, J.O., Carlsson, S., Engstrand, L., Morcos, E., Wiklund, N.P., Weitzberg, E., *Urinary nitrite: More than a marker of infection*. *Urology*, 1997. **50**(2): p. 189-191.

61. Lauer, T., Preik, M., Rassaf, T., Strauer, B.E., Deussen, A., Feelisch, M., Kelm, M., *Plasma nitrite rather than nitrate reflects regional endothelial nitric oxide synthase activity but lacks intrinsic vasodilator action* PNAS, 2001. **98**(22): p. 12814-12819.
62. Dzierzak, E., Philipsen, E., *Erythropoiesis: Development and Differentiation*. Cold Spring Harbor Perspectives in Medicine, 2013. **3**(4): p. a011601.
63. Helms, C., Kim-Shapiro, D.B., *Hemoglobin-mediated nitric oxide signaling*. Free Radic Biol Med, 2013. **61**: p. 464-472.
64. Canham, P.B., Burton, A.C., *Distribution of size and shape in populations of normal human red cells*. Circ Res, 1968. **22**(3): p. 405-422.
65. Parthasarathi, K., Lipowsky, H.H., *Capillary recruitment in response to tissue hypoxia and its dependence on red blood cell deformability*. Am J Physiol, 1999. **277**(6): p. H2145-2157.
66. Cokelet, G.R., Meiselman, H.J., *Rheological Comparison of Hemoglobin Solutions and Erythrocyte Suspensions*. Science, 1968. **162**(3850): p. 275-277.
67. Wood, K.C., Cortese-Krott, M.M., Kovacic, J.C., Noguchi, A., Liu, V.B., Wang, X., Raghavachari, N., Boehm, M., Kato, G.J., Kelm, M., Gladwin, M.T., *Circulating blood endothelial nitric oxide synthase contributes to the regulation of systemic blood pressure and nitrite homeostasis*. Arterioscler Thromb Vasc Biol, 2013. **33**(8): p. 1861-71.
68. Benz, P.M., Fleming, I., *Can erythrocytes release biologically active NO?* Cell Commun Signal, 2016. **14**(1): p. 22.
69. Cortese-Krott, M.M., Kramer, C.M., Kelm, M., *NOS, NO, and the Red Cell*, in *Nitric Oxide (Third Edition)*. 2017. p. 185-194.
70. Cassoly, R., Gibson, Q.H., *Conformation, co-operativity and ligand binding in human hemoglobin*. Journal of Molecular Biology, 1975. **91**(3): p. 301-313.
71. Herold, S., *The outer-sphere oxidation of nitrosyliron(II)hemoglobin by peroxynitrite leads to the release of nitrogen monoxide*. Inorg. Chem., 2004. **43**: p. 3783-3785.
72. Rassaf, T., Bryan, N.S., Maloney, R.E., Specian, V., Kelm, M., Kalyanaraman, B., Rodriguez, J., Feelisch, M., *NO adducts in mammalian red blood cells: too much or too little?* Nature Medicine, 2003. **9**: p. 481-482.
73. Jia, L., Bonaventura, C., Bonaventura, J., Stamler, J.S., *S-nitrosohaemoglobin: a dynamic activity of blood involved in vascular control*. Nature, 1996. **380**(6571): p. 221-6.
74. Gladwin, M.T., Lancaster Jr., J.R., Freeman, B.A., Schechter, A.N., *Nitric oxide's reactions with hemoglobin: a view through the SNO-storm*. Nature Medicine, 2003. **9**: p. 496-500.

75. Vitturi, D.A., Teng, X., Toledo, J.C., Matalon, JS., Lancaster Jr., J.R., Patel R.P., *Regulation of nitrite transport in red blood cells by hemoglobin oxygen fractional saturation*. Am. J. Physiol. Heart Circ. Physiol., 2009. **296**: p. H1398-H1407.
76. Dejam, A., Hunter, C.J., Pelletier, M.M., Hsu, L.L., Machado, R.F., Shiva, S., Power, G.G., Kelm, M., Gladwin, M.T., Schechter, A.N., *Erythrocytes are the major intravascular storage sites of nitrite in human blood*. Blood, 2005. **106**: p. 734-739.
77. Cortese-Krott, M.M., Rodriguez-Mateos, A., Sansone, R., Kuhnle, G.G., Thasian-Sivarajah, S., Krenz, T., Horn, P., Krisp, C., Wolters, D., Heiss, C., Kroncke, K. D., Hogg, N., Feelisch, M., Kelm, M., *Human red blood cells at work: identification and visualization of erythrocytic eNOS activity in health and disease*. Blood, 2012. **120**(20): p. 4229-37.
78. Kleinbongard, P., Schulz, R., Rassaf, T., Lauer, T., Dejam, A., Jax, T., Kumara, I., Gharini, P., Kabanova, S., Ozuyaman, B., Schnurch, H. G., Godecke, A., Weber, A. A., Robenek, M., Robenek, H., Bloch, W., Rosen, P., Kelm, M., *Red blood cells express a functional endothelial nitric oxide synthase*. Blood, 2006. **107**(7): p. 2943-51.
79. Kang, E.S., Ford, K., Grokulsky, G., Wang, Y.-B., Chiang, T.M., Acchiardo, S.R., *Normal circulating adult human red blood cells contain inactive NOS proteins*. J Lab Clin Med, 2000. **135**(6): p. 444-451.
80. Ulker, P., Gunduz, F., Meiselman, H.J., Baskurt, O.K., *Nitric oxide generated by red blood cells following exposure to shear stress dilates isolated small mesenteric arteries under hypoxic conditions*. Clin Hemorheol Microcirc, 2013. **54**(4): p. 357-369.
81. Hobbs, A.J., Gladwin, M.T., Patel, R.P., Williams, D.L.H., Butlere, A.R., *Haemoglobin: NO transporter, NO inactivator or NO one of the above?* Trends Pharmacol Sci, 2002. **23**(9).
82. Joshi, M.S., Ferguson Jr., T.B., Han, T.H., Hyduke, D.R., Liao, J.C., Rassaf, T., Bryan, N., Feelisch, M., Lancaster Jr., J.R., *Nitric oxide is consumed, rather than conserved, by reaction with oxyhemoglobin under physiological conditions*. Proc Natl Acad Sci U S A, 2002. **99**(16): p. 10341-10346.
83. Robinson, J.M., Lancaster Jr., J.R., *Hemoglobin-Mediated, Hypoxia-Induced Vasodilation via Nitric Oxide: Mechanism(s) and Physiologic versus Pathophysiologic Relevance*. Am J Respir Cell Mol Bio, 2005. **32**(4): p. 257-261.
84. Basu, S., Grubina, R., Huang, J., Conradie, J., Huang, Z., Jeffers, A., Jiang, A., He, X., Azarov, I., Seibert, R., Mehta, A., Patel, R., King, S.B., Hogg, N., Ghosh, A., Gladwin, M.T., Kim-Shapiro, D.B., *Catalytic generation of N₂O₃ by the concerted nitrite reductase and anhydrase activity of hemoglobin*. Nat Chem Biol, 2007. **3**: p. 785-794.

85. Rodkey, F.L., *A mechanism for the conversion of oxyhemoglobin to methemoglobin by nitrite*. Clin Chem, 1976. **22**(12): p. 1986-1990.
86. Shingles, R., Roh, M.H., McCarty, R.E., *Direct Measurement of Nitrite Transport Across Erythrocyte Membrane Vesicles Using the Fluorescent Probe, 6-Methoxy-N-(3-sulfopropyl) quinolinium*. Journal of Bioenergetics and Biomembranes, 1997. **29**: p. 611-616.
87. Jensen, F.B., Rohde, S., *Comparative analysis of nitrite uptake and hemoglobin-nitrite reactions in erythrocytes: sorting out uptake mechanisms and oxygenation dependencies*. Am J Physiol Cell Physiol, 2010. **298**: p. R972-R982.
88. Rifkind, J.M., Mohanty, J.G., Nagababu, E., Salgado, M.T., Cao, Z., *Potential Modulation of Vascular Function by Nitric Oxide and Reactive Oxygen Species Released From Erythrocytes*. Front Physiol, 2018. **9**.
89. Locovei, S., Bao, L., Dahl, G., *Pannexin 1 in erythrocytes: Function without a gap*. PNAS, 2006. **103**: p. 7655-7659.
90. Sridharan, M., Adderley, S.P., Bowles, E.A., Egan, T.M., Stephenson, A.H., Ellsworth, M.L., Sprague, R.S., *Pannexin 1 is the conduit for low oxygen tension-induced ATP release from human erythrocytes*. AJP: Heart Circ. Physiol., 2010. **299**: p. H1146-H1152.
91. Forsyth, A.M., Wan, J., Owrutsky, P.D., Abkarian, M., Stone, H.A., *Multiscale approach to link red blood cell dynamics, shear viscosity, and ATP release*. Proc. Natl. Acad. Sci., 2011. **108**: p. 10986-10991.
92. Wan, J., Forsyth, A.M., Stone, H.A., *Red blood cell dynamics: from cell deformation to ATP release*. Integr. Biol., 2011. **3**: p. 972-981.
93. Ellsworth, M.L., Forrester, T., Ellis, C.G., Dietrich, H.H., *The erythrocyte as a regulator of vascular tone*. Am. J. Physiol. Heart Circ. Physiol., 1995. **269**: p. H2155-H2161.
94. Ellsworth, M.L., Sprague, R.S., *Regulation of blood flow distribution in skeletal muscle: role of erythrocyte-released ATP*. J. Physiol., 2012. **590**: p. 4985-4991.
95. Gonzalez-Alonso, J., *ATP as a mediator of erythrocyte-dependent regulation of skeletal muscle blood flow and oxygen delivery in humans*. J. Physiol., 2012. **590**: p. 5001-5013.
96. Chen, L.Y., Mehta, J.L., *Variable Effects of L-Arginine Analogs on L-Arginine-Nitric Oxide Pathway in Human Neutrophils and Platelets May Relate to Different Nitric Oxide Synthase Isoforms*. J Biol Chem, 1998. **269**(40): p. 25062-25066.
97. De Frutos, T., De Miguel, L.S., Farré, J., Gómez, J., Romero, J., Marcos-Alberca, P., Nuñez, A., Rico, L., López-Farré, A., *Expression of an endothelial-type nitric oxide synthase isoform in human neutrophils: modification by tumor necrosis factor-alpha and during acute myocardial infarction*. J Am Coll Cardiol, 2001. **37**(3): p. 800-807.

98. Mühl, H., Pfeilschifter, J., *Endothelial nitric oxide synthase: a determinant of TNF α production by human monocytes/macrophages*. *Biochem Biophys Res Commun*, 2003. **310**(3): p. 677-680.
99. Saluja, R., Jyoti, A., Chatterjee, M., Habib, S., Verma, A., Mitra, K., Barthwal, VM.K., Bajpai, V.K., Dikshit, M., *Molecular and biochemical characterization of nitric oxide synthase isoforms and their intracellular distribution in human peripheral blood mononuclear cells*. *Biochim Biophys Acta*, 2011. **1813**(10): p. 1700-1707.
100. Sase, K., Michel, T., *Expression of constitutive endothelial nitric oxide synthase in human blood platelets*. *Life Sciences*, 1995. **57**(22): p. 2049-2055.
101. Radomski, M.W., Palmer, R.M., Moncada, S., *An L-arginine/nitric oxide pathway present in human platelets regulates aggregation*. *PNAS*, 1990. **87**(13): p. 5193-5197.
102. Schaeue, D., Micewicz, E.D., Ratikan, J.A., Xie, M.W., Cheng, G., McBride, W.H., *Radiation and Inflammation*. *Seminars in Radiation Oncology*, 2015. **25**(1): p. 4-10.
103. Gladwin, M.T., Schechter, A.N., Kim-Shapiro, D.B., Patel, R.P., Hogg, N., Shiva, S., Cannon III, R.O., Kelm, M., Wink, D.A., Espey, M.G., Oldfield, E.H., Pluta, R.M., Freeman, B.A., Lancaster Jr., J.R., Feelisch, M., Lundberg, J.O., *The emerging biology of the nitrite anion*. *Nat Chem Biol*, 2005. **1**(6): p. 308-314.
104. Cosby, K., Partovi, K.S., Crawford, J.H., Patel, R.P., Reiter, C.D., Martyr, S., Yang, B.K., Waclawiw, M.A., Zalos, G., Xu, X., Huang, K.T., Shields, H., Kim-Shapiro, D.B., Schechter, A.N., Cannon III, R.O., Gladwin, M.T., *Nitrite reduction to nitric oxide by deoxyhemoglobin vasodilates the human circulation*. *Nat Med*, 2003. **9**(12): p. 1498-1505.
105. Webb, A.J., Milsom, A.B., Rathod, K.S., Chu, W.L., Qureshi, S., Lovell, M.J., Lecomte, F.M.J., Perrett, D., Raimondo, C., Khoshbin, E., Ahmed, Z., Uppal, R., Benjamin, N., Hobbs, A.J., Ahluwalia, A., *Mechanisms Underlying Erythrocyte and Endothelial Nitrite Reduction to Nitric Oxide in Hypoxia*. *Circ Res*, 2008. **103**: p. 957-964.
106. Crawford, J.H., Isbell, T.S., Huang, Z., Shiva, S., Chacko, B.K., Schechter, A.N., Darley-Usmar, V.M., Kerby, J.D., Lang, Jr., J.D., Kraus, D., Ho, C., Gladwin, M.T., Patel, R.P., *Hypoxia, red blood cells, and nitrite regulate NO-dependent hypoxic vasodilation*. *Blood*, 2006. **107**(2): p. 566-574.
107. Aamand, R., Dalsgaard, T., Jensen, F.B., Simonsen, U., Roepstorff, A., Fago, A., *Generation of nitric oxide from nitrite by carbonic anhydrase: a possible link between metabolic activity and vasodilation*. *Am J Physiol*, 2009. **297**(6): p. H2068-2074.
108. Ghosh, S.M., Kapil, V., Fuentes-Calvo, I., Bubb, K.J., Pearl, V., Milsom, A.B., Khambata, R., Maleki-Toyserkani, S., Yousuf, M., Benjamin, N., Webb, A.J., Caulfield, M.J., Hobbs, A.J., Ahluwalia, A., *Enhanced Vasodilator Activity of Nitrite in Hypertension: critical Role for*

- Erythrocytic Xanthine Oxidoreductase and Translational Potential*. Hypertension, 2013. **61**(5): p. 1091-1102.
109. Deem, S., Gladwin, M.T., Berg, J.T., Kerr, M.E., Swenson, E.R., *Effects of S-Nitrosation of Hemoglobin on Hypoxic Pulmonary Vasoconstriction and Nitric Oxide Flux*. American Journal of Respiratory and Critical Care Medicine, 2001. **163**(5).
110. Huang, Z., Ucer, K.B., Murphy, T., Williams, R.T., King, S.B., Kim-Shapiro, D.B., *Kinetics of Nitric Oxide Binding to R-State Hemoglobin*. Biochem Biophys Res Commun, 2002. **292**(4): p. 812-818.
111. Isbell, T.S., Sun, C.-W., Wu, L.-C., Teng, X., Vitturi, D.A., Branch, B.G., Kevil, C.G., Peng, N., Wyss, J.M., Ambalavanan, N., Schwiebert, L., Ren, J., Pawlik, K.M., Renfrow, M.B., Patel, R.P., Townes, T.M., *SNO-hemoglobin is not essential for red blood cell-dependent hypoxic vasodilation*. Nature Medicine, 2008. **14**(7): p. 773-777.
112. Gladwin, M.T., Shelhamer, J.H., Schechter, A.N., Pease-Fye, M.E., Waclawiw, M.A., Panza, J.A., Ognibene, F.P., Cannon III, R.O., *Role of circulating nitrite and S-nitrosohemoglobin in the regulation of regional blood flow in humans*. PNAS, 2000. **97**(21): p. 11482-11487.
113. Liu, C., Wajih, N., Li, X., Basu, S., Janes, J., Marvel, M., Keggi, C., Helms, C.C., Lee, A.N., Belanger, A.M., Diz, D.I., Laurienti, P.J., Caudell, D.L., Wang, J., Gladwin, M.T., Kim-Shapiro, D.B., *Mechanisms of Human Erythrocytic Bioactivation of Nitrite*. J Biol Chem, 2015. **290**(2): p. 1281-1294.
114. Gambaryan, S., Subramanian, H., Kehrer, L., Mindukshev, I., Sudnitsyna, J., Reiss, C., Rukoyatkina, N., Friebe, A., Sharina, I., Martin, E., Walter, U., *Erythrocytes do not activate purified and platelet soluble guanylate cyclases even in conditions favourable for NO synthesis*. Cell Commun Signal, 2016. **14**(1): p. 16.
115. Tziakas, D.N., Chalikias, G., Pavlaki, M., Kareli, D., Gogiraju, R., Hubert, A., Bohm, E., Stamoulis, P., Drosos, I., Kikas, P., Mikroulis, D., Giatromanolaki, A., Georgiadis, G.S., Konstantinou, F., Argyriou, C., Munzel, T., Konstantinides, S.V., Schafer, K., *Lysed Erythrocyte Membranes Promote Vascular Calcification: Possible Role of Erythrocyte-Derived Nitric Oxide*. Circulation, 2019.
116. Diederich, L., Suvorava, T., Sansone, R., Keller, T.C.S., Barbarino, F., Sutton, T.R., Kramer, C.M., Luckstadt, W., Isakson, B.E., Gohlke, H., Feelisch, M., Kelm, M., Cortese-Krott, M.M., *On the Effects of Reactive Oxygen Species and Nitric Oxide on Red Blood Cell Deformability*. Front Physiol, 2018. **9**: p. 332.
117. Helms, C.C., Gladwin, M.T., Kim-Shapiro, D.B., *Erythrocytes and Vascular Function: Oxygen and Nitric Oxide*. Front Physiol, 2018. **9**: p. 125.

118. Spector, E.B., Rice, S.C., Kern, R.M., Hendrickson, R., Cederbaum, S.D., *Comparison of arginase activity in red blood cells of lower mammals, primates, and man: Evolution to high activity in primates*. Am J Hum Genet, 1985. **37**(6): p. 1138-1145.
119. Yang, J., Gonon, A.T., Sjöquist, P.-O., Lundberg, J.O. Pernow, J., *Arginase regulates red blood cell nitric oxide synthase and export of cardioprotective nitric oxide bioactivity*. Proceedings of the National Academy of Sciences, 2013. **110**(37): p. 15049-15054.
120. Cortese-Krott, M.M., Mergia, E., Kramer, C.M., Luckstadt, W., Yang, J., Wolff, G., Panknin, C., Bracht, T., Sitek, B., Pernow, J., Stasch, J.P., Feelisch, M., Koesling, D., Kelm, M., *Identification of a soluble guanylate cyclase in RBCs: preserved activity in patients with coronary artery disease*. Redox Biol, 2018. **14**: p. 328-337.
121. Peterson, K.R., Fedosyuk, H., Zelenchuk, L., Nakamoto, B., Yannaki, E., Stamatoyannopoulos, G., Ciciotte, S., Peters, L.L., Scott, L.M., Papayannopoulou, T., *Transgenic Cre expression mice for generation of erythroid-specific gene alterations*. Genesis, 2004. **39**(1): p. 1-9.
122. Schwenk, F., Baron, U., Rajewsky, K., *A cre-transgenic mouse strain for the ubiquitous deletion of loxP-flanked gene segments including deletion in germ cells*. Nucleic Acids Res, 1995. **23**(24): p. 5080-1.
123. Nagy, A., *Cre recombinase: the universal reagent for genome tailoring*. Genesis, 2000. **26**(2): p. 99-109.
124. Kwan, K.-M., *Conditional alleles in mice: practical considerations for tissue-specific knockouts*. Genesis, 2002. **32**(2): p. 46-62.
125. Lakso, M., Sauer, B., Mosinger Jr., B., Lee, E.J., Manning, R.W., Yu, S.H., Mulder, K.L., Westphal, H., *Targeted oncogene activation by site-specific recombination in transgenic mice*. PNAS, 1992. **89**(14): p. 6232-6236.
126. Orban, P.C., Chui, aD., Marth, J.D., *Tissue- and site-specific DNA recombination in transgenic mice*. PNAS, 1992. **89**(15): p. 6861-6865.
127. Kuhn, R., Schwenk, F., Aguet, M., Rajewsky, K., *Inducible gene targeting in mice*. Science, 1995. **269**(5229): p. 1427-1429.
128. Kilkenny, C., Browne, W.J., Cuthill, I.C., Emerson, M., Altman, D.G., *Improving Bioscience Research Reporting: The ARRIVE Guidelines for Reporting Animal Research*. PLOS Biology, 2010. **8**(6): p. e1000412.
129. Sörensen, I., Adams, R.H., Gossler, A., *DLL1-mediated Notch activation regulates endothelial identity in mouse fetal arteries*. Blood, 2009. **113**(22): p. 5680-5688.
130. Lowry, O.H., Rosebrough, N.J., Farr, A.L., Randall, R.J., *Protein measurement with the Folin phenol reagent*. Journal of Biological Chemistry, 1951. **193**: p. 256-275.

131. Erkens, R., Kramer, C.M., Luckstadt, W., Panknin, C., Krause, L., Weidenbach, M., Dirzka, J., Krenz, T., Mergia, E., Suvorava, T., Kelm, M., Cortese-Krott, M.M., *Left ventricular diastolic dysfunction in Nrf2 knock out mice is associated with cardiac hypertrophy, decreased expression of SERCA2a, and preserved endothelial function*. Free Radic Biol Med, 2015. **89**: p. 906-17.
132. Feelisch, M., Rassaf, T., Mnaimneh, S., Singh, N., Bryan, N.S., Jour'dHeuil, D., Kelm, M., *Concomitant S-, N-, and heme-nitros(yl)ation in biological tissues and fluids: implications for the fate of NO in vivo*. Faseb j, 2002. **16**(13): p. 1775-1785.
133. Hussain, M.B., MacAllister, R.J., Hobbs, A.J., *Reciprocal regulation of cGMP-mediated vasorelaxation by soluble and particulate guanylate cyclases*. Am J Physiol Heart Circ Physiol, 2001. **280**(3): p. H1151-9.
134. Brandes, R.P., Kim, D., Schmitz-Winnenthal, F.H., Amidi, M., Gödecke, A., Mülsch, A., Busse, R., *Increased nitrovasodilator sensitivity in endothelial nitric oxide synthase knockout mice: role of soluble guanylyl cyclase*. Hypertension, 2000. **35**(1 Pt 2): p. 231-6.
135. Moncada, S., Rees, D.D., Schulz, R., Palmer, R.M., *Development and mechanism of a specific supersensitivity to nitrovasodilators after inhibition of vascular nitric oxide synthesis in vivo*. Proceedings of the National Academy of Sciences, 1991. **88**(6): p. 2166-2170.
136. Cokic, V.P., Andric, S. A., Stojilkovic, S. S., Noguchi, C. T., Schechter, A. N., *Hydroxyurea nitrosylates and activates soluble guanylyl cyclase in human erythroid cells*. Blood, 2008. **111**(3): p. 1117-23.
137. Mitchell, J.A., Förstermann, U., Warner, T.D., Pollock, J.S., Schmidt, H.H.H.W., Heller, M., Murad, F., *Endothelial cells have a particulate enzyme system responsible for EDRF formation: Measurement by vascular relaxation*. Biochem Biophys Res Commun, 1991. **176**(3): p. 1417-1423.
138. Palmer, R.M.J., Ferrige, A.G., Moncada, S., *Nitric oxide release accounts for the biological activity of endothelium-derived relaxing factor*. Nature, 1987. **327**(6122): p. 524-526.
139. Martin, W., Furchgott, R.F., Villani, G.M., Jothianandan, D., *Depression of contractile responses in rat aorta by spontaneously released endothelium-derived relaxing factor*. Journal of Pharmacology and Experimental Therapeutics, 1986. **237**(2): p. 529-538.
140. Suvorava, T., Stegbauer, J., Thieme, M., Pick, S., Friedrich, S., Rump, L.C., Hohlfeld, T., Kojda, G., *Sustained hypertension despite endothelial-specific eNOS rescue in eNOS-deficient mice*. Biochem Biophys Res Commun, 2015. **458**(3): p. 576-83.
141. Sayed, N., Baskaran, P., Ma, X., Van den Akker, F., Beuve, A., *Desensitization of soluble guanylyl cyclase, the NO receptor, by S-nitrosylation*. PNAS, 2007. **104**(30): p. 12312-12317.
142. Stamler, J.S., Lamas, S., Fang, F.C., *Nitrosylation. The prototypic redox-based signaling mechanism*. Cell, 2001. **106**(6): p. 675-683.

143. Foster, M.W., McMahon, T.J., Stamler, J.S., *S-nitrosylation in health and disease*. Trends in Molecular Medicine, 2003. **9**(4): p. 160-168.
144. Liu, L., Yan, Y., Zeng, M., Zhang, J., Hanes, M.A., Ahearn, G., McMahon, T.J., Dickfeld, T., Marshall, H.E., Que, L.G., Stamler, J.S., *Essential roles of S-nitrosothiols in vascular homeostasis and endotoxic shock*. Cell, 2004. **116**(4): p. 617-628.
145. Gow, A.J., Chen, Q., Hess, D.T., Day, B.J., Ischiropoulos, H., Stamler, J.S., *Basal and Stimulated Protein S-Nitrosylation in Multiple Cell Types and Tissues*. Journal of Biological Chemistry, 2002. **277**(12): p. 9637-9640.
146. Jensen, D.E., Belka, G.K., Du Bois, G.C., *S-Nitrosoglutathione is a substrate for rat alcohol dehydrogenase class III isoenzyme*. Biochemical Journal, 1998. **331**(Pt.2): p. 659-668.
147. Liu, L., Hausladen, A., Zeng, M., Que, L., Heitman, J., Stamler, J.S., *A metabolic enzyme for S-nitrosothiol conserved from bacteria to humans*. Nature, 2001. **410**: p. 490-494.
148. Dei Zotti, F., Lobysheva, I.I., Balligand, J. L., *Nitrosyl-hemoglobin formation in rodent and human venous erythrocytes reflects NO formation from the vasculature in vivo*. PLoS One, 2018. **13**(7): p. e0200352.
149. Heiss, C., Rodriguez-Mateos, A., Kelm, M., *Central Role of eNOS in the Maintenance of Endothelial Homeostasis*. Antioxid Redox Signal, 2015. **22**(14): p. 1230-1242.
150. Schuler, D., Sansone, R., Freudenberger, T., Rodriguez-Mateos, A., Weber, G., Momma, T.Y., Goy, C., Altschmied, J., Haendeler, J., Fischer, J.W., Kelm, M., Heiss, C., *Measurement of endothelium-dependent vasodilation in mice--brief report*. Arterioscler Thromb Vasc Biol, 2014. **34**(12): p. 2651-2657.
151. Lundberg, J.O., Weitzberg, E., *NO Generation From Nitrite and Its Role in Vascular Control*. Arterioscler Thromb Vasc Biol, 2005. **25**(5): p. 915-922.
152. Stamler, J.S., Jia, L., Eu, J.P., McMahon, T.J., Demchenko, I.T., Bonaventura, J., Gernert, K., Piantadosi, C.A., *Blood Flow Regulation by S-Nitrosohemoglobin in the Physiological Oxygen Gradient*. Science, 1997. **276**(5321): p. 2034-2037.
153. McMahon, T.J., Stamler, J.S., *Concerted nitric oxide/oxygen delivery by hemoglobin*. Methods in Enzymology, 1999. **391**: p. 99-106.
154. McMahon, T.J., Moon, R.E., Luschinger, B.P., Carraway, M.S., Stone, A.E., Stolp, B.W., Gow, A.J., Pawloski, J.R., Watke, P., Singel, D.J., Piantadosi, C.A., Stamler, J.S., *Nitric oxide in the human respiratory cycle*. Nat Med, 2002. **8**(7): p. 711-717.
155. Gladwin, M.T., Wang, X., Reiter, C.D., Yang, B.K., Vivas, E.X., Bonaventura, C., Schechter, A.N., *S-Nitrosohemoglobin Is Unstable in the Reductive Erythrocyte Environment and Lacks O2/NO-linked Allosteric Function*. J Biol Chem, 2002. **277**(31): p. 27818-27828.

156. Gladwin, M.T., Ognibene, F.P., Pannell, L.K., Nichols, J.S., Pease-Fye, M.E., Shelhamer, J.H., Schechter, A.N., *Relative role of heme nitrosylation and β -cysteine 93 nitrosation in the transport and metabolism of nitric oxide by hemoglobin in the human circulation*. Proc Natl Acad Sci U S A, 2000. **97**(18): p. 9943-9948.
157. Piknova, B., Gladwin, M.T., Schlechter, A.N., Hogg, N., *Electron paramagnetic resonance analysis of nitrosylhemoglobin in humans during NO inhalation*. J Biol Chem, 2005. **280**(49): p. 40583-40588.
158. Cannon III, R.O., Schechter, A.N., Panza, J.A., Ognibene, F.P., Pease-Fye, M.E., Waclawiw, M.A., Shelhamer, J.H., Gladwin, M.T., *Effects of inhaled nitric oxide on regional blood flow are consistent with intravascular nitric oxide delivery*. J Clin Invest, 2001. **108**(2): p. 279-287.
159. Lipton, A.J., Johnson, M.A., Macdonald, T., Lieberman, M.W., Gozal, D., Gaston, B., *S-Nitrosothiols signal the ventilatory response to hypoxia*. Nature, 2001. **413**: p. 171-174.
160. McMahon, T.J., Stone, A.E., Bonaventura, J., Singel, D.J., Stamler, J.S., *Functional coupling of oxygen binding and vasoactivity in S-nitrosohemoglobin*. J Biol Chem, 2000. **275**(22): p. 16738-16745.
161. Grubina, R., Huang, Z., Shiva, S., Joshi, M.S., Azarov, I., Basu, S., Ringwood, L.A., Jiang, A., Hogg, N., Kim-Shapiro, D.B., *Concerted nitric oxide formation and release from the simultaneous reactions of nitrite with deoxy- and oxyhemoglobin*. Journal of Biological Chemistry, 2007. **282**(17): p. 12916-12927.
162. Kleschyov, A.L., *The NO-heme signaling hypothesis*. Free Radical Biology and Medicine, 2017. **112**: p. 544-552.
163. Gilchrist, M., Shore, A.C., Benjamin, N., *Inorganic nitrate and nitrite and control of blood pressure*. Cardiovasc Res, 2011. **89**(3): p. 492-498.
164. Godber, B.L.J., Doel, J.J., Sapkota, G.P., Blake, D.R., Stevens, C.R., Eisenthal, R., Harrison, R., *Reduction of Nitrite to Nitric Oxide Catalyzed by Xanthine Oxidoreductase*. J Biol Chem, 2000. **275**(11): p. 7757-7763.
165. Li, H., Samouilov, A., Liu, X., Zweier, J.L., *Characterization of the Magnitude and Kinetics of Xanthine Oxidase-catalyzed Nitrite Reduction: EVALUATION OF ITS ROLE IN NITRIC OXIDE GENERATION IN ANOXIC TISSUES*. J Biol Chem, 2001. **276**(27): p. 24482-24489.
166. Millar, T.M., Stevens, C.R., Benjamin, N., Eisenthal, R., Harrison, R., Blake, D.R., *Xanthine oxidoreductase catalyses the reduction of nitrates and nitrite to nitric oxide under hypoxic conditions*. FEBS Letters, 1998. **427**(2): p. 225-228.

167. Gautier, C., Faassen, E., Mikula, I., Martasek, P., Slama-Schwok, A., *Endothelial nitric oxide synthase reduces nitrite anions to NO under anoxia*. *Biochem Biophys Res Commun*, 2006. **341**(3): p. 816-821.
168. Castello, P.R., David, P.S., McClure, T., Crook, Z., Poyton, R.O., *Mitochondrial cytochrome oxidase produces nitric oxide under hypoxic conditions: Implications for oxygen sensing and hypoxic signaling in eukaryotes*. *Cell Metabolism*, 2006. **3**(4): p. 277-287.
169. Hunter, C.J., Dejam, A., Blood, A.B., Shields, H., Kim-Shapiro, D.B., Machado, R.F., Tarekegn, S., Mulla, N., Hopper, A.O., Schechter, A.N., Power, G.G., Gladwin, M.T., *Inhaled nebulized nitrite is a hypoxia-sensitive NO-dependent selective pulmonary vasodilator*. *Nat Med*, 2004. **10**(10): p. 1122-1127.
170. Webb, A., Bond, R., McLean, P., Uppal, R., Benjamin, N., Ahluwalia, A., *Reduction of nitrite to nitric oxide during ischemia protects against myocardial ischemia-reperfusion damage*. *Proc Natl Acad Sci U S A*, 2004. **101**(37): p. 13683-13688.
171. Duranski, M.R., Greer, J.J.M., Dejam, A., Jaganmohan, S., Hogg, N., Langston, W., Patel, R.P., Yet, S.-F., Wang, X., Kevil, C.G., Gladwin, M.T., Lefer, D.J., *Cytoprotective effects of nitrite during in vivo ischemia-reperfusion of the heart and liver*. *J Clin Invest*, 2005. **115**(5): p. 1232-1240.
172. Pitulescu, M.E., Schmidt, I., Benedito, R., Adams, R.H., *Inducible gene targeting in the neonatal vasculature and analysis of retinal angiogenesis in mice*. *Nat Protoc*, 2010. **5**(9): p. 1518-34.
173. Jones, S.P., Girod, W.G., Palazzo, A.J., Granger, D.N., Grisham, M.B., Jourd'Heuil, D., Huang, P.L., Lefer, D.J., *Myocardial ischemia-reperfusion injury is exacerbated in absence of endothelial cell nitric oxide synthase*. *Am J Physiol*, 1999. **276**(5 Pt 2): p. H1567-1573.
174. Pong, T., Atochin, D.N., Bloch, K.D., Huang, P.L., *Phosphomimetic Modulation of eNOS Improves Myocardial Reperfusion and Mimics Cardiac Postconditioning in Mice*. *PLoS One*, 2014. **9**(1): p. e85946.
175. Feil, S., Krauss, J., Thunemann, M., Feil, R., *Genetic inducible fate mapping in adult mice using tamoxifen-dependent Cre recombinases*. *Methods Mol Biol*, 2014. **1194**: p. 113-39.

7. Acknowledgements

The experimental work for this dissertation was done in the Myocardial Infarct Research Laboratory, Division of Cardiology, Pulmonology and Angiology, Medical Faculty of the Heinrich-Heine-University.

I am especially thankful to my mentor Prof. Dr. rer. nat. Miriam M. Cortese-Krott. I would like to thank her for the scientific topics she assigned me and the brilliant and lively discussions we had; a special thank for the trust she put on me and the scientific and personal guidance she gave me during my PhD.

Prof. Dr. rer. nat. Jens Fischer, I would like to thank for his mentorship and the revision of my doctoral thesis.

I would like to thank Prof. Brant E. Isakson, PhD, for the great opportunity to work in his laboratory at the Cardiovascular Research Center at the University of Virginia; thanks for including me as a complete member of his team and for his big every-day support.

I am grateful for the funding by the “Internationales Graduiertenkolleg 1902” (IRTG 1902; Deutsche Forschungsgemeinschaft) with the speaker Prof. Dr. rer. nat. Axel Gödecke and the scientific coordinator Dr. Sandra Berger. I would like to thank for the great opportunity they gave me to spend part of my PhD studies abroad, at the University of Virginia, which was of great value for my education and personal experience. Moreover I would like to thank for the scientific training offered and for the big help and support given me during my PhD period.

I am extremely grateful to all my colleagues of the Myocardial Infarction Research Laboratory that have been not only colleagues but friends and family. We faced busy days and we shared many experiences together, always smiling and taking care of each other. Thank for your correctional help to this work and a very special thank you for everything you did for and with me, Sophia Heuser, Anthea Lo Bue and Junjie Li.

To the Isakson Laboratory, that included me in the team as I was always part of it and for guiding me into new techniques and new experiences. Thank you, Claire Ruddiman, Abigail Antoine, Edgar Macal, Angela Best, Scott Johnstone.

One special thank goes to the Pharmacology and Physiology department at the Heinrich-Heine-University. To Dr. rer. nat. Rebekka Schnekman for teaching me how to isolate cells and for becoming a true friend, enjoying with me every experiment and every coffee we had together. Thanks to Dr. med. André Heinen for helping me in the setup of an essential experiment in the Laboratory of Prof. Axel Gödecke and for being always ready to help and smile at every inconvenience I had.

One more thank to Stefanie Becher for teaching me the Millar catheterization procedure and for the continuous support offered me in these years.

Thank you, to all that contributed with their data to my dissertation. Dr. Lukas Vornholtz, for analysis of aortic rings *ex vivo*, Dr. Tatsiana Suvorava for FMD measurements and for teaching me the ultrasound *in vivo* techniques, Carina Nihlén for measuring nitrate content in the drinking water (Karolinska Institute, Stockholm, Sweden), Prof. Martin Feelisch, PhD, Bernadette O. Fernandez, PhD and Dr. Frederik Barbarino for the NO metabolites data. Thanks to Eugenia Piragine for performing qPCR, Anthea Lo Bue, Sivatharsini Thasian-Sivarajah and Wiebke Lückstädt for help with the western blots and Sophia Heuser for Ter119⁺ cells isolation and qPCR analyses.

8. Curriculum vitae

Name/Surname: Francesca Leo
 Date and place of birth: August 2, 1993 – Massa, (IT)
 Place of birth: Massa, Italy
 Nationality: Italian
 Personal email: francescaleoms@gmail.com



WORKING EXPERIENCE

09/17 – 01/2022 Doctoral researcher – Heinrich-Heine-University – Düsseldorf, (DE)
 07/2017 -08/2017 Pharmacist - "Farmacia Nobile Dr. Benedetto" – Marina di Massa, (IT)
 02/2017 – 06/2017 Part-time counseling for freshmen at the University of Pisa, (IT)

EDUCATION

09/2017 - today Doctoral researcher – Heinrich Heine Universität – Düsseldorf, (DE)
Title: “Endothelial eNOS and red blood cell eNOS independently regulate blood pressure and nitric oxide metabolites”
 Supervisor: Prof. Dr. rer. nat. Miriam M. Cortese-Krott
 09/2012- 06/2017 MD in Pharmacy and Medicinal Chemistry (with honours):
 110/110 cum laude – Department of Pharmacy, University of Pisa, (IT)
Title: “Modulatori dell’attività dell’enzima SIRT1 come strategia per contenere l’aging e le patologie cardiovascolari correlate”
 Supervisor: Prof. Vincenzo Calderone, Dr. Lara Testai

FORMATION

01/2020 – 04/2020 Visiting scholar at University of Virginia – Charlottesville (VA), USA
 Supervisor: Prof. Brant E. Isakson – Robert M. Berne Cardiovascular Research Center – Department of Molecular Physiology and Biological Physics – University of Virginia Health System
 10/2017 – 01/2018 “Versuchstierkundlicher Kurs” – FELASA
 Heinrich-Heine-University – Düsseldorf, (DE)
 06/2017 – 07/2017 State examination for qualification as a pharmacist – Pisa, (IT)
 03/2016 – 10/2016 Professional internship at a Pharmacy
 Pharmacy: "Farmacia Nobile Dr. Benedetto" – Marina di Massa, (IT)
 Tutor: Dr. Benedetto Nobile, Dr. Giovanni Nobile
 02/2016 BLS-D: theoretical and practical course of basic life support with the use of semi-automatic defibrillator, to lay rescuers – Livorno, (IT)

VOLUNTEERING

06/206 – 06/2013 Leader of a children's volunteer parish group every summer for 2 weeks